UNIVERSITY OF ALBERTA
LIBRARY

Regulations Regarding Theses and Dissertations

Typescript copies of theses and dissertations for Master's and Doctor's degrees deposited in the University of Alberta Library, as the official Copy of the Faculty of Graduate Studies, may be consulted in the Reference Reading Room only.

A second copy is on deposit in the Department under whose supervision the work was done. Some Departments are willing to loan their copy to libraries, through the inter-library loan service of the University of Alberta Library.

These theses and dissertations are to be used only with due regard to the rights of the author. Written permission of the author and of the Department must be obtained through the University of Alberta Library when extended passages are copied. When permission has been granted, acknowledgement must appear in the published work.

This thesis or dissertation has been used in accordance with the above regulations by the persons listed below. The borrowing library is obligated to secure the signature of each user.

Please sign below:

Date	Signature	Institution

THE UNIVERSITY OF ALBERTA

THE INFLUENCE OF HOMOGENEOUS REACTIONS AND OF REACTOR SURFACE UPON N-PROPANOL DECOMPOSITION

BY

TAMOTSU IMAI

C

A THESIS

SUBMITTED TO THE FACULTY OF GRADUATE STUDIES

IN PARTIAL FULFILMENT OF THE REQUIREMENTS FOR THE

DEGREE OF MASTER OF SCIENCE

IN

CHEMICAL ENGINEERING

FACULTY OF ENGINEERING

DEPARTMENT OF CHEMICAL AND PETROLEUM ENGINEERING

EDMONTON, ALBERTA

SEPTEMBER, 1967

[illegible]

[illegible]
[illegible]

[illegible]

[illegible]

[illegible]
[illegible]
[illegible]
[illegible]

[illegible]

[illegible]

[illegible]
[illegible]

[illegible]
[illegible]

UNIVERSITY OF ALBERTA

FACULTY OF GRADUATE STUDIES

The undersigned certify that they have read, and recommend to the Faculty of Graduate Studies for acceptance a thesis entitled THE INFLUENCE OF HOMOGENEOUS REACTIONS AND OF REACTOR SURFACE UPON n-PROPANOL DECOMPOSITION submitted by Tamotsu Imai in partial fulfilment of the requirements for the degree of Master of Science in Chemical Engineering.

ABSTRACT

The homogeneous thermal decomposition of n-propanol and the catalytic effects of Pyrex Glass and type 316 stainless steel reactor surfaces were investigated in a Pyrex Glass flow reactor. Experiments to study the thermal decomposition of n-propanol were carried out at temperatures of 380°C, 400°C, 420°C, 440°C and 463°C and at 705 mm Hg. The effect of Pyrex Glass surface on the decomposition of n-propanol was studied at 463°C and at 705 mm Hg. The effect of type 316 stainless steel surface was investigated at 463°C, and at five space velocity levels of 0.1135, 0.0511, 0.0372, 0.0226 and 0.0151 [(gm-mole of n-propanol feed)/(hr)(gm of stainless steel)].

In the homogeneous thermal decomposition of n-propanol, a maximum n-propanol conversion of 0.8651 mole % was obtained at the residence time, 38.0 sec, and at the temperature of 463°C. The experimental results were discussed from the points of view of chemical species, stoichiometry of the product compounds, and chemical kinetics. It was believed that radical reactions, initiated by a foreign gas such as oxygen, were occuring. A chain reaction was also believed to proceed at temperatures above 440°C but not at temperatures below 400°C.

The effect of Pyrex Glass on the decomposition of n-propanol was found to be negligible.

It was found that in the presence of type 316 stainless steel, the dehydrogenation of n-propanol produced propionaldehyde and hydrogen. The condensations of n-propanol with aldehydes to produce propionaldehyde

dipropyl acetal and acetaldehyde dipropyl acetal were also encountered.

On the basis of this work, continuing studies of catalyzed reactions of n-propanol can be performed in Pyrex Glass reactors with negligible interference from homogeneous decomposition at temperatures below 463°C, especially at high n-propanol conversion.

ACKNOWLEDGEMENTS

The author is indebted to Dr. I. G. Dalla Lana of the Department of Chemical and Petroleum Engineering, University of Alberta, for his guidance and supervision during the course of this investigation.

The helpful discussions and suggestions of Dr. H. Kubota, Dr. K. Obi and Dr. A. Saxena are greatly appreciated. Appreciation is also expressed to Miss J. Vinkenborg for her patience and assistance in preparing the manuscript.

The financial support received from the National Research Council of Canada and the University of Alberta is gratefully acknowledged.

TABLE OF CONTENTS

LIST OF FIGURES

LIST OF TABLES

I. INTRODUCTION

In a recent investigation, the effect of silica-alumina treated with NaOH in catalizing the dehydrogenation reactions of n-propanol has been reported (1). During this work, both thermal decomposition of n-propanol and catalytic effects from the type 316 stainless steel reactor walls were encountered.

The present investigation was carried out to obtain information about the nature and magnitude of these undesirable side-reactions. Detailed knowledge of these reactions is necessary if one is to interpret kinetic data consistent with the reaction chemistry encountered in the dehydrogenation of n-propanol on silica-alumina catalyst treated with NaOH.

II. THEORY AND LITERATURE SURVEY

Extensive work has been done on catalytic and noncatalytic decomposition reactions of organic compounds. Semenov (2), Steacie (3), Hinshelwood (4) and Rice (5) did extensive studies on the thermal decomposition of organic compounds, and their books give an excellent review of this subject.

However, very few investigations of the thermal decomposition and stainless steel catalyzed decomposition of alcohols have been reported (1), (6). Wanke (1) studied the thermal decomposition of n-propanol in a glass reactor at 460°C and in a stainless steel reactor at 440°C. He obtained propionaldehyde, methyl ethyl ketone, and hydrogen as products in the glass reactor and propionaldehyde, methyl ethyl ketone, propylene, and hydrogen in the stainless steel reactor. He did not analyze the products quantitatively and the reaction mechanism was not studied.

In the literature, for the thermal decomposition of organic compounds, molecular and free-radical mechanisms have been proposed. In the free-radical mechanism, the influence of a foreign gas, such as oxygen, on the thermal decomposition may play an important role in the initiation of the reaction. These mechanisms and the catalytic effects

of stainless steel on the thermal decomposition of n-propanol will be described in the following section.

A. Thermal Decomposition

1. Reaction Mechanisms

There is considerable uncertainty concerning the manner in which organic compounds decompose at high temperatures (7). Two main mechanisms are believed to occur.

a) the molecular mechanism

In this case, the compound splits into its final stable decomposition products in a single step. This step involves the simultaneous rupture of two valence bonds and the formation of at least one new one, as in the following example,

$$CH_3 \!+\! \underset{\underset{O}{\|}}{C} \!+\! H \longrightarrow CH_4 + CO \qquad (1)$$

It is apparent, therefore, that the activation energy of the process will bear no simple relation to the bond strengths. The activation energy of a molecular reaction is always somewhat less than the energy corresponding to the breaking of a bond, since the energy set free in the stabilization of the products contributes toward reducing the latter energy (8).

b) the free-radical mechanism

In this case, the primary step consists of the rupture of only a single bond, giving rise to unsaturated

radicals. Then, these radicals undergo chain reactions which ultimately lead to the final stable products. The activation energy of the primary step in this mechanism will be a dissociation energy (7), (9).

Some values of dissociation energies are shown in Table II-1 and II-2 (See Appendix VI). It is difficult to discuss the reactivity of the various primary reactions quantitatively based on the dissociation energies shown in Table II-2 because these values may be in error up to 4 Kcal.

Rice (31) has indicated that if there is a difference of 4 Kcal in the activation energies of two reactions, the relative reaction rate at 600°C is exp(4,000/2x873):1, that is about 9:1. The relative reaction rate is 500:1 if the difference between the activation energies is 10 Kcal. According to this, reaction (2) and (3) may possibly occur as the primary steps in the thermal decomposition of n-propanol.

$$CH_3CH_2CH_2OH \longrightarrow CH_3 + CH_2CH_2OH \qquad (2)$$

$$CH_3CH_2CH_2OH \longrightarrow CH_3CH_2 + CH_2OH \qquad (3)$$

2. The Activation Energies of Chain Reactions

Many reactions, having the characteristics of chain reactions, show induction periods during which the rate of change is apparently almost zero, and at the end

[illegible]

Table II-1

Values of Bond Dissociation Energies (10)

Values in Kcal/mole

R	R-H	R-CH_3	R-OH	RO-H
CH_3	104.0	88.0	91.0	102.0
C_2H_5	98.0	85.0	91.0	102.0
C_3H_7	98.0	-	92.5*	103.0
$(CH_3)_2CH$	94.5	83.0	92.0	103.0

* This value calculated by author (See Appendix VI).

Table II-2

Values of Bond Dissociation Energies in n-Propanol

Values in Kcal/mole

Bond	Bond Dissociation Energy
CH_3-CH_2CH_2OH	79.2*
CH_3CH_2-CH_2OH	82.4*
$CH_3CH_2CH(OH)$-H	90-92 **
$CH_3CH_2CH_2$-OH	92.5**
$CH_3CH_2CH_2O$-H	103 (10)

* Values calculated by author

** The value estimated from similar reactions (See Appendix VI).

[illegible]

[illegible]

[illegible]

[illegible]	[illegible]	[illegible]	[illegible]	[illegible]
[illegible]	[illegible]	[illegible]	[illegible]	[illegible]
[illegible]	[illegible]	[illegible]	[illegible]	[illegible]
[illegible]	[illegible]	[illegible]	[illegible]	[illegible]
[illegible]	[illegible]	[illegible]	[illegible]	[illegible]

[illegible]

[illegible]

[illegible]

[illegible]

[illegible]	[illegible]
[illegible]	[illegible]
[illegible]	[illegible]
[illegible]	[illegible]
[illegible]	[illegible]
[illegible]	[illegible]

[illegible]

[illegible]

[illegible]

of which measurable reaction sets in (11). The experimental activation energies of the chain reactions are usually far smaller than the dissociation energies of the primary steps. This is explained by the Rice-Herzfeld mechanism as follows:

		E, Kcal	
M_1	$\xrightarrow{k_1} R_1 + R_1'$	80	(4)
$R_1 + M_1$	$\xrightarrow{k_2} R_1H + R_2$	15	(5)
R_2	$\xrightarrow{k_3} R_1 + M_3$	38	(6)
$R_1 + R_2$	$\xrightarrow{k_4} M_4$	8	(7)

The molecule M_1 is assumed to decompose into radicals R_1 and R_1'. The radical R_1' is assumed to play no part in the reaction, but R_1 initiates the chain of reactions (5), (6) and (7). The radical R_1 reacts with a fresh molecule of the reactant, abstracts a hydrogen atom, and forms the stable substance R_1H and the radical R_2. R_2 then decomposes into a radical and a molecule M_3. A chain reaction is thus established since steps (5) and (6) are repetitive. The chain is finally broken when the radicals combine to form a stable molecule according to reaction (7).

Assuming that long chains occur and that the concentration of the radicals is constant, it is possible to write equations (8) and (9) for the steady state:

[illegible]

[illegible]

[illegible]

[illegible]

$$\frac{d[R_1]}{dt} = 0 = k_1[M_1] - k_2[R_1][M_1] + k_3[R_2] - k_4[R_1][R_2] \quad (8)$$

$$\frac{d[R_2]}{dt} = 0 = k_2[R_1][M_1] - k_3[R_2] - k_4[R_1][R_2] \quad (9)$$

Whence, by eliminating $[R_2]$ and solving the quadratic equation obtained from the equations (8) and (9),

$$[R_1] = \frac{k_1}{4k_2} + [(\frac{k_1}{4k_2})^2 + (\frac{k_1 k_3}{2k_2 k_4})]^{\frac{1}{2}} \quad (10)$$

The negative value of $[R_1]$ was discarded. If it is assumed that k_1 is very small, and that $k_1 << k_2$,

$$[R_1] \simeq (\frac{k_1 k_3}{2k_2 k_4})^{\frac{1}{2}} \quad (11)$$

The overall rate of decomposition of M_1 is given by

$$-\frac{d[M_1]}{dt} = k_1[M_1] + k_2[R_1][M_1] \quad (12)$$

Substituting for $[R_1]$ from equation (11),

$$-\frac{d[M_1]}{dt} \simeq k_1[M_1][1 + (\frac{k_2 k_3}{2k_1 k_4})^{\frac{1}{2}}] \quad (13)$$

Since $k_1 x k_4$ is small compared with $k_2 x k_3$ according to the activation energies, the term in parentheses is large compared with unity, so that the rate is given approximately by

$$-\frac{d[M_1]}{dt} \simeq k_1[M_1](\frac{k_2 k_3}{2k_1 k_4})^{\frac{1}{2}} = [M_1](\frac{k_1 k_2 k_3}{k_4})^{\frac{1}{2}} \quad (14)$$

According to the Arrhenius equation which gives the

temperature dependency of the rate constant, the overall activation energy is thus calculated to be

$$E_{overall} \simeq \tfrac{1}{2}(E_1 + E_2 + E_3 - E_4)$$

Using the values given previously for the activation energies of the elementary reactions,

$$E_{overall} \simeq 62.5 \text{ Kcal}$$

which is much less than the 80 Kcal assumed for the primary step.

3. Chemical Reactions

Rice (5) has reported that the mechanism of decomposition of primary alcohols is a direct separation of molecular hydrogen from the alcohol to form the corresponding aldehyde,

$$R\ CH_2OH \longrightarrow RCHO + H_2 \qquad (15)$$

According to the free-radical mechanism, the primary steps induce the chain reactions. The radicals, CH_3, CH_2CH_2OH, CH_3CH_2 and CH_2OH, which are formed by the reactions (2) and (3) may induce the chain reactions. A detailed discussion of the postulated chemical reactions will be presented in a later section.

4. The Influence of Foreign Gases

The influence of foreign gases on the rate of decomposition has been extensively investigated. Certain substances such as oxygen, iodine, bromine, nitric oxide, nitrous oxide, and hydrogen sulfide catalyze the reaction, and mechanisms involving the introduction of new free-radical processes have been proposed (32). Letort (13) has found the sensitizing action of oxygen as initiator in the thermal decomposition of acetaldehyde. Hinshelwood (14) reported that traces of oxygen induce the decomposition of organic compounds, such as acetaldehyde, at temperatures below 400°C, where acetaldehyde is thermally stable. Morris (15) suggested that some oxidizing impurity, which was removed by hydroquinone, was responsible for the initiation of chain processes in ordinary acetaldehyde. The decomposition of acetaldehyde catalyzed by oxygen is first order with respect to the oxygen concentration. The amount of acetaldehyde catalytically decomposed by a given quantity of oxygen is greater, the greater the excess of acetaldehyde (16). A search through the literature has revealed that the influence of foreign gases on the decomposition of n-propanol has not been studied. This investigation has provided some information on this subject and the results will be discussed in a later section.

B. The Effects of Stainless Steel as a Catalyst

The work of Wanke (1), as cited previously, has indicated that stainless steel significantly affects the decomposition of n-propanol and n-propanol conversion with stainless steel is increased compared to the homogeneous thermal decomposition of n-propanol. Kozlov and coworkers (6) reported that stainless steel produces decomposition of secondary and tertiary butyl alcohols into butylene at temperatures higher than 150°C.

The surface of stainless steel contains oxides of Cr, Fe, Ni and Mo (17) and these may be responsible for the catalytic effects of the stainless steels. Due to the complex nature of the catalytic action of the multi-component catalyst, it is difficult to assess the overall catalytic activity of a stainless steel in terms of the catalytic activities of these metal oxides. However, since both NiO and Cr_2O_3 are very active catalysts for dehydrogenation and dehydration of organic compounds (18), type 316 stainless steel may also be expected to possess a similar character.

C. The Formation of Acetals

Aldehydes and alcohols in the liquid phase easily form acetals in the presence of acid catalysts (19). Acetals are also obtained from olefins and alcohols by oxidation with metals of variable valence, e.g. Cu and

Fe chlorides, in the presence of Pd salts in the liquid phase (20). In the noncatalytic vapor phase oxidation of hydrocarbons (21), Robertson has reported formation of acetal together with other products, such as aldehydes, ketones, alcohols and oxides.

D. Summary of Published Results

Much work has been done on the decomposition of organic compounds such as hydrocarbons, aldehydes, esters, and ethers. However, there is a lack of information on the thermal decomposition of primary alcohols.

Various possible mechanisms for the thermal decomposition of n-propanol have been considered. These include: the molecular mechanism, the free-radical mechanism, and the influence of foreign gases on the initiation of the reaction.

Very few workers have reported the catalytic effects of stainless steels on the decomposition of alcohols. Catalytic activities resulting in dehydration and dehydrogenation have been suggested.

[illegible]

[illegible]

[illegible]

[illegible]

[illegible]

III. EQUIPMENT AND OPERATING PROCEDURE

A. Equipment

The experimental equipment, as represented in Figures III-1 and III-2, consists of the n-propanol feed system, the vaporization system, the reaction system, and the sampling system. Figure 1 is a schematic representation of the overall layout of the equipment and the instrumentation used to control the feed rate, the vaporizer and reactor temperature, and to condense the product gases. An acrylic acid resin sheet was placed in front of the vaporization and reaction systems for safty against splashes of heated oil and melted salt.

Each of the above systems will be discussed in detail.

1. Feed System

To obtain precise and stable feed rates, a micro-feeder manufactured by Azuma Denki Kogyo Co. Ltd., Tokyo, Japan was used. The n-propanol was fed by a 100 cc glass syringe with a synchronous motor acting on the piston. Different velocities of the piston were obtained by changing the combination of transmission gears. In the present investigation, four syringe piston velocities were used to give different residence times in the reactor. These were 10 mm/hr, 15 mm/hr, 20 mm/hr,

[illegible]

[illegible]

[illegible]

[illegible]

[illegible]

and 40 mm/hr, corresponding to 6.8819, 10.2505, 13.6506 and 27.3429 grams of n-propanol feed per hour, all at 80 °F. The calibration of the micro-feeder is shown in Appendix I.

2. Vaporization System

The vaporizer was fabricated from a 1 meter length of 1/16 inch O.D. type 316 stainless steel tubing turned into spirals of 3 cm diameter. The vaporizer was heated by immersing it in an oil bath. The oil used was mineral oil. The oil was heated by a 1000 watt calrod heater placed as a helical coil on the inside wall of the 12 cm diameter, 30 cm high vessel containing the oil and the vaporizer. A schematic cross-section of this system showing the location of the vaporizer in the oil bath is given in Figure III-1. The oil bath was lifted and lowered by a pneumatic lift which simplified the handling of the oil bath. The container was surrounded by 5 cm thickness of asbestos insulation. The bath was also equipped with a stirrer, driven by a three-speed electric motor. The oil temperature was measured by a ceramic-insulated, metal-sheathed 1/16 inch O.D. iron-constantan thermocouple, purchased from Thermo Electric Company (Catalog No. 5J0411E). The oil temperature was controlled by a R7161J Versatronik SCR Trigger Controller with Digital Setpoint, purchased from Honeywell. Good

[illegible]

[illegible]

[illegible]

[illegible]

temperature control was obtained with this apparatus and the bath temperature did not fluctuate more than 1°C when n-propanol was fed at the above feed rates.

The outlet line was made of 25 cm length of ¼ inch stainless steel tubing with a 12/5 female metal ball-socket joint at the end.

3. Reaction System

The reactor was fabricated from Pyrex glass. Figure III-2 shows a vertical cross section of the reactor giving dimensions and construction details. The inlet of the reactor was jointed to the outlet of the vaporizer by a 12/5 male glass ball-socket joint. After this joint, the reactant and the product flow lines were all made of Pyrex glass. The upper dead volumes within the reactor above the inlet and the outlet were decreased by placing the Pyrex glass tubes inside the reactor (See Figure III-2). The thermocouples were located inside these tubes to prevent the reactant and products from contacting the stainless steel of the thermocouple (See Figure III-2). Three thermocouples were used to measure the inlet, the reactor bed, and the outlet temperatures.

The reactor was heated by a eutectic composition salt bath, i.e. a salt composed of 50 wt % Sodium Nitrate and 50 wt % Potassium Nitrate, which melts at

approximately 120°C. The salt was heated by a 2500 watt calrod heater placed as a helical coil on the inside wall of the 13.5 cm diameter, 35 cm high vessel containing the salt and the reactor. A schematic cross section of this system showing the location of the reactor in the salt bath is given in Figure III-1. The salt bath was lifted and lowered by the pneumatic lift. The container was surrounded by 5 cm of asbestos insulation. The bath was also equipped with a stirrer driven by a three-speed electric motor.

The temperature in the salt bath was controlled by a Foxboro Model 64100 FO temperature recorder-controller. A Foxboro type 693 EMF converter equipped with a ¼ inch iron-constantan thermocouple supplied the input to the controller which regulated the current to the calrod heater. Excellent temperature control was obtained in this way and the bath temperature did not fluctuate more than 0.5°C once a steady temperature in the bath was obtained. The temperature range over which the controller will regulate the temperature depends on the range unit in the EMF converter. A 300° to 500°C range unit was sufficient for the present program.

The thermocouples used for measuring the temperature inside the reactor were ceramic-insulated, metal-sheathed 1/16 inch O.D., iron-constantan thermocouples, purchased

from Thermo Electric Company (Catalogue No. 5JO411E).

The pressure difference between the system and atmospheric pressure was measured by a manometer placed before the wet-test meter. It was always found to be negligible (See Appendix VII).

4. Temperature Recording

The three thermocouples from the reactor were connected to a Speedomax Type G Leeds and Northrup' 12 point variable range variable zero temperature recorder. The time required to complete the 12 point cycle was 48 seconds. The range, normally set on this recorder, was checked and adjusted prior to every experimental run by feeding voltages into the recorder from a potentiometer, equivalent to those produced by an iron-constantan thermocouple at 300°C and at 500°C. An ice-water cold junction was used for all thermocouples other than the one attached to the temperature controller, since the controller was equipped with a cold junction compensator.

5. Sampling System

To prevent condensation of the vapor products in the line between the reaction system exit and the condenser, asbestos tapes were wrapped around this line. During start-up and shut-down, the products were vented through the 3-way stopcock located after the condenser. At steady state, defined by constant temperature and

constant feed-rate, the products were passed through an ice-cooled water condenser and then into a cold trap. The cold trap was immersed in an ice-water mixture. The trap was built so that it could easily be removed from the rest of the apparatus and weighed without having to transfer the liquid from the container, thereby avoiding any loss of liquid product.

The noncondensable gases passed from the cold trap to a 250 cc gas sampling tube and then to the wet-test meter. All of the gas volume inside the sampling system from the inlet of the condenser to the outlet of the wet-test meter was replaced by helium gas before start-up. This operation increased the accuracy of the analysis by gas phase chromatography. The wet-test meter used was of Precision make with a 0.1 cu. ft. capacity per revolution. The accuracy of the wet-test meter at flow rates of 0.00 to 0.01 cu. ft. per hour was checked and found to be within ±6% of the actual gas flow (See Appendix VIII).

B. Operation of Equipment

A detailed discussion of the start-up, sampling, material feeding, and shut-down phases of the operation follows.

1. Start-up

The calrod heater and temperature controller of the oil bath were switched on after immersing the vaporizer in the oil bath. Approximately one hour of heating time was required to achieve the set temperature, 120°C.

The reactor was immersed in the salt bath after the salt temperature reached 300°C, the salt being melted completely. A proportional band setting of 20% with a 3 minute reset was then used on the automatic temperature controller to give a minimum of cycling or overshooting. Approximately three hours of heating time was required to achieve and hold the set temperature in the bath. Once steady state temperature conditions in the reactor and vaporizer were obtained, the experimental test and sampling commenced.

2. Sampling

After the air in the sampling system was replaced by helium gas for twenty minutes, the n-propanol feed was started. Steady state temperature conditions were regained in thirty minutes after the n-propanol feed was started. The products obtained during this period were discarded by venting through the 3-way stopcock located after the condenser. The water-ice cold trap was installed and ice-cooled water was circulated through the condenser. The sampling was started by diverting the product flow with the 3-way stopcock. The sampling time was recorded by

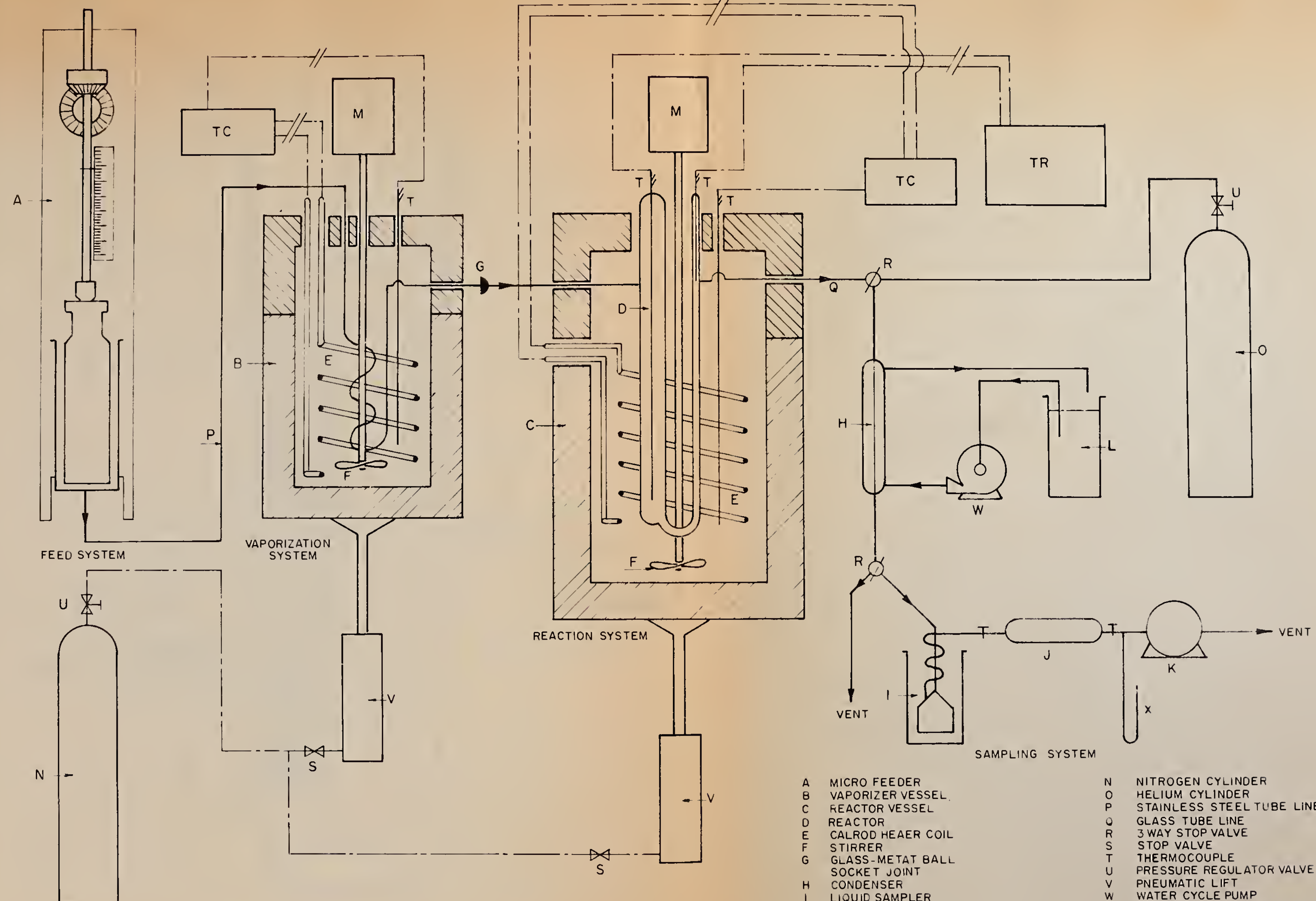

A	MICRO FEEDER	N	NITROGEN CYLINDER
B	VAPORIZER VESSEL	O	HELIUM CYLINDER
C	REACTOR VESSEL	P	STAINLESS STEEL TUBE LINE
D	REACTOR	Q	GLASS TUBE LINE
E	CALROD HEAER COIL	R	3 WAY STOP VALVE
F	STIRRER	S	STOP VALVE
G	GLASS-METAT BALL SOCKET JOINT	T	THERMOCOUPLE
H	CONDENSER	U	PRESSURE REGULATOR VALVE
I	LIQUID SAMPLER	V	PNEUMATIC LIFT
J	GAS SAMPLER	W	WATER CYCLE PUMP
K	WET TEST METER	X	MANOMETER
L	ICE WATER	TC	TEMPERATURE CONTROLER
M	MOTOR	TR	TEMPERATURE RECORDER

FIGURE III-1 SCHEMATIC LAYOUT OF EQUIPMENT

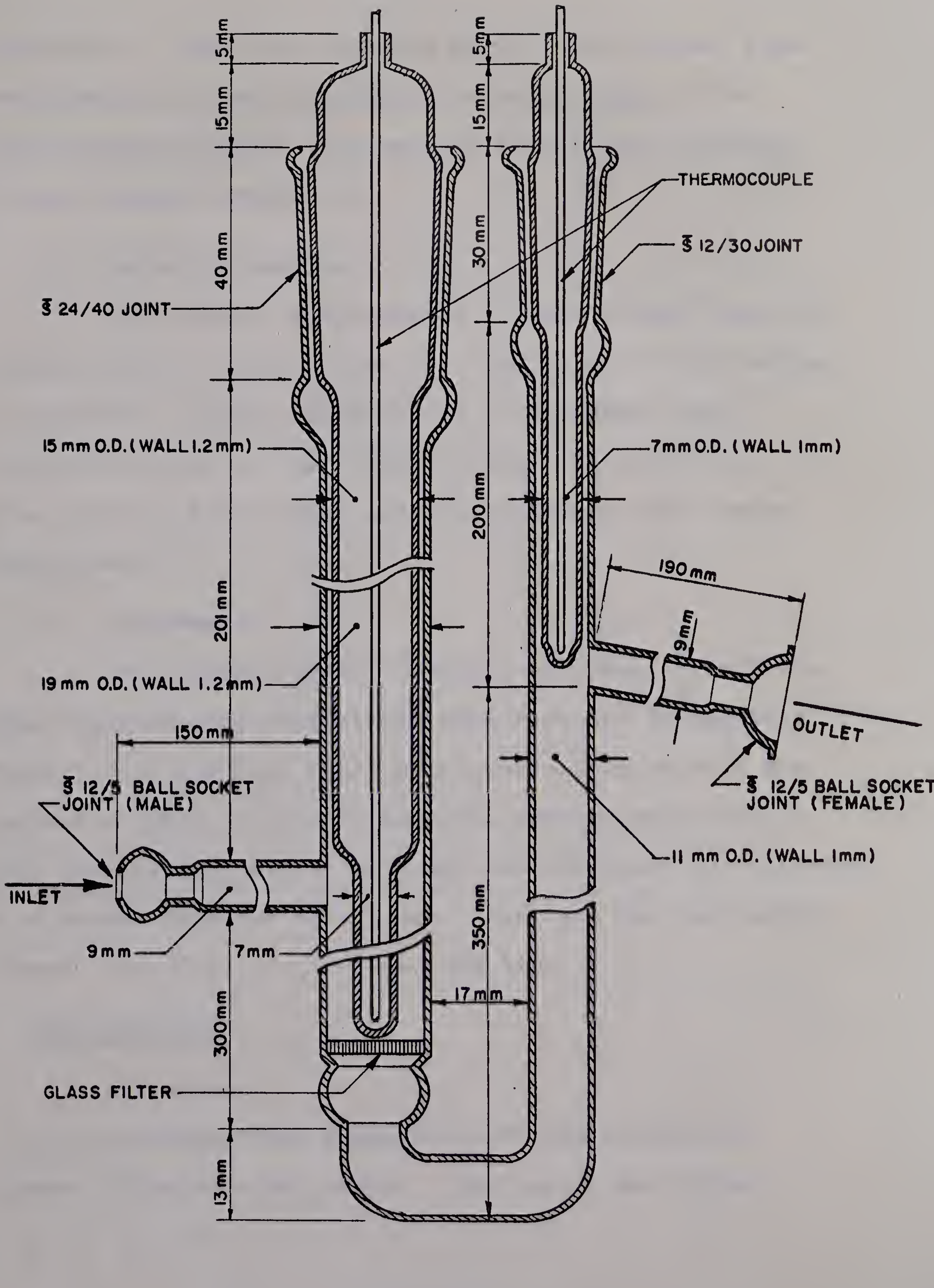

FIGURE III-2 CROSS-SECTION OF REACTOR SCALE 1/1

stop-watch. After the sampling period, the product flow was changed to vent through the 3-way stopcock. The liquid product sample obtained was sealed with stoppers and was weighed immediately.

3. Material Feeding

The reactor was designed so that solids could be loaded into the reactor from the side inlet of the reactor, if required. Either glass pieces or stainless steel pieces were used in this test program. This could be done within a few minutes without disturbing the steady conditions.

4. Shut-down

The liquid feeder, heaters, stirrers, circulation pump, recorders and controllers were shut off in sequence. The oil bath and salt bath vessels were lowered with the pneumatic lifts. The salt bath was lowered while the salt was melting, since the glass reactor might be destroyed by a stress when the salt froze. Nitrogen gas was passed through the flow line to clean the line.

C. Raw Material

1. n-Propanol

n-Propanol was supplied by Fisher Scientific Company (Catalogue No. A-414). The purity was higher

than 99.97% by the peak area % of gas phase chromatography analysis by using Ucon-chromosorb column (See chapter III-D-1). Traces of aldehydes, such as acetaldehyde and propionaldehyde, methyl ethyl ketone, and some unknown higher compounds were included in the n-propanol. These traces of impurities were detected in the gas phase chromatography analysis. Physical properties (22) of n-propanol are shown as follows.

Molecular Weight	60.09	
Boiling Point	97.8	°C
Specific Gravity	0.804 20/4	
Density at 80°F	0.767*	gm/cc

* The value calculated by author (See Appendix IX).

2. Stainless Steel Packing

Stainless steel packing was made of type 316 stainless steel screen (500 mesh). The size of the packing piece was approximately 3 x 3 mm.

The packing was washed with acetone and dried before it was used.

The properties of type 316 stainless steel packing are shown as follows.

Surface Area*	1.3	sq m/gm
Density (33)	0.29	lb/cu in

* measured by SORPTOMAT

Composition (33)

Chromium	18	%	
Nickel	11	%	
Molybdenum	25	%	
Carbon	0.10	%	maximum
Iron	balance		

3. Pyrex Glass Packing

Pyrex Glass packing was provided by crushing Pyrex Glass tubing of which quality is the same as that of the reactor. The packing was washed with acetone, aqueous HCl solution, aqueous NaOH solution, and water before it was used.

Properties of Pyrex Glass packing are shown as follows.

Size	-10 + 20	mesh fraction
Surface Area*	0.3	sq m /gm
Density (23)	2.23	gm /cc
Thermal Conductivity (23) at 25°C	0.0023	cal/(sec)(sq cm)(°C/cm)
Mean Specific Heat (23) 25°C - 175°C	0.20	cal/(gm)(°C)
Composition (23)		
Silica	80	%
Boric Oxide	14	%
Soda	4	%
Alumina	2	%

* measured by SORPTOMAT

D. Analysis of Product

1. Liquid Products

The components of the liquid phase product were separated by gas-liquid chromatography using a Beckman Model G.C.-4. The chromatogram peak areas of the components were integrated by using an Aerograph Model 471 Digital Integrator manufactured by Infotronics Corporation. The following is a description of the type of column used and the operating conditions under which the liquid analysis was carried out.

Column: 1/8 inch diameter, 35 feet, copper tubing packed with 30% Ucon on acid washed Chromosorb W (-80+100 mesh). The Ucon, designated as Ucon Lubricant LB-1800X, was supplied by the Union Carbide Chemical Company.

Column Temperature:

100°C for lower molecule components and 150°C for higher molecule components than n-propanol were used.

Detector Temperature:	250°C
Detector Current:	200mA
Sample Size:	2 microliters
Carrier and Reference Gas:	Helium
Gas Flow Rate:	Carrier side 20 cc/min
	Reference side 20 cc/min

The products which were separated in the course of this work and which were identified under the above conditions included: ethane, propylene plus propane, acetaldehyde, propionaldehyde, methyl ethyl ketone, n-propanol, acetaldehyde dipropyl acetal, propionaldehyde dipropyl acetal. Propane, propylene, acetaldehyde, propionaldehyde, methyl ethyl ketone and n-propanol were identified by using chromatographic retention times (See Appendix III). Vasudeva (24), Wanke (1), or Anderson (25) also identified these components using chromatographic retention times by Ucon-celite column, infrared spectroscopy, and/or nuclear magnetic resonance. Ethane, carbon dioxide, and ethylene appeared at the same retention time using the Ucon column. It was found, however, that carbon dioxide and ethylene were not present in the product. Gas chromatographic analysis using a silica gel column which could separate ethane from ethylene and carbon dioxide was used in this test. Acetaldehyde dipropyl acetal and propionaldehyde dipropyl acetal were identified in the corresponding fractions which were collected in chromatographic analyses by analyses with infrared spectroscopy, mass spectroscopy and nuclear magnetic resonance. The typical chromatographic charts are shown in Appendix III. Relative thermal conductivity responses were used to calculate the mole per

cent of the components in the products. Relative thermal conductivity responses are shown in Appendix IV.

2. Gaseous Products

Three separate columns were required to analyse the gas product sample. The following is a description of the columns, the operating conditions used, and the products analysed with each column.

a) Column: 30% Ucon on chromosorb W (same as for liquid product)

Column Temperature: 70°C

Detector Temperature: 150°C

Detector Current: 200mA

Carrier and Reference Gas: Helium

Gas Flow Rate: Carrier side 20 cc/min
Reference side 20 cc/min

The products separated under the above conditions were ethane and propane plus propylene.

b) Column: 1/8 inch diameter, 15 feet long, copper tubing packed with high activity charcoal. The charcoal was supplied by the Burrell Corporation (Catalogue No. 341-10).

Column Temperature: 90°C

Detector Temperature:	150°C
Detector Current:	200mA
Carrier and Reference Gas:	Helium
Gas Flow Rate:	Carrier side 20 cc/min
	Reference side 20 cc/min

The products separated under the above conditions were hydrogen, carbon monoxide, and methane.

c) Column:	¼ inch diameter, 25 feet long, copper tubing packed with silica gel containing 3% di-n-decyl phthalate purchased from Eastman Organic Chemicals.
Column Temperature:	130°C
Detector Temperature:	200°C
Detector Current:	200mA
Carrier and Reference Gas:	Helium
Gas Flow Rate:	Carrier side 30 cc/min
	Reference side 30 cc/min

The products separated under the above conditions were ethane, ethylene, propane and propylene.

The products were identified by their respective retention times, verified by passing pure samples of the gas involved through the appropriate column. For

quantitative analysis, a calibration chart of peak area versus mole per cent was prepared for hydrogen (See Appendix II). Quantitative analyses of methane, carbon monoxide, and ethane were done by passing the pure gases and taking the peak area ratios of product gases to the pure gases.

It was verified that the product gas included propane and propylene. Quantitative analysis was not done for these individual gases, since their amounts present were too small to analyse separately. Only the sum of propane and propylene was determined using the relative thermal conductivity response of propylene.

IV. EXPERIMENTAL PROGRAM AND RESULTS

The present investigation was carried out at approximately 705 mm Hg and at temperatures up to 463°C with the following objectives:

1. to investigate the thermal decomposition of n-propanol;
2. to investigate the influence of Pyrex Glass, if any, upon the thermal decomposition of n-propanol;
3. to investigate the effects of stainless steel 316 surfaces in catalyzing reactions of n-propanol or on the thermal decomposition of n-propanol.

The latter materials were of interest because of their frequent use in constructing experimental reactors.

A. Definition of Terms

1. Space Velocity

The term space velocity as used in the present investigation is defined in the following ways:

a) homogeneous thermal decomposition of n-propanol:

$$\text{Space Velocity } [\text{sec}^{-1}] = \frac{\left\{\begin{matrix}\text{Volume of n-propanol feed at } 0°\text{C} \\ \text{and 760 mm Hg as gas [cc/sec]}\end{matrix}\right\}}{\text{Volume of reactor [cc]}} \tag{16}$$

b) thermal decomposition of n-propanol in the

presence of Pyrex Glass packing:

$$\text{Space Velocity } [\text{mole.hr}^{-1}\ .\text{gm}^{-1}] = \frac{\text{gm-moles of n-propanol feed } [\text{mole/hr}]}{\text{grams of Pyrex Glass } [\text{gm}]} \tag{17}$$

c) thermal decomposition of n-propanol in the presence of 316 stainless steel packing:

$$\text{Space Velocity } [\text{mole.hr}^{-1}\ .\text{gm}^{-1}] = \frac{\text{gm-moles of n-propanol feed } [\text{mole/hr}]}{\text{grams of 316 stainless steel } [\text{gm}]} \tag{18}$$

2. Space Time

The term, space time, when used with tubular homogeneous or heterogeneous reactors is defined as

$$\text{Space time } [\text{sec}] = \frac{1}{\text{Space Velocity } [\text{sec}^{-1}]} \tag{19}$$

3. Residence Time

The term, residence time, cannot be measured accurately and is used in an arbitrary manner mainly in the case of homogeneous thermal decomposition of n-propanol. In this investigation, the n-propanol conversion is so small that the residence time will be defined in the following way.

Residence Time [sec] =

$$\frac{\text{Volume of reactor [cc]}}{\text{Volume of n-propanol feed at the reaction conditions [cc/sec]}} \qquad (20)$$

4. n-Propanol Conversion

The term n-propanol conversion is defined as

n-Propanol Conversion [mole %] =

$$= 100 - \frac{\text{moles of n-propanol in the product}}{\text{moles of n-propanol in the feed}} \times 100 \qquad (21)$$

5. Material Accountability

Material accountability was used as a measure of the reliability of chemical analysis in accounting for the products. Carbon, hydrogen, and oxygen accountabilities were obtained by calculating the corresponding material balances.

Carbon Accountability [%] =

$$\frac{\text{[g-atoms] of carbon in analyzed products per mole of n-propanol feed}}{\text{[g-atoms] of carbon per mole of n-propanol feed}} \times 100 \qquad (22)$$

Similar definitions applied to the hydrogen and oxygen cases.

B. <u>The Thermal Decomposition of n-Propanol</u>

Twenty runs were performed to investigate the effects of the reaction temperatures and the residence times upon the thermal stability of the n-propanol molecule.

1. The Effect of Reaction Temperature

The reaction was studied at bath temperatures of 380°, 400°, 420°

440° and 463°C. The temperature difference between the salt bath and the reactor bed is less than 3°C for the worst case (See Appendix VII). Four runs with different residence times were performed at each reaction temperature. The experimental results are shown in Tables IV-1 to IV-4 and in Figures IV-6 to IV-13. The curves of n-propanol in Figures IV-6 to IV-13 show the n-propanol conversions.

2. The Effect of Residence Time

The residence times studied were approximately 10, 20, 30 and 40 sec at each of the four reaction temperatures. The experimental results are shown in Tables IV-1 to IV-4 and in Figures IV-1 to IV-5. The curves of n-propanol in Figures IV-1 to IV-5 show the n-propanol conversions.

3. The Effects of Residence Time and Temperature on n-Propanol Conversion

The n-propanol conversion is influenced by the residence time and the reaction temperatures. Figure IV-14 shows the n-propanol conversion curves versus the residence time and the reaction temperature. The values of the n-propanol conversions in Figure IV-14 were read from Figures IV-1 to IV-13.

4. Initial Reaction Rate and Activation Energy

Table IV-7 gives the initial rates of n-propanol decomposition versus the reciprocal of temperature calculated from Figures IV-1 to IV-5. These values are plotted on semi-logarithmic coordinates as shown in Figure IV-17.

The initial rate of n-propanol decomposition is given by

$$Y_o = -\left(\frac{d[\text{n-propanol}]}{dt}\right)_{t=o} \tag{23}$$

Figure IV-17 shows that the apparent overall activation energies are definitely different between the higher and lower temperature regions. In the higher temperature region, from line A in Figure IV-17, the activation energy is 35 Kcal. On the other hand, in the lower temperature region, the activation energy is 8 Kcal. The difference in the activation energy may be caused by the difference in the reaction mechanism. This will be discussed later on.

C. The Effect of Pyrex Glass on the Termal Decomposition of n-Propanol

The effect of Pyrex Glass was investigated at a constant temperature, 463°C, and approximately the same n-propanol feed rate, 0.24 moles/ hr, by packing three different amounts of Pyrex Glass packing, 5, 10 and 15 grams. The experimental results from Runs 18, 21, 22 and 23 are shown in Table IV-5 and Figure IV-15. The space time shown in Table IV-5 was calculated as follows;

$$\text{Space Time [sec]} = \frac{\{(\text{The volume of reactor}) - (\text{The volume of Pyrex Glass packing})\}[\text{cc}]}{\text{The volume of n-propanol feed as gas at } 0^\circ\text{C and } 760 \text{ mm Hg}[\text{cc/sec}]} \tag{24}$$

D. Effect of Stainless Steel on Decomposition of n-Propanol

Runs 24, 25, 26, 27 and 28 were performed to investigate the effect of type 316 stainless steel on the thermal decomposition of n-

propanol. The reaction temperature was at 463°C and the weights of stainless steel which were packed into the reactor were 2, 4, 6, 10 and 15 grams. The experimental results are shown in Table IV-6 and Figure IV-16.

[illegible]

[illegible]

Table IV-1 Effects of Temperature and Reaction Residence Time on Product Distribution

No. of Run		1	2	3	4	5
Reaction Temp.	[°C]	380	380	380	380	400
Residence Time	[sec]	10.6	21.1	28.6	42.0	10.2
Space Time	[sec]	4.4	8.8	12.0	17.6	4.1
Product	[mole%]					
Hydrogen		0.0002	0.0004	0.0006	0.0009	0.0009
Carbon monoxide		0.0000	0.0006	0.0014	0.0065	0.0005
Methane		0.0039	0.0099	0.0147	0.0229	0.0049
Ethane		0.0109	0.0174	0.0204	0.0223	0.0138
Propane+Propylene		0.0038	0.0082	0.0122	0.0202	0.0060
Acetaldehyde		0.0138	0.0275	0.0367	0.0534	0.0178
Propionaldehyde		0.0207	0.0280	0.0294	0.0288	0.0368
n-Propanol		99.9468	99.9081	99.8848	99.8451	99.9204
Accountability	[%]					
Carbon		100.01	100.02	100.02	100.03	100.01
Hydrogen		100.00	100.01	100.01	100.02	100.00
Oxygen		100.00	100.00	100.00	100.01	100.00

Table IV-2 Effects of Temperature and Reaction Residence Time on Product Distribution

No. of Run		6	7	8	9	10
Reaction Temp.	[°C]	400	400	400	420	420
Residence Time	[sec]	20.5	26.9	41.9	10.1	20.2
Space Time	[sec]	8.3	10.9	17.0	4.0	8.0
Product	[mole%]					
Hydrogen		0.0025	0.0030	0.0045	0.0018	0.0053
Carbon monoxide		0.0013	0.0033	0.0148	0.0014	0.0047
Methane		0.0126	0.0178	0.0257	0.0123	0.0291
Ethane		0.0217	0.0238	0.0272	0.0193	0.0271
Propane+Propylene		0.0136	0.0194	0.0332	0.0097	0.0225
Acetaldehyde		0.0309	0.0375	0.0484	0.0284	0.0524
Propionaldehyde		0.0544	0.0713	0.1100	0.0282	0.0581
n-Propanol		99.8634	99.8241	99.7361	99.8990	99.8008
Accountability	[%]					
Carbon		100.03	100.03	100.05	100.02	100.04
Hydrogen		100.01	100.01	100.04	100.01	100.01
Oxygen		100.00	100.01	100.02	100.00	100.01

Table IV-3 Effects of Temperature and Reaction Residence Time on Product Distribution

No. of Run		11	12	13	14	15
Reaction Temp.	(°C)	420	420	440	440	440
Residence Time	(sec)	26.4	41.2	10.0	19.4	27.0
Space Time	(sec)	10.6	16.6	3.8	7.4	10.3
Product	(mole%)					
Hydrogen		0.0071	0.0100	0.0054	0.0114	0.0149
Carbon monoxide		0.0090	0.0242	0.0020	0.0074	0.0136
Methane		0.0397	0.0555	0.0281	0.0599	0.0781
Ethane		0.0317	0.0378	0.0241	0.0331	0.0441
Propane+Propylene		0.0316	0.0535	0.0157	0.0346	0.0483
Acetaldehyde		0.0661	0.0906	0.0579	0.0956	0.1290
Propionaldehyde		0.0765	0.1129	0.0265	0.0377	0.0420
n-Propanol		99.7384	99.6157	99.8403	99.7203	99.6301
Accountability	(%)					
Carbon		100.05	100.08	100.03	100.06	100.08
Hydrogen		100.02	100.03	100.02	100.04	100.05
Oxygen		100.01	100.03	100.01	100.02	100.03

Table IV-4 Effects of Temperature and Reaction Residence Time on Product Distribution

No. of Run		16	17	18	19	20
Reaction Temp.	(°C)	440	463	463	463	463
Residence Time	(sec)	37.6	9.5	19.0	26.3	38.0
Space Time	(sec)	14.4	3.5	7.5	9.8	14.1
Product	(mole%)					
Hydrogen		0.019	0.0127	0.0264	0.0388	0.0522
Carbon monoxide		0.0369	0.0032	0.0106	0.0186	0.0616
Methane		0.0996	0.0516	0.0884	0.1231	0.1568
Ethane		0.0559	0.0329	0.0568	0.0799	0.1046
Propane+Propylene		0.0809	0.0285	0.0592	0.0861	0.1524
Atcetaldehyde		0.1595	0.1165	0.1747	0.2138	0.2601
Propionaldehyde		0.0469	0.0352	0.0492	0.0582	0.0775
n-Propanol		99.5013	99.7195	99.5347	z9.3817	99.1349
Accountatility	(%)					
Carbon		100.12	100.05	100.10	100.14	100.22
Hydrogen		100.07	100.03	100.06	100.10	100.15
Oxygen		100.04	100.02	100.03	100.04	100.07

Table IV-5 Effects of Pyrex Glass on the Thermal Decomposition of n-Propanol

No. of Run		18	21	22	23
Pyrex Glass Added	[gm]	0	5	10	15
Reaction Temp.	[°C]	463	463	463	463
Space Time	[sec]	7.1	6.8	6.6	6.3
Product	[mole%]				
Hydrogen		0.0264	0.0257	0.0255	0.0218
Carbon monoxide		0.0106	0.0093	0.0085	0.0096
Methane		0.0884	0.0899	0.0882	0.0862
Ethane		0.0568	0.0564	0.0540	0.0522
Propane+Propylene		0.0592	0.0576	0.0586	0.0608
Acetaldehyde		0.1747	0.1735	0.1682	0.1655
Propionaldehyde		0.0492	0.0488	0.0458	0.0471
n-Propanol		99.5347	99.5388	99.5512	99.5568
Accountability	[%]				
Carbon		100.10	100.09	100.09	100.08
Hydrogen		100.06	100.06	100.06	100.06
Oxygen		100.03	100.03	100.03	100.02

Table IV-6 Effects of Stainless Steel on the Thermal Decomposition of n-Propanol

No. of Run		18	24	25	26	27	28
S.S.* Added	[gm]	0	2	4	6	10	15
Space Velocity	[moles/gm hr]	-	0.1135	0.0571	0.0372	0.0226	0.0151
Reaction Temp.	[°C]	463	463	463	463	463	463
Product	[mole%]						
Hydrogen		0.0264	0.0646	0.0899	0.1244	0.1489	0.1837
Carbon monoxide		0.0146	0.0078	0.0054	0.0048	0.0064	0.0058
Methane		0.0884	0.0833	0.0732	0.0565	0.0466	0.0326
Ethane		0.0568	0.0322	0.0308	0.0224	0.0225	0.0178
Propane+Propylene		0.0592	0.0562	0.0576	0.0498	0.0515	0.0397
Acetaldehyde		0.1747	0.1362	0.1233	0.1015	0.0854	0.0775
Propionaldehyde		0.0492	0.1055	0.1499	0.1689	0.2126	0.3441
n-Propanol		99.5347	99.5141	99.4519	99.4345	99.3584	99.2129
Acetaldehyde di-propyl acetal		0.0000	0.0000	0.0139	0.0168	0.0224	0.0153
Propionaldehyde di-propyl acetal		0.0000	0.0000	0.0042	0.0205	0.0456	0.0706

* 316 Stainless Steel Packing

Table IV-7

Effect of Temperature on Initial Rate for n-Propanol Decomposition

Temperature [°C]	$1/T[°K^{-1}]$ x 10^3	Rate [Moles/(Feed Moles)(sec)] x 10^4
380	1.5314	0.80
400	1.4859	0.98
420	1.4430	1.26
440	1.4025	1.95
463	1.3587	4.15

[illegible]

[illegible]

[illegible]

[illegible]

[illegible]	[illegible]	[illegible]
[illegible]	[illegible]	[illegible]
[illegible]	[illegible]	[illegible]
[illegible]	[illegible]	[illegible]
[illegible]	[illegible]	[illegible]
[illegible]	[illegible]	[illegible]

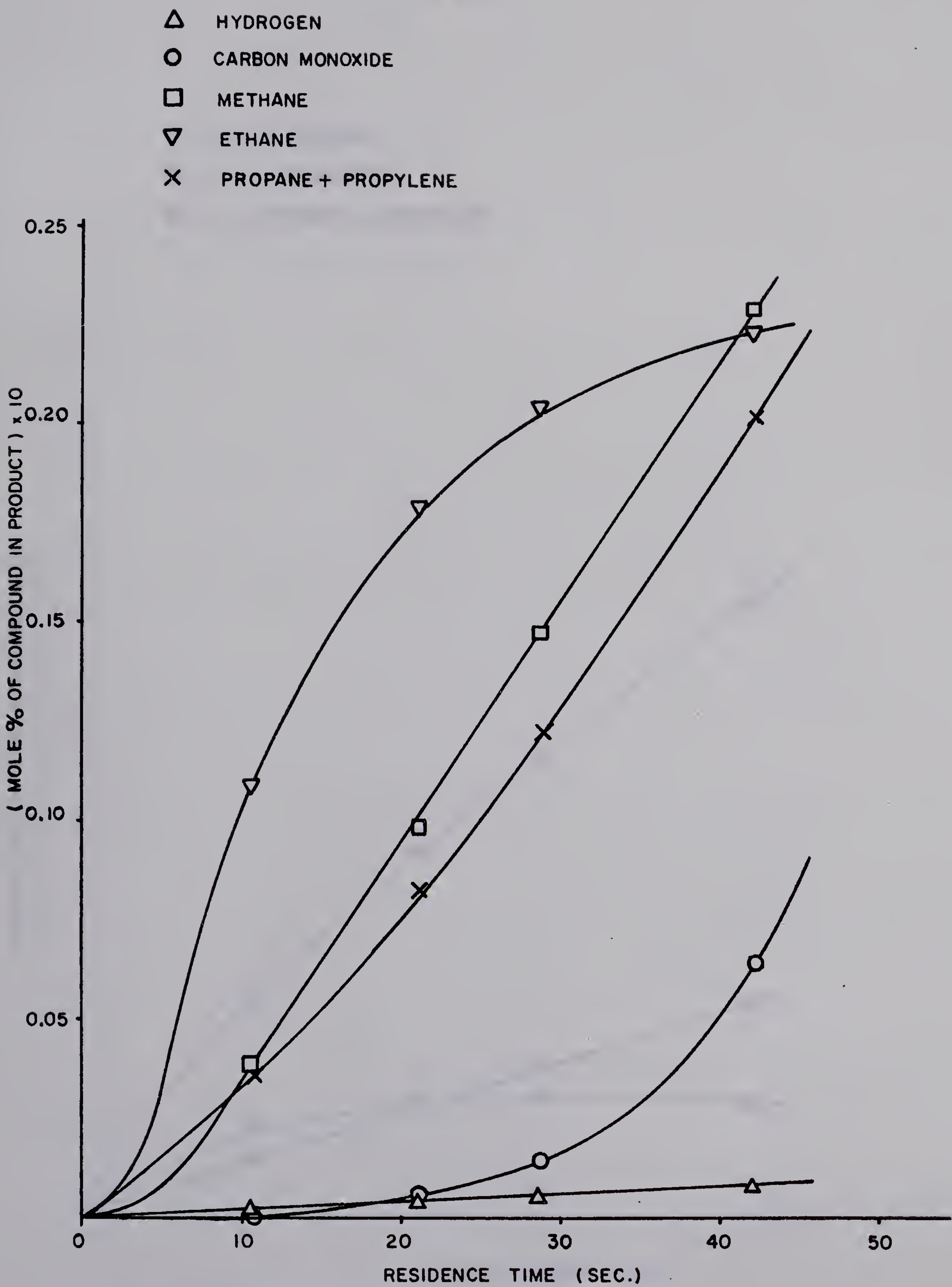

FIGURE IV-1-A: EFFECT OF RESIDENCE TIME ON THERMAL DECOMPOSITION OF n-PROPANOL AT 380°C

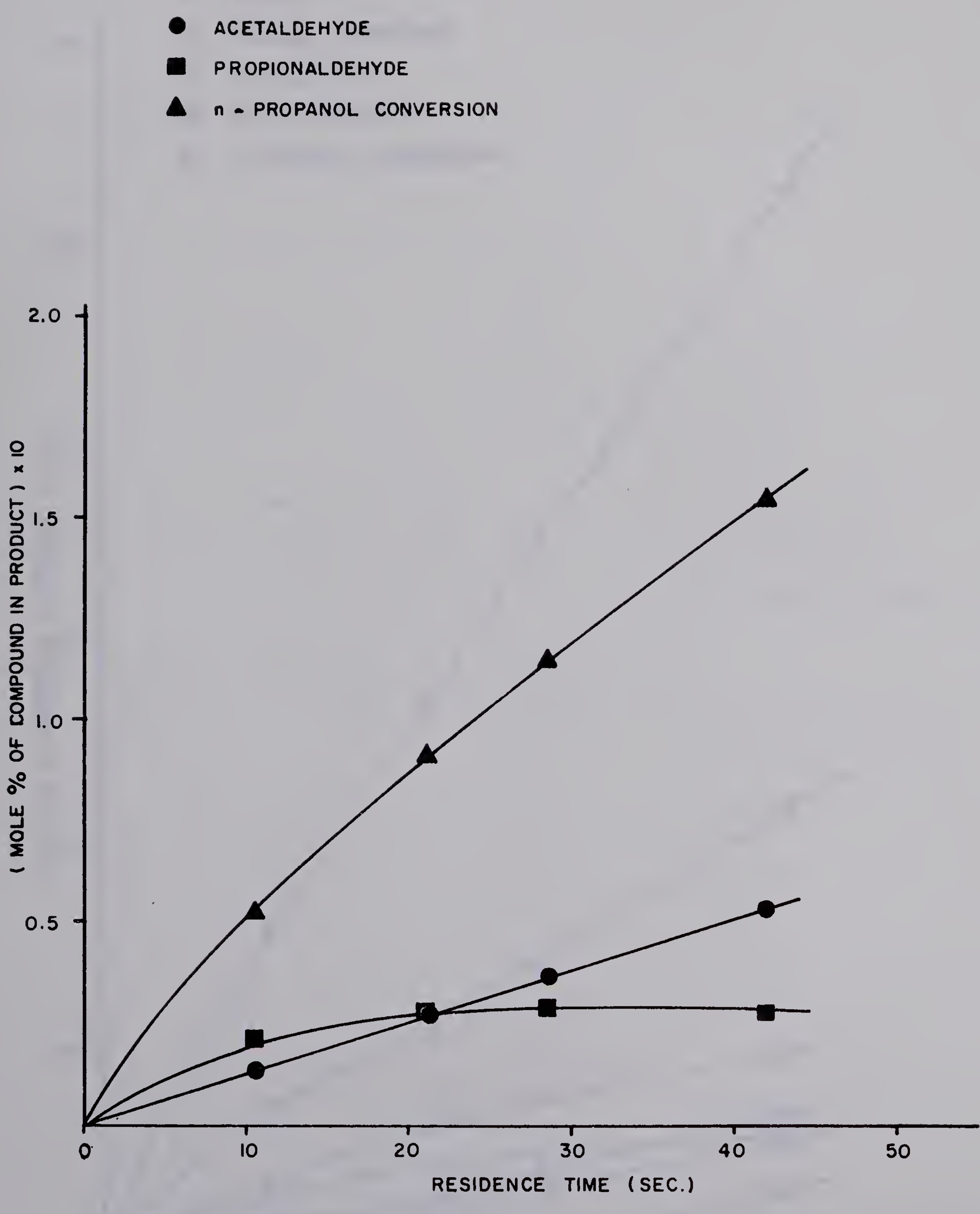

FIGURE IV-1-B: EFFECT OF RESIDENCE TIME ON THERMAL DECOMPOSITION OF n-PROPANOL AT 380°C

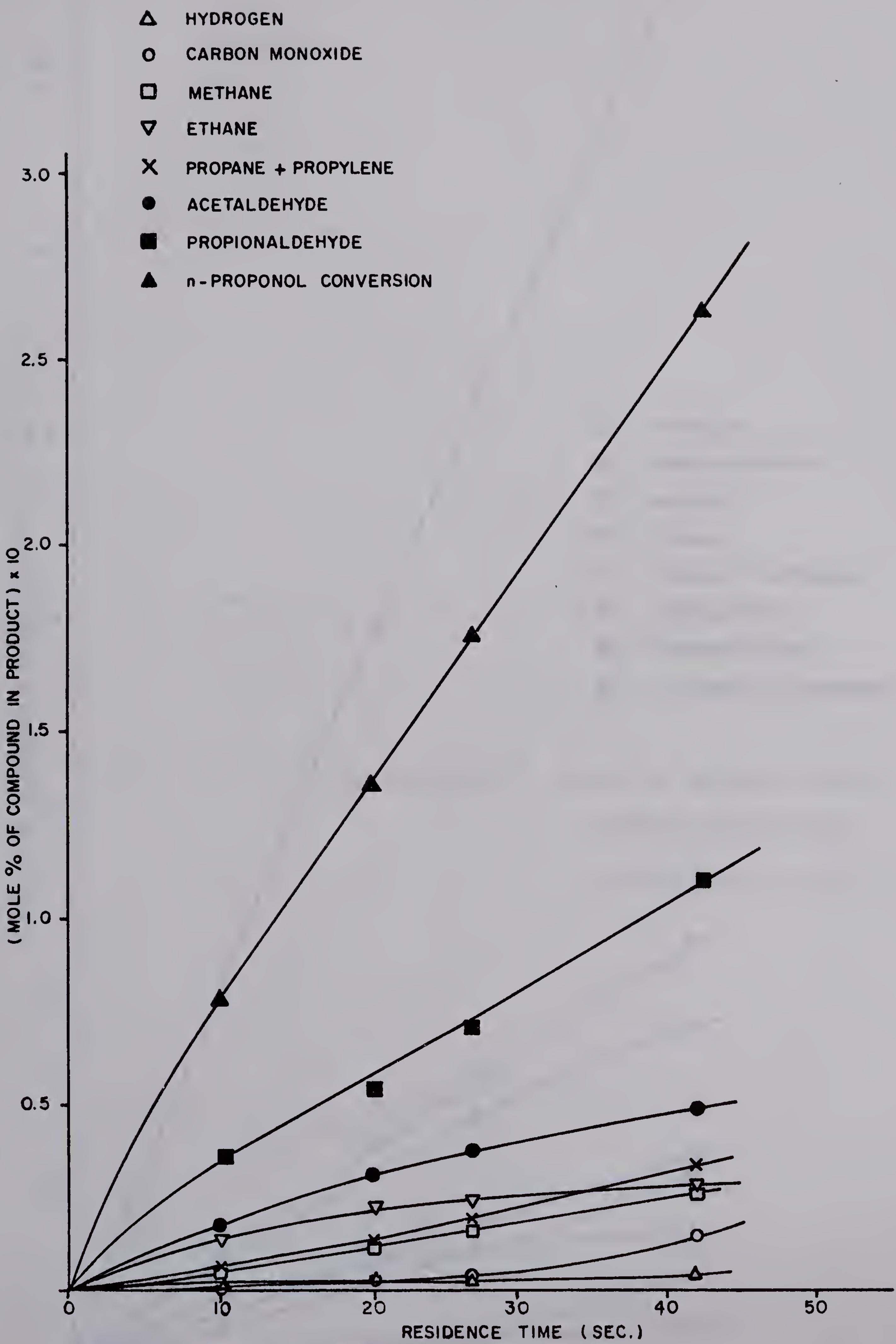

FIGURE IV-2: EFFECT OF RESIDENCE TIME ON THERMAL DECOMPOSITION OF n-PROPANOL AT 400°C

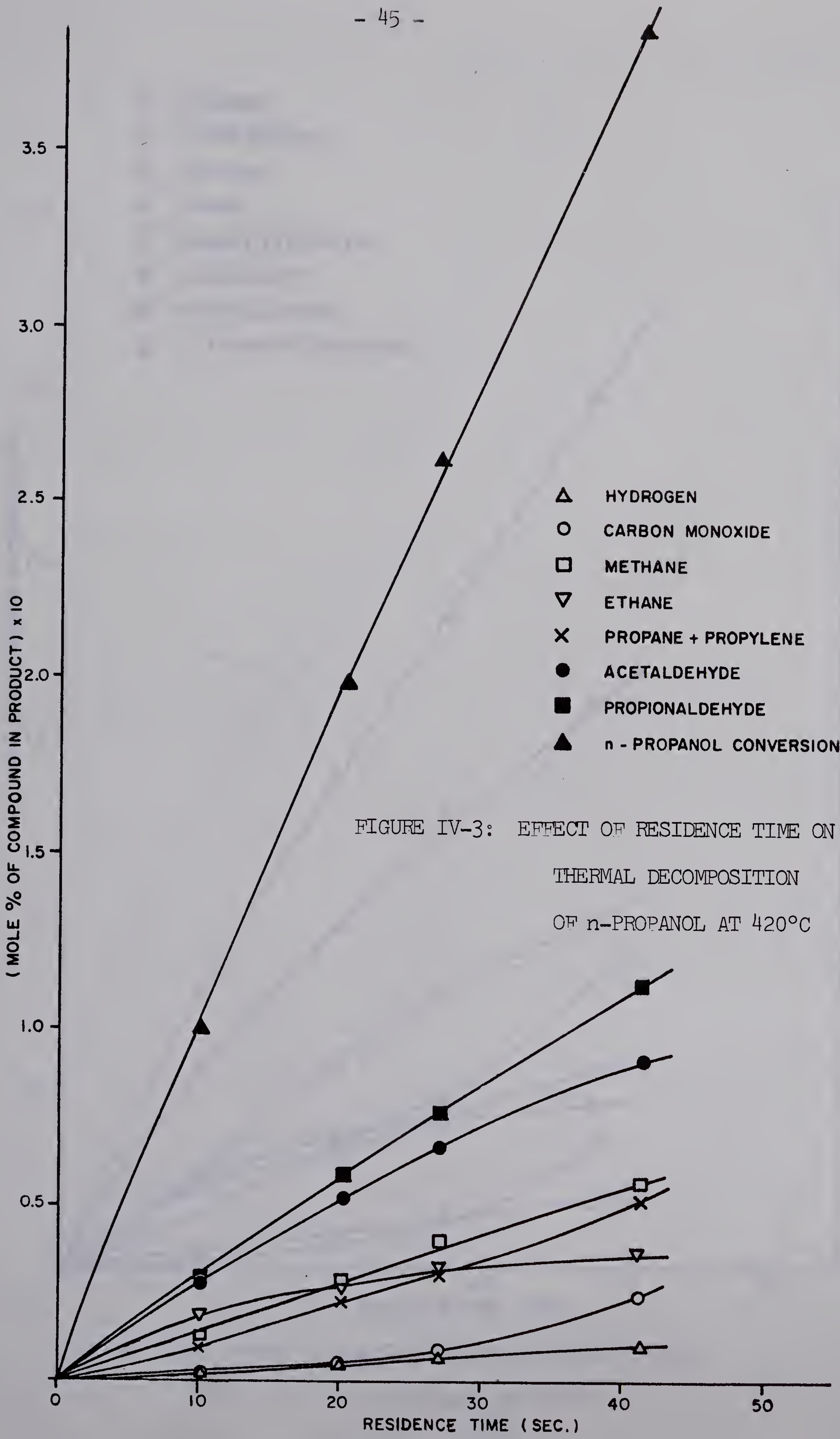

FIGURE IV-3: EFFECT OF RESIDENCE TIME ON THERMAL DECOMPOSITION OF n-PROPANOL AT 420°C

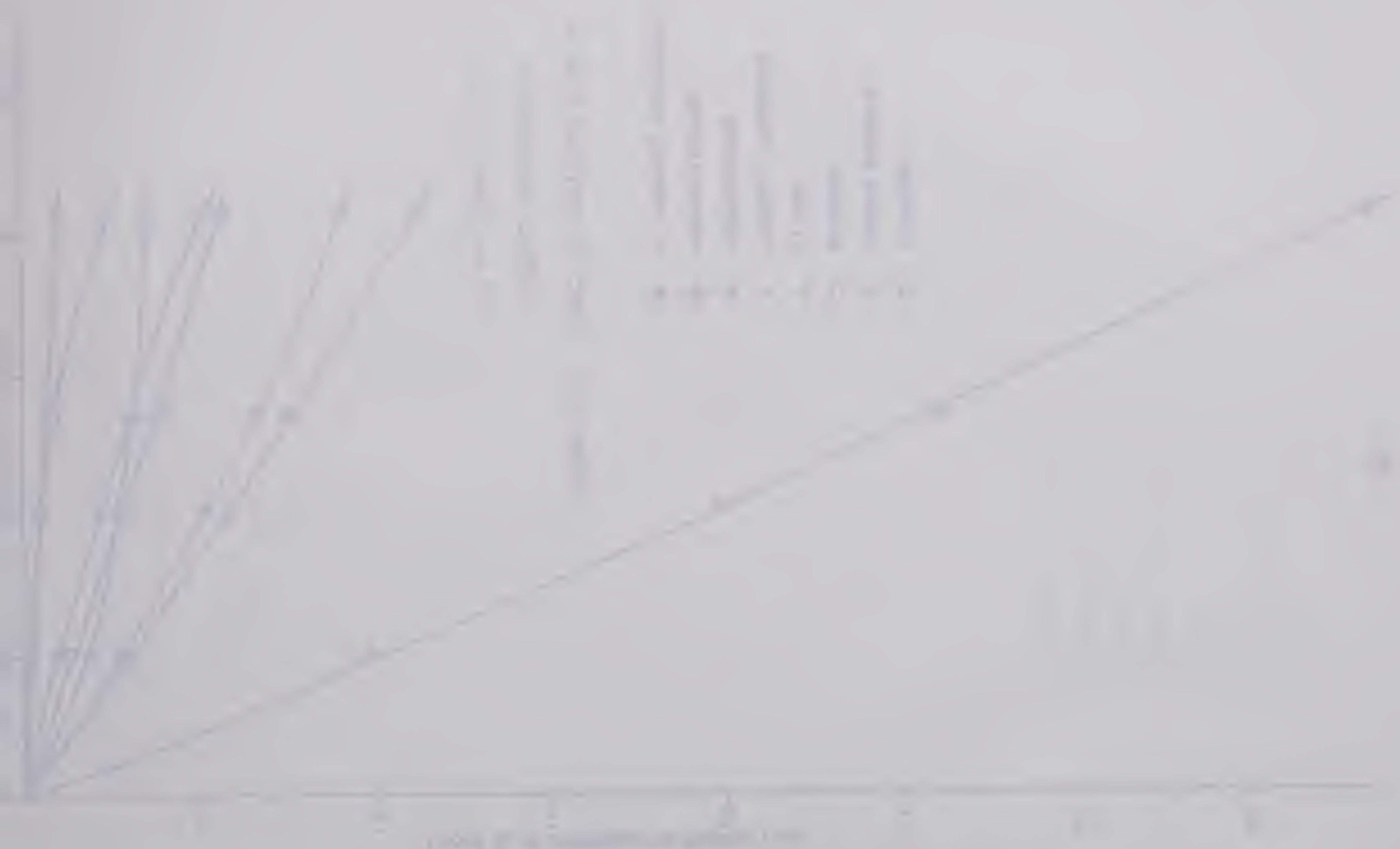

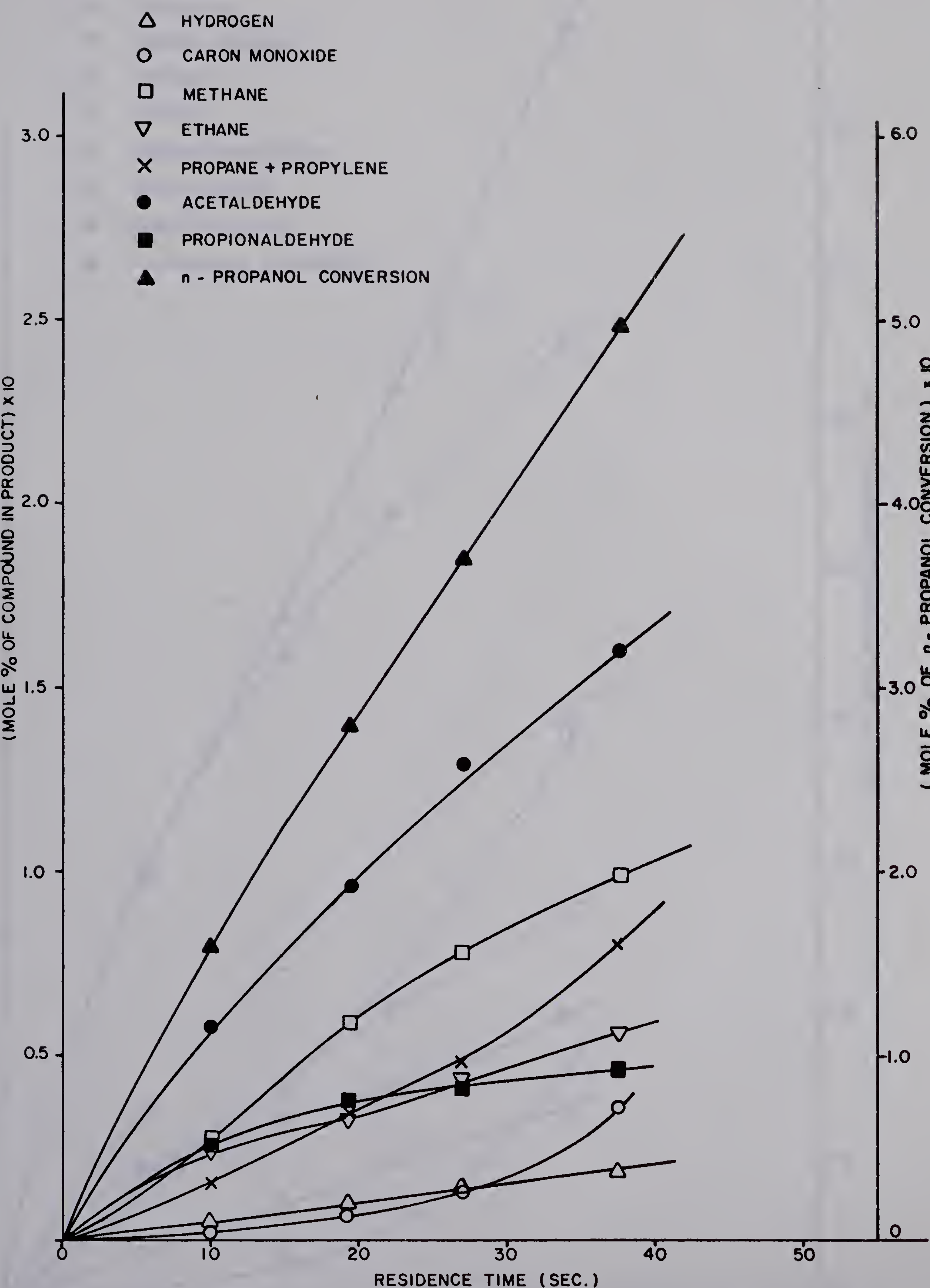

FIGURE IV-4: EFFECT OF RESIDENCE TIME ON DECOMPOSITION

OF n-PROPANOL AT 440°C

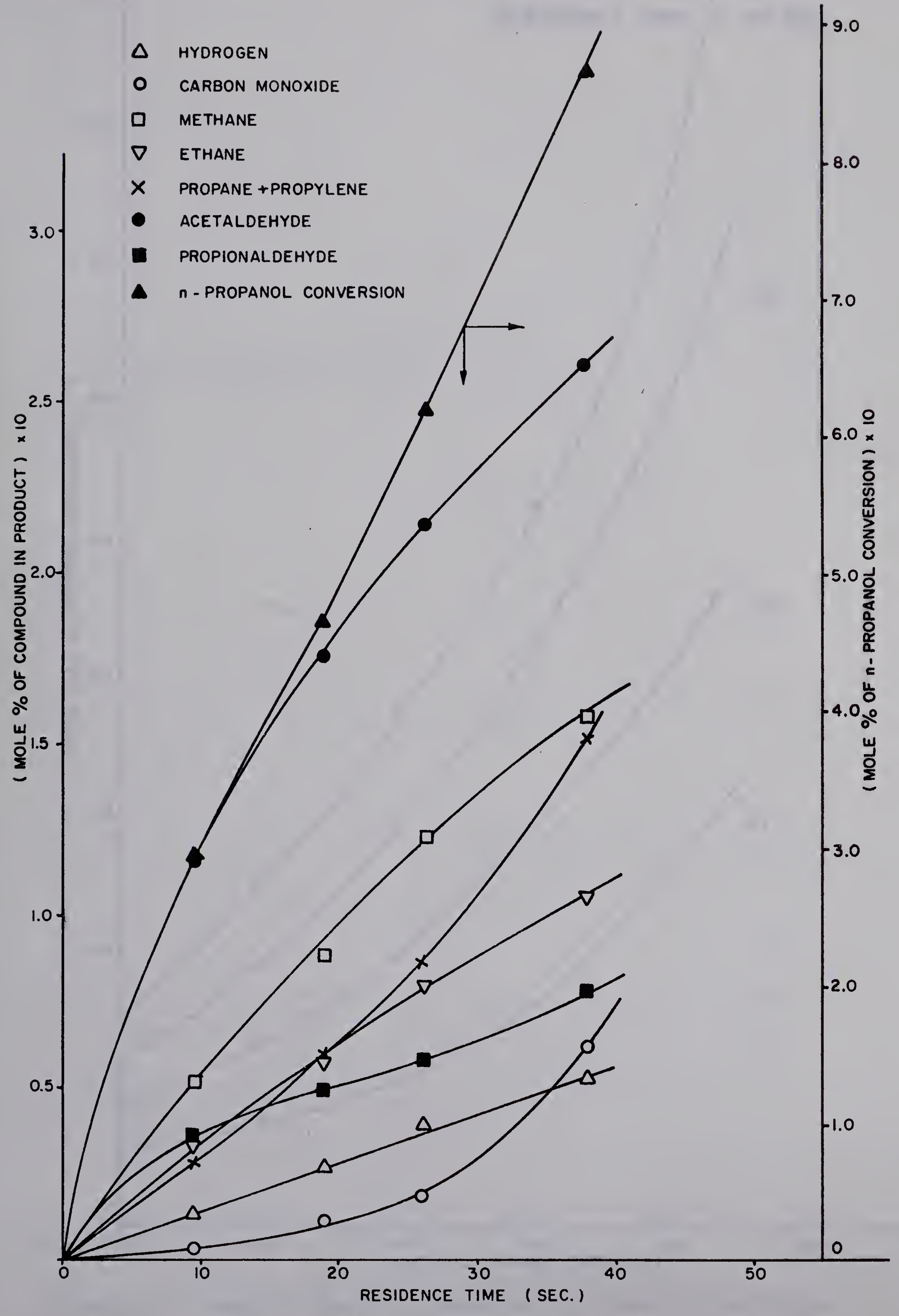

FIGURE IV-5: EFFECT OF RESIDENCE TIME ON THERMAL DECOMPOSITION OF n-PROPANOL AT 463°C

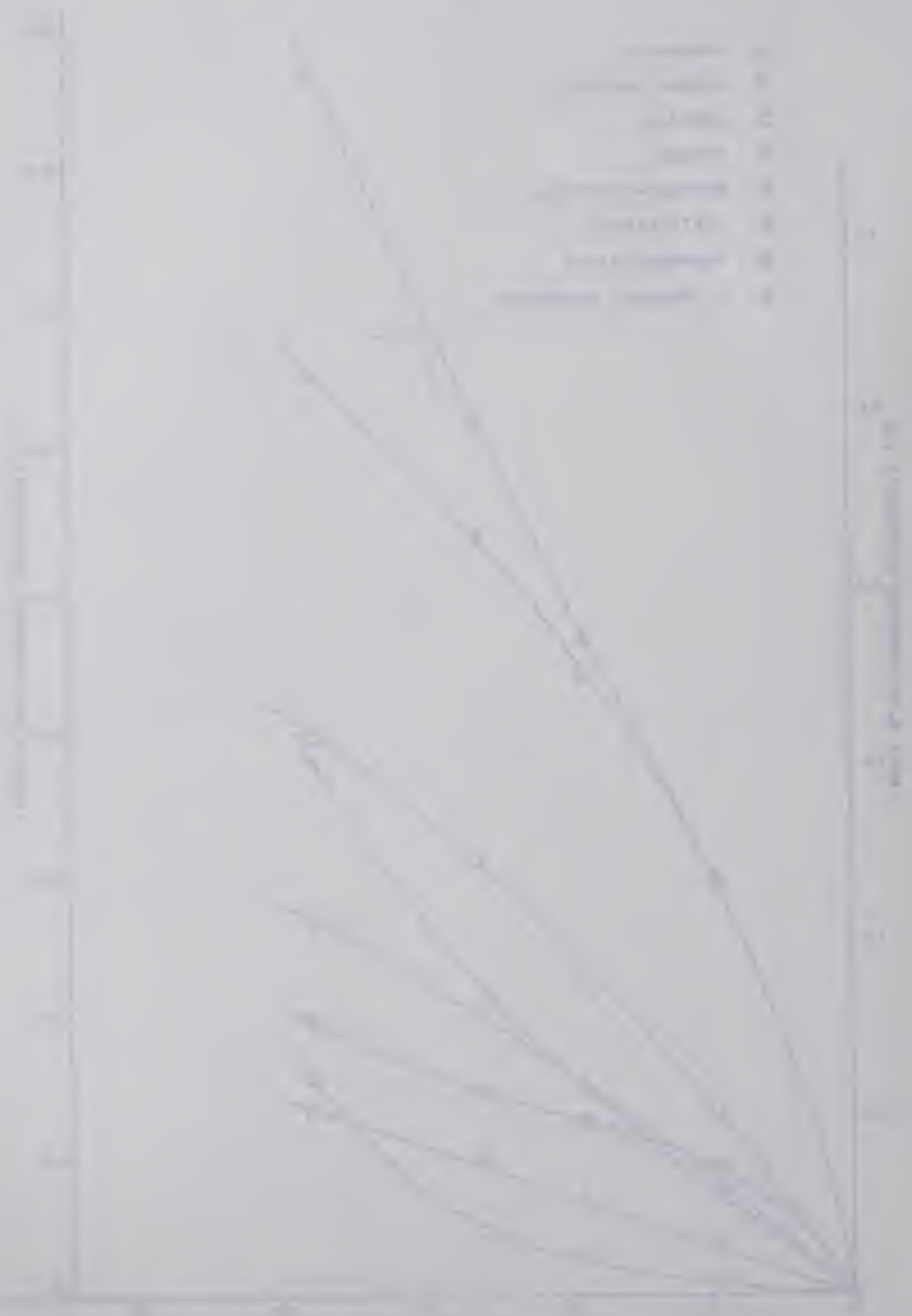

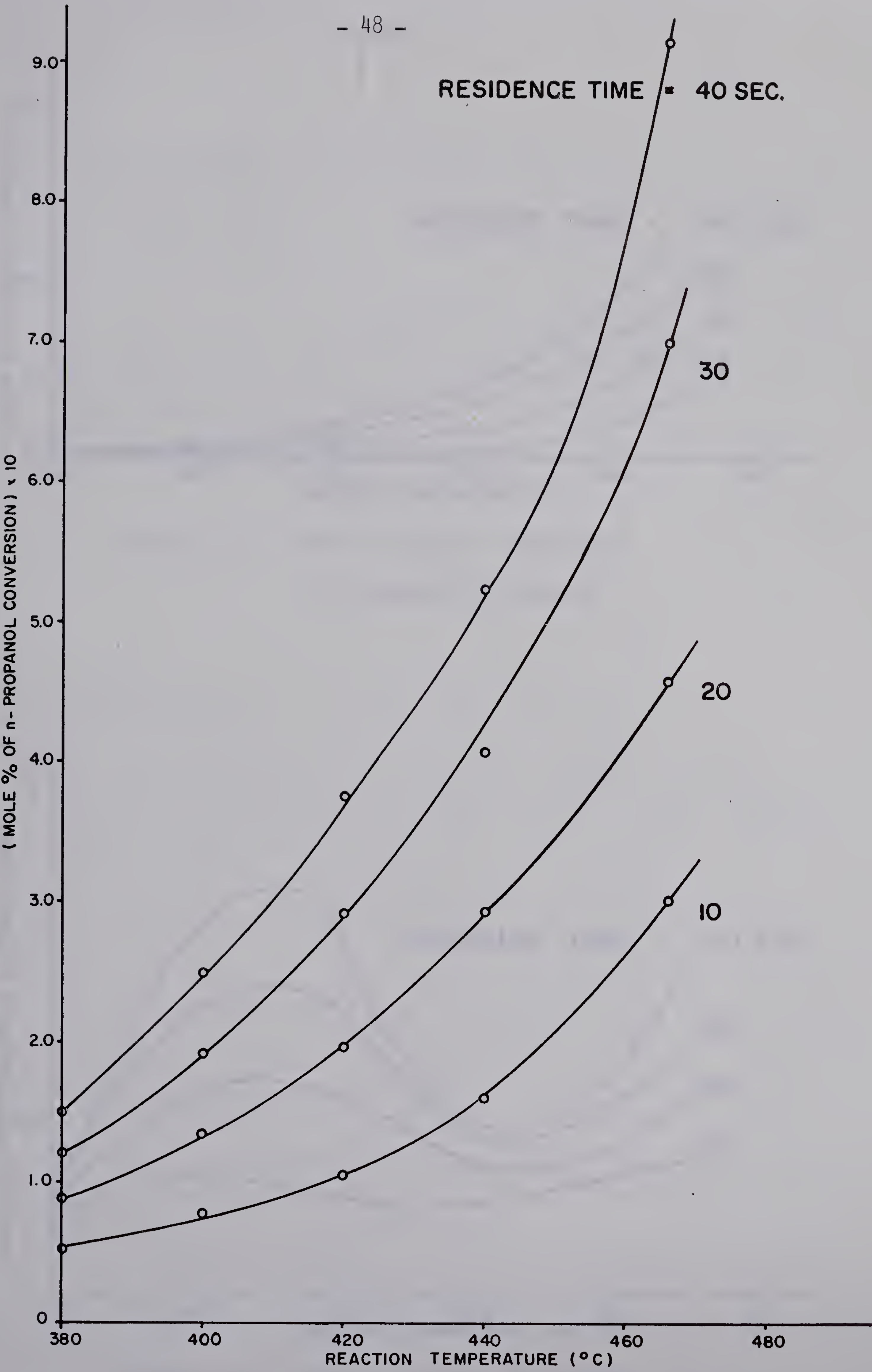

FIGURE IV-6: EFFECT OF REACTION TEMPERATURE ON THERMAL DECOMPOSITION OF n-PROPANOL

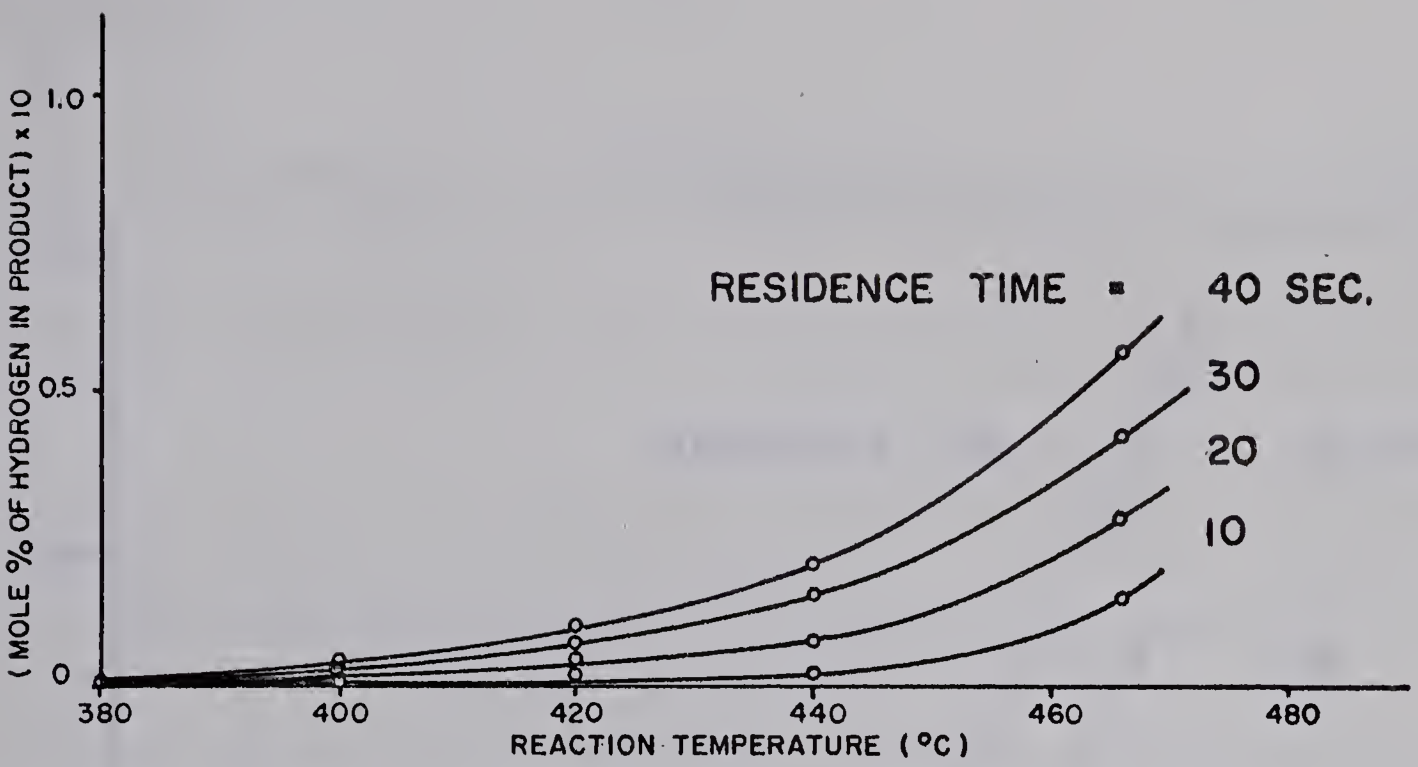

FIGURE IV-7: EFFECT OF REACTION TEMPERATURE ON FORMATION OF HYDROGEN

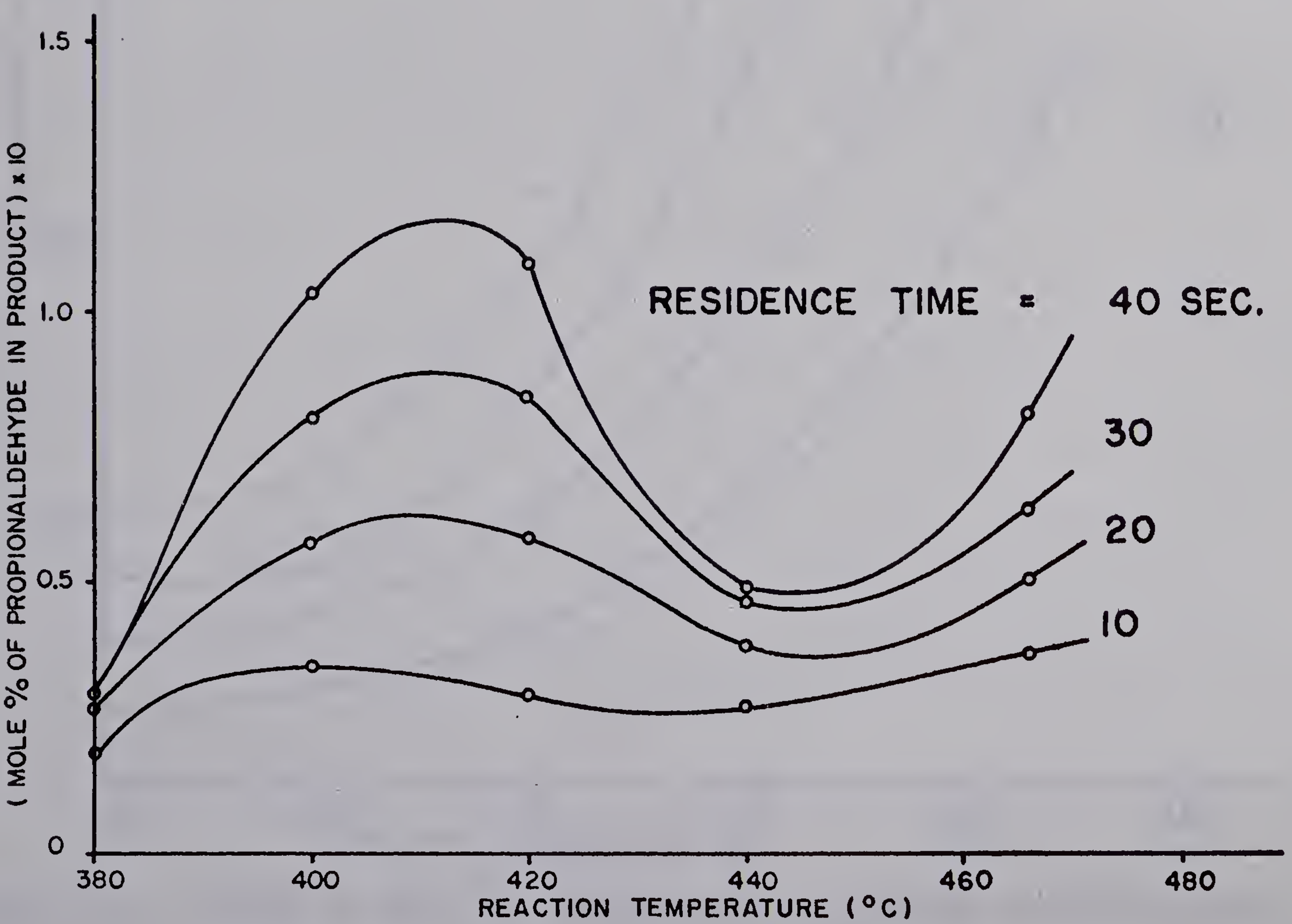

FIGURE IV-8: EFFECT OF REACTION TEMPERATURE ON FORMATION OF PROPIONALDEHYDE

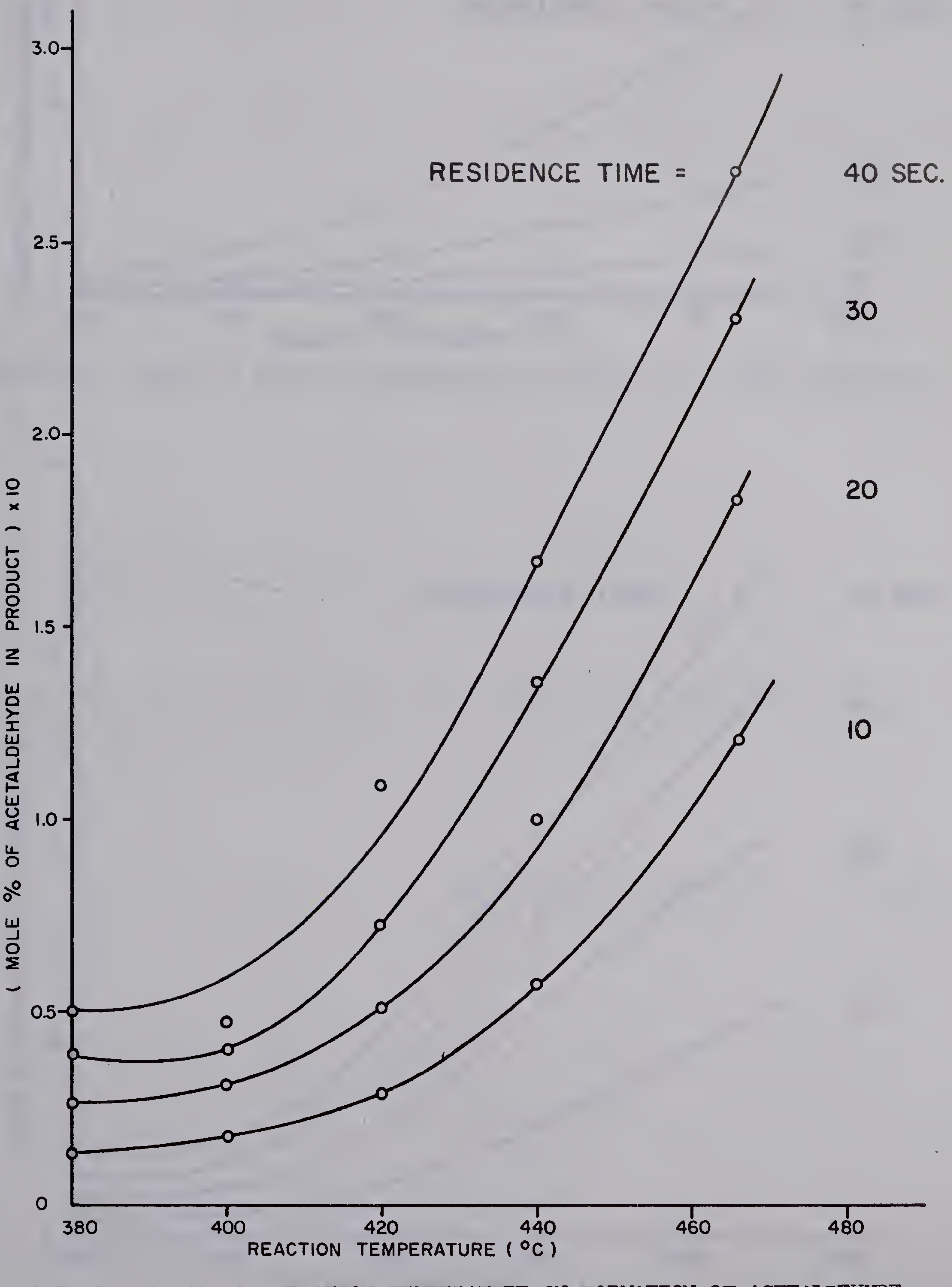

FIGURE IV-9: EFFECT OF REACTION TEMPERATURE ON FORMATION OF ACETALDEHYDE

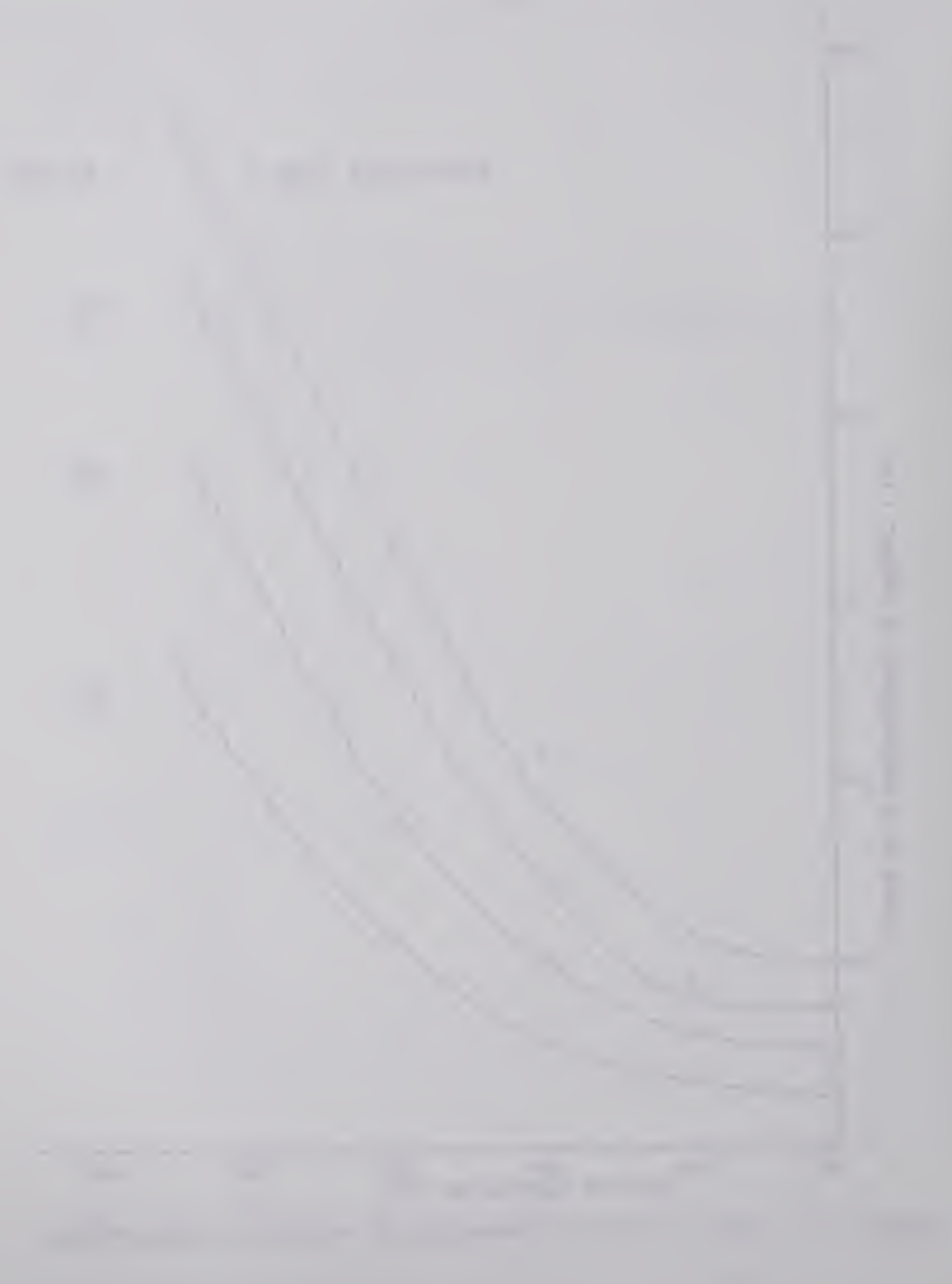

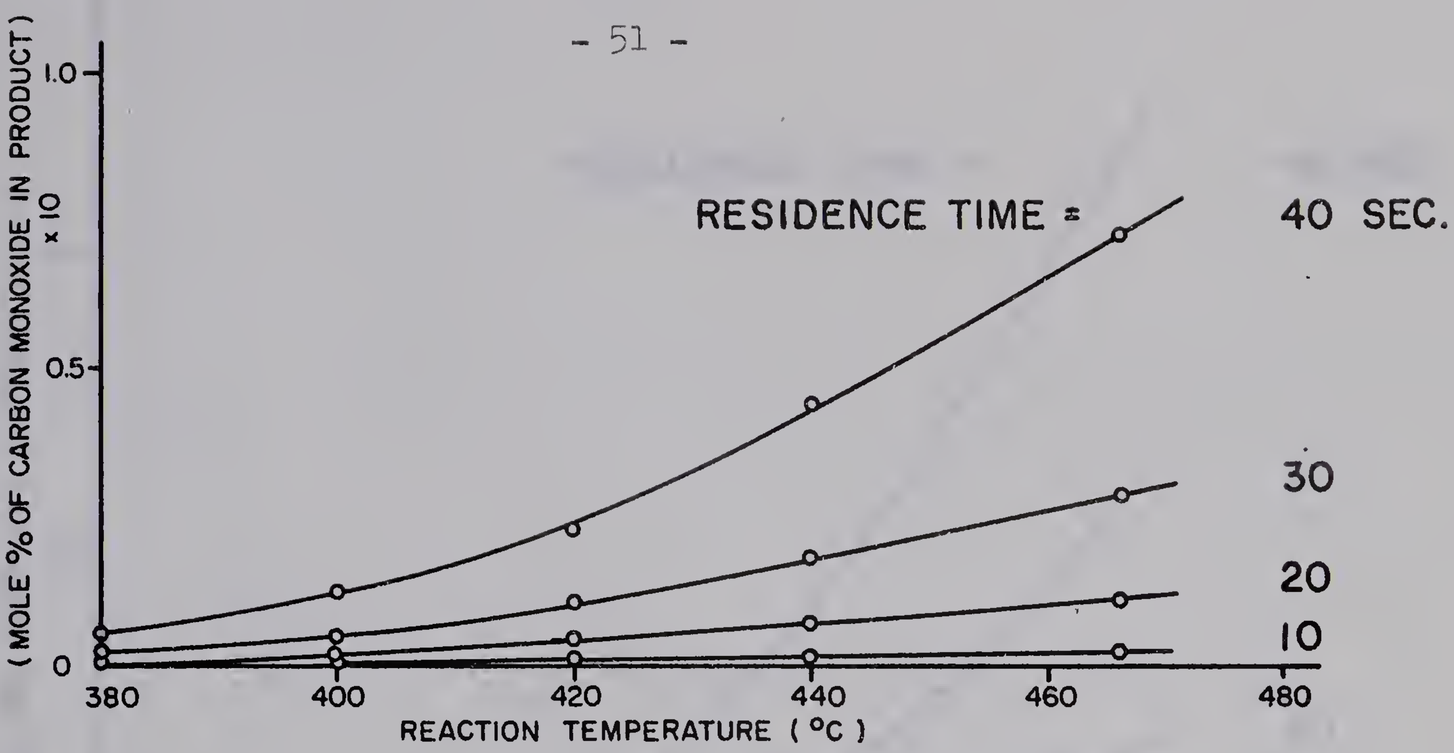

FIGURE IV-10: EFFECT OF REACTION TEMPERATURE ON FORMATION OF CARBON MONOXIDE

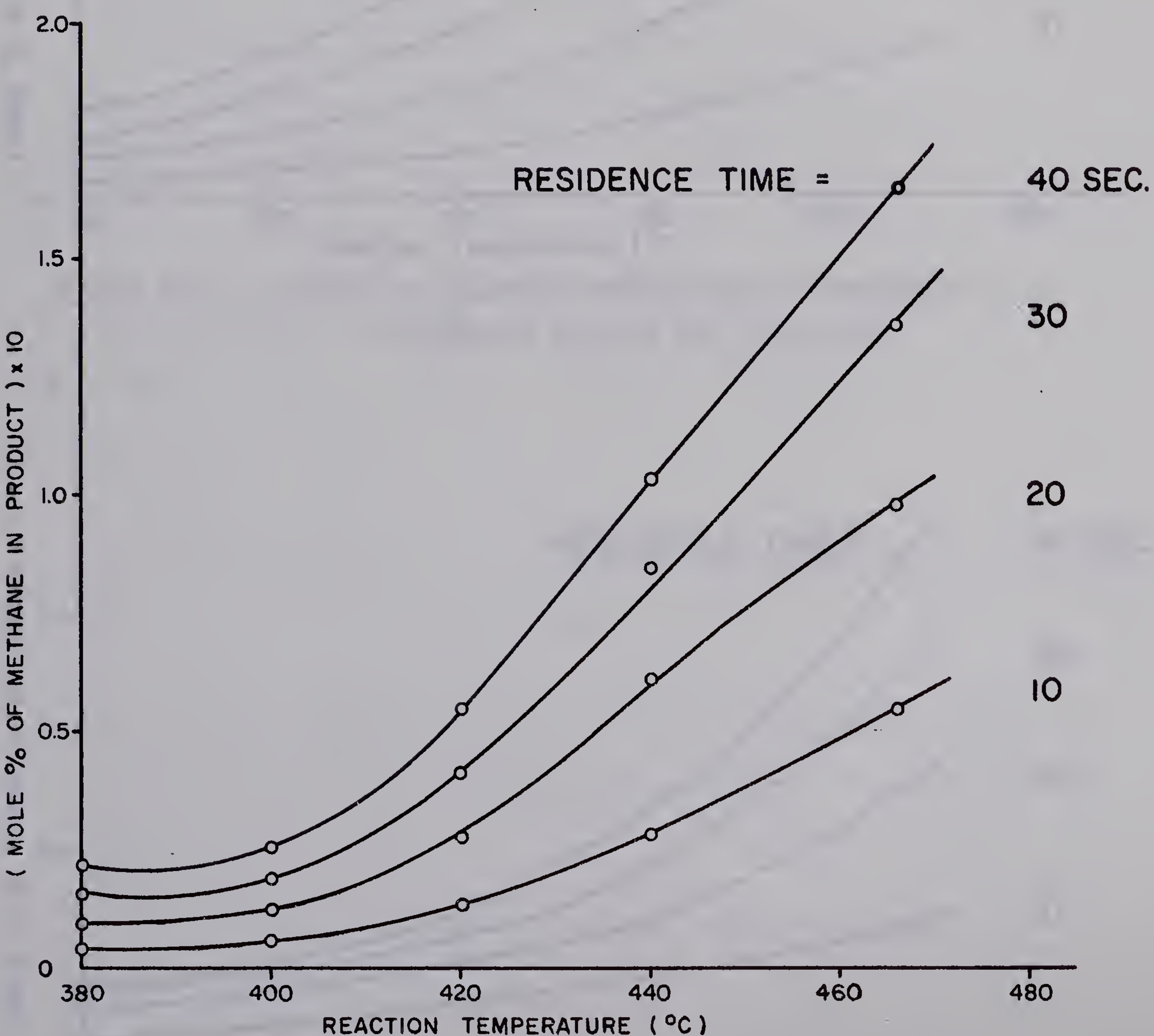

FIGURE IV-11: EFFECT OF REACTION TEMPERATURE ON FORMATION OF METHANE

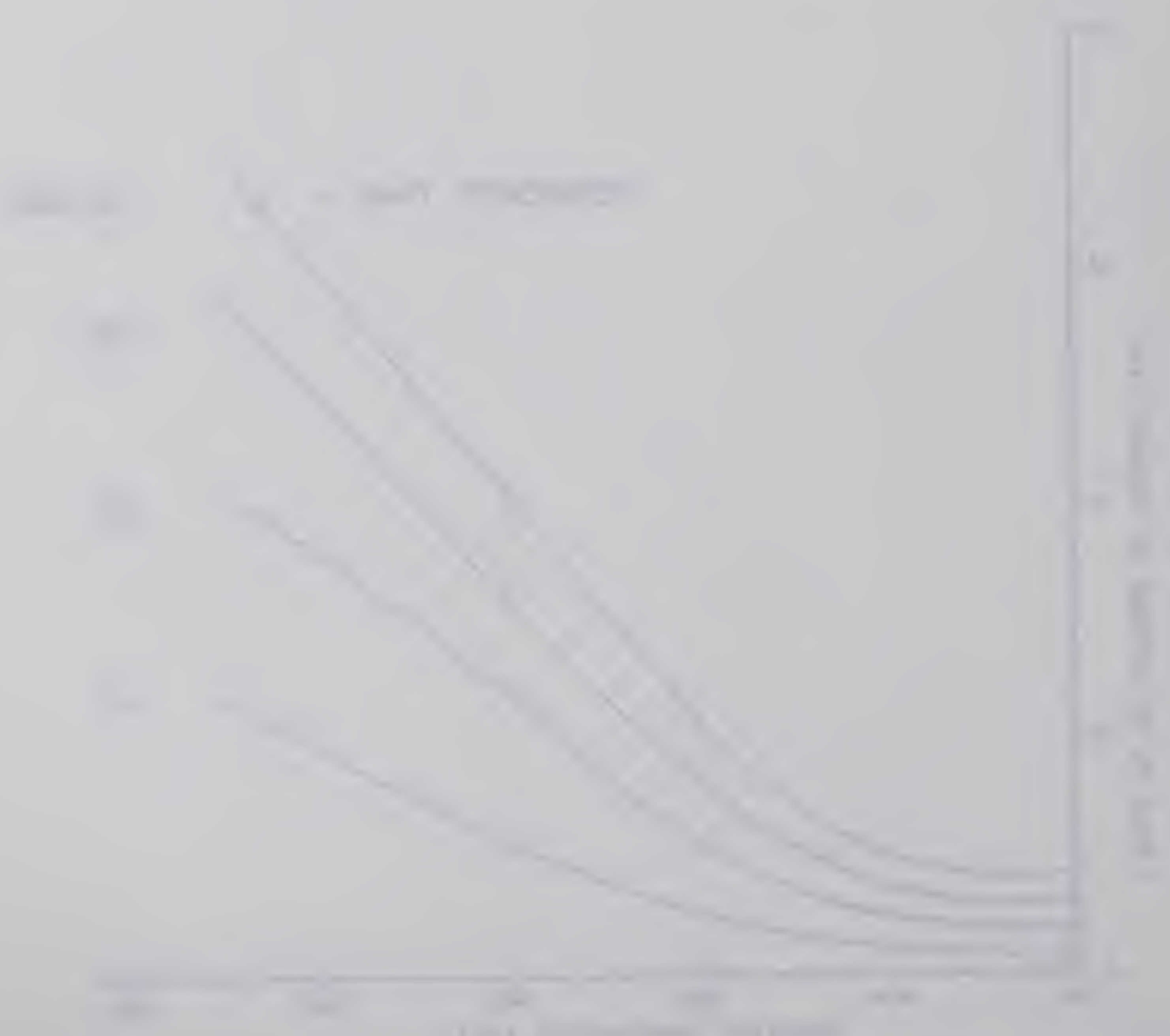

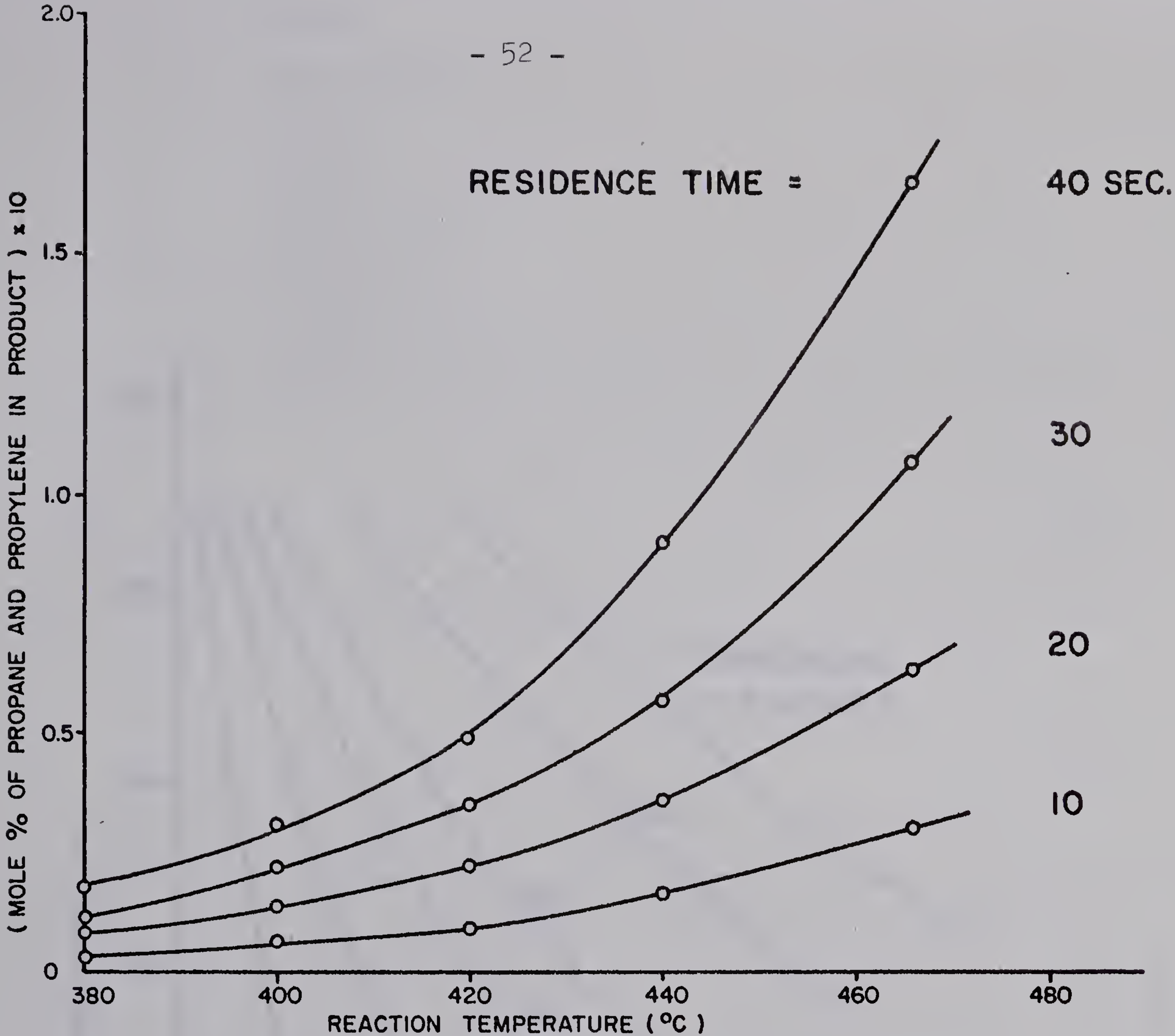

FIGURE IV-12: EFFECT OF REACTION TEMPERATURE ON FORMATION OF COMBINED PROPANE AND PROPYLENE

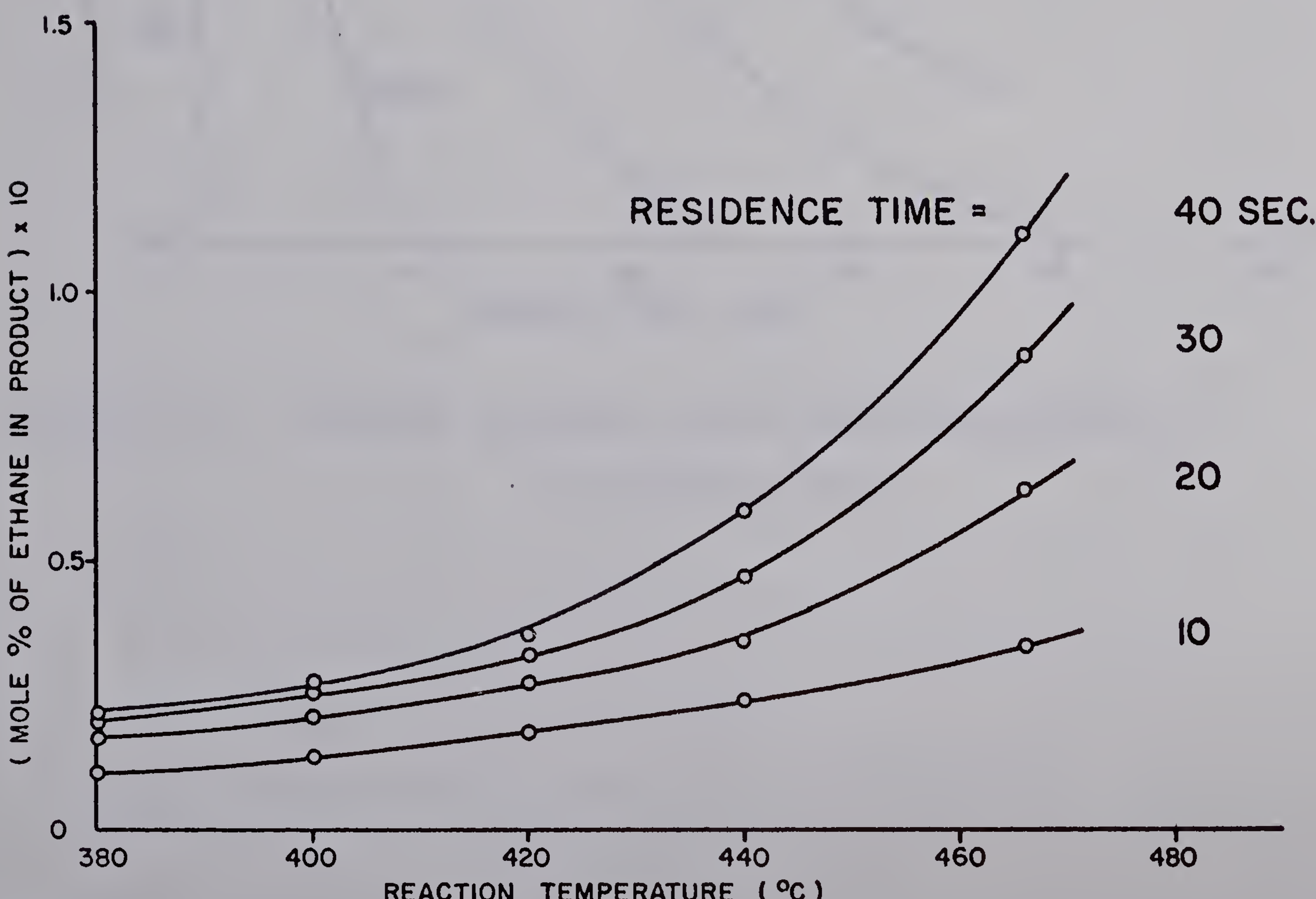

FIGURE IV-13: EFFECT OF REACTION TEMPERATURE ON FORMATION OF ETHANE

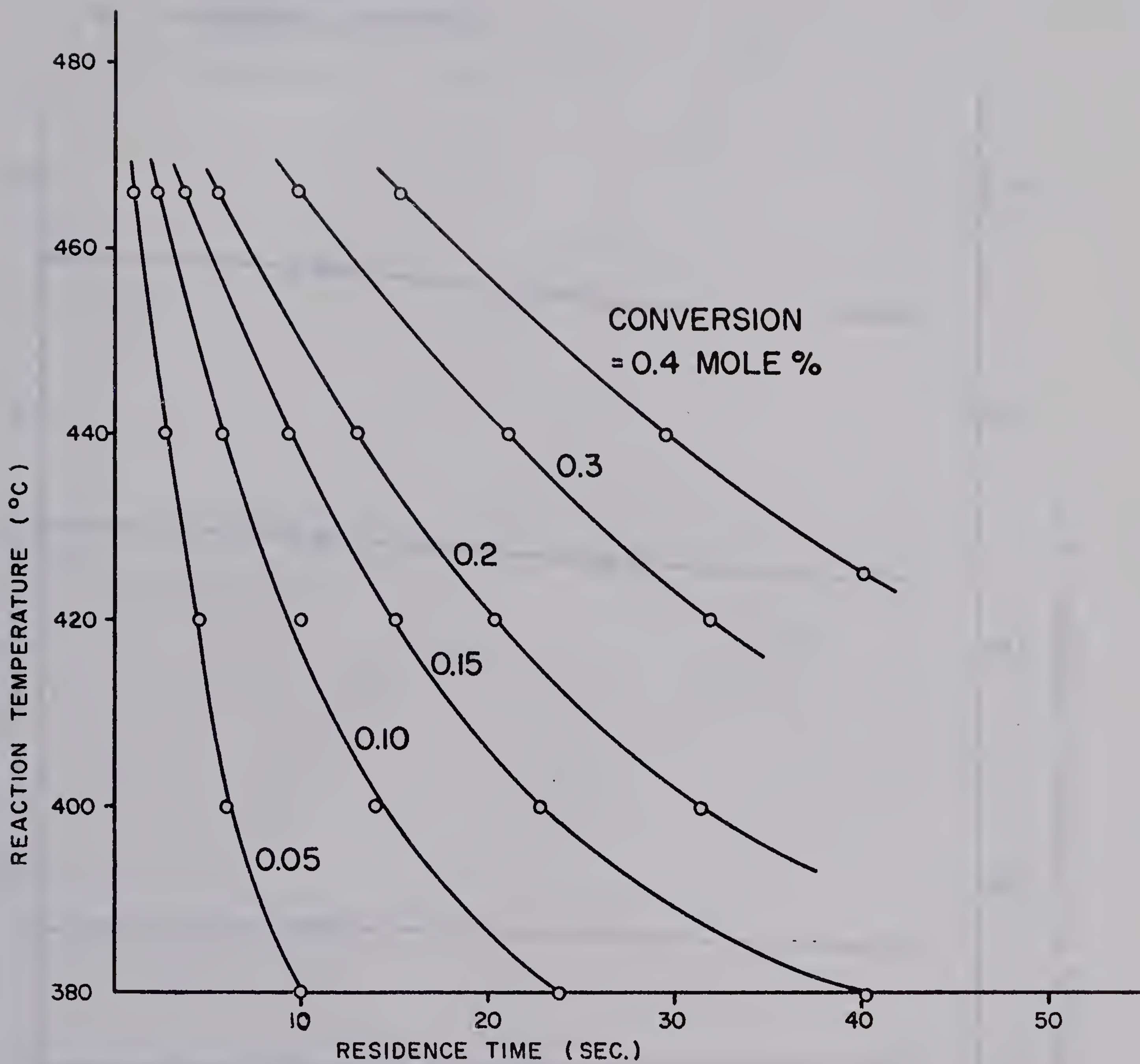

FIGURE IV-14: n-PROPANOL CONVERSION VERSUS REACTION TEMPERATURE AND RESIDENCE TIME

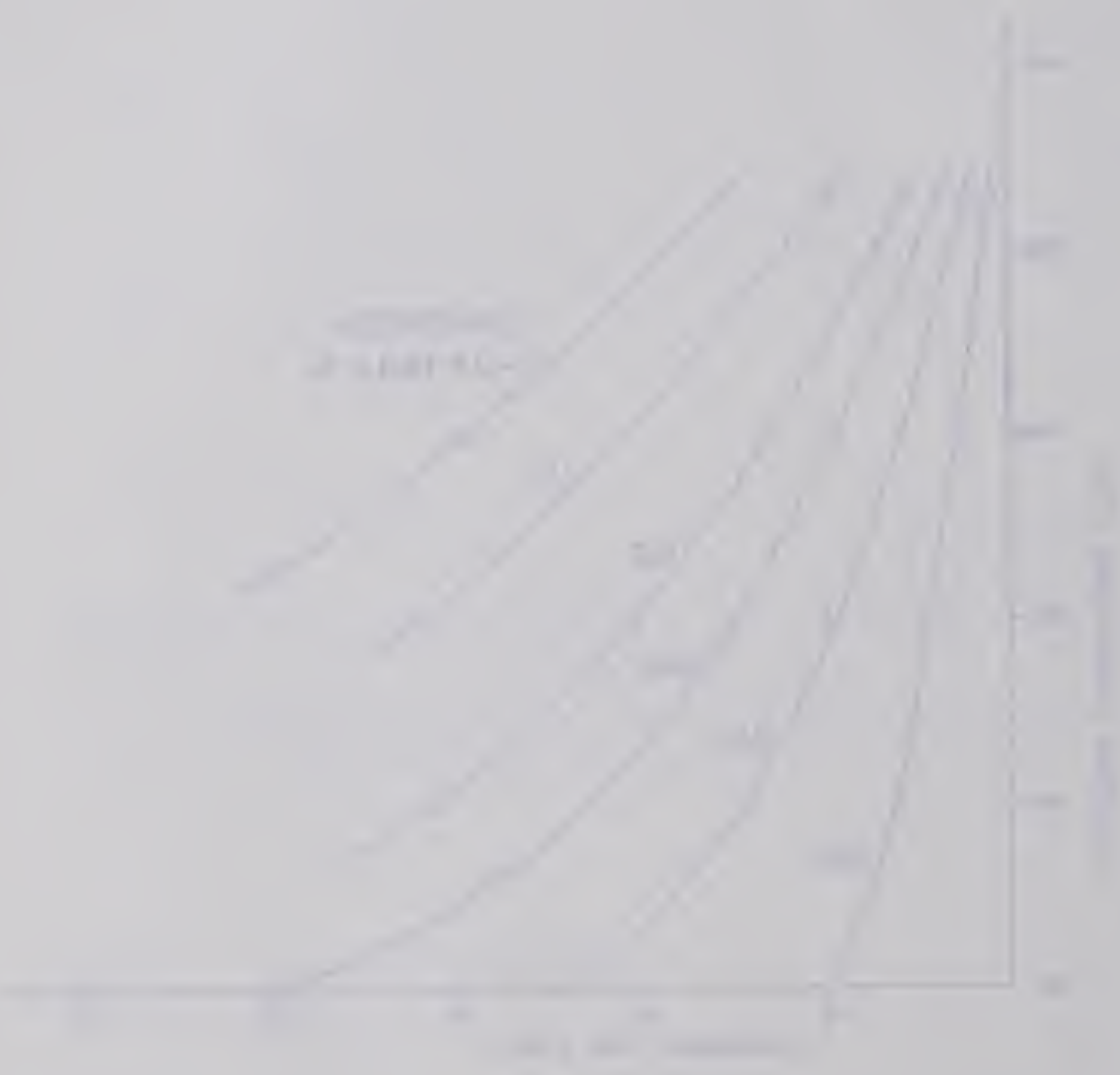

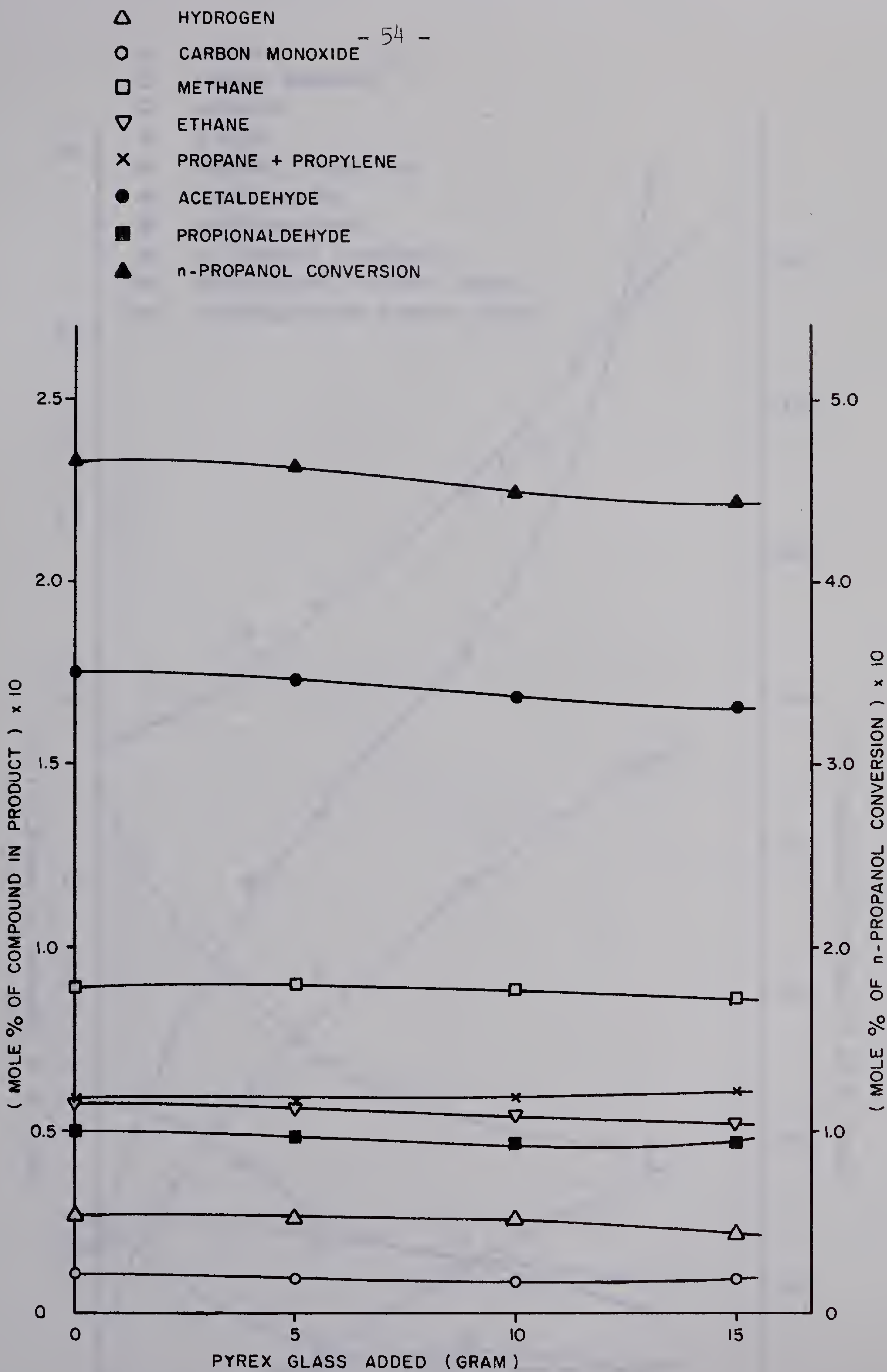

FIGURE IV-15: EFFECT OF PYREX GLASS ON DECOMPOSITION OF n-PROPANOL AT 463°C

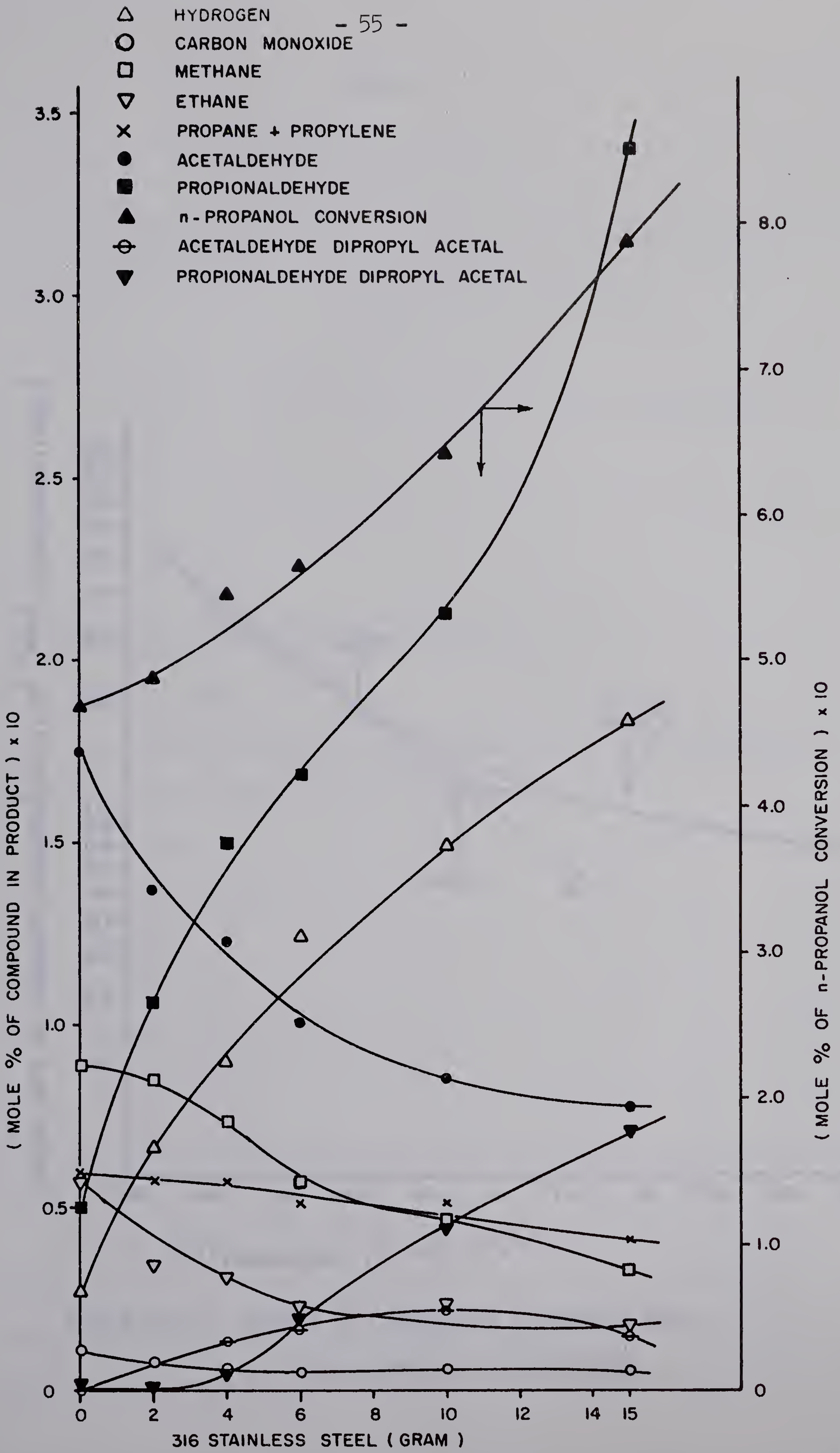

FIGURE IV-16: EFFECT OF TYPE 316 STAINLESS STEEL ON DECOMPOSITION OF n-PROPANOL AT 463°C

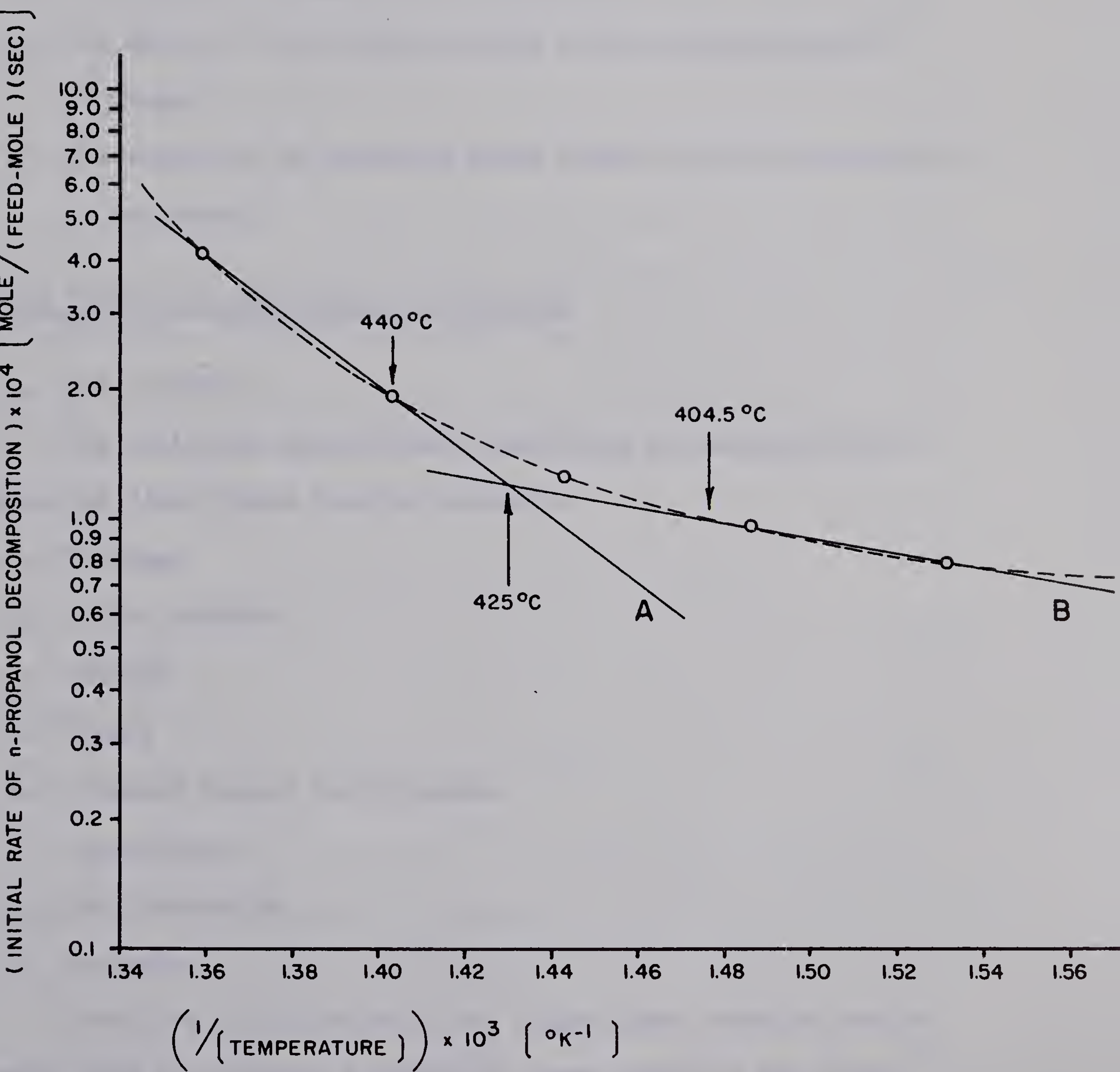

FIGURE IV-17: EFFECT OF TEMPERATURE ON INITIAL RATE FOR n-PROPANOL DECOMPOSITION

V. DISCUSSION OF RESULTS

The experimental results presented in the preceding chapter will be analyzed and discussed under the following sections:

A. The thermal decomposition of n-propanol

B. The effect of Pyrex Glass surface on the decomposition of n-propanol

C. The effect of 316 stainless steel surface on the decomposition of n-propanol

A. The Thermal Decomposition of n-Propanol

1. The Products

The following compounds were identified and analyzed in the gaseous and liquid phase reaction products:

a. Hydrogen

b. Carbon monoxide

c. Methane

d. Ethane

e. Combined propane and propylene

f. Acetaldehyde

g. Propionaldehyde

h. n-Propanol

Water was also detected in the liquid phase reaction product chromatograph by injecting a relatively large amount of the liquid product into a gas-liquid chromatograph. However, due to the small amount of water present and the tendency for profound tailing of the

water peak in the chromatograph, a quantitative analysis of the water present could not be obtained. The Karl Fischer titration was also employed in an attempt to obtain the analysis of water present, but the results obtained were not satisfactory.

The amount of water in the sample was so small that a single drop of Karl Fischer reagent exceeded the end point (See Appendix V).

Mixtures of known amounts of water and n-propanol were analyzed by gas-liquid chromatography. No peak for water appeared at concentrations of water below 0.6 mole %, which amount was expected to be the largest amount of water in any product sample. The maximum combined concentration of propane and propylene in the product was 0.1524 mole % in the present investigation. The amount of water should correspond at most to that of the propylene present, if the water is formed by dehydration of n-propanol.

2. The Molecular Mechanism and Chemical Reactions

According to the molecular mechanism (34, 21), the following reactions may occur:

$$2n - C_3H_7OH \rightleftharpoons n - C_3H_7OH + n - C_3H_7OH^* \quad (25)$$

The activation of n-propanol by collision may occur by the reaction (25). The activated n-propanol, $n - C_3H_7OH^*$, may then decompose into the product compounds, for example,

$$n - C_3H_7OH^* \longrightarrow H_2 + C_2H_5CHO \quad (26)$$

$$n - C_3H_7OH^* \longrightarrow CH_4 + CH_3CHO \qquad (27)$$

Since hydrogen and methane are normally chemically stable between 380° and 460°C (7, 10), not only hydrogen and propionaldehyde but also methane and acetaldehyde should exist in equivalent amounts if this mechanism is to be valid. It is seen, however, that Figures IV-1 to IV-5 show far smaller amount of hydrogen and methane compared to those of the two aldehydes.

Although a considerable amount of ethane is formed in the reaction products, the formation of ethane through the decomposition of activated n-propanol cannot be expected according to the molecular mechanism because formaldehyde, HCOH, should be formed if this reaction occurs. Formaldehyde was not obtained in the products. A possible explanation for the formation of ethane by the molecular mechanism may involve the decomposition of activated propionaldehyde according to reaction (28).

$$CH_3CH_2CHO^* \longrightarrow CH_3CH_3 + CO \qquad (28)$$

Again as in the case of reactions (26) and (27), the amounts of products, ethane and carbon monoxide encountered were not consistent with those for reaction (28). Furthermore, a significant difference occurs in the shape of the curves describing the formation of ethane and carbon monoxide, as shown in Figures IV-1 to IV-5. From the exponentially shaped curves for carbon monoxide at increasing residence time, it is apparent that carbon monoxide is the product of secondary reaction, whereas ethane is not.

The formation of propane should not be expected according to the molecular mechanism since, if propane is produced from the activated n-propanol, an oxygen atom must be produced. This is contrary to the concept of molecular mechanisms as discussed earlier. Although the dehydration reaction (29) may occur, it is difficult to speculate further due to the lack of accurate information on the amounts of water and propylene present.

$$n - C_3H_7OH^* \longrightarrow C_3H_6 + H_2O \tag{29}$$

If the reactions (25), (26), (27) and (29) are considered from a homogeneous kinetics treatment, it may be possible to make additional useful observations. Consider that the decomposition of n-propanol may be presented by the following molecular mechanism:

$$2n - C_3H_7OH \underset{k_2}{\overset{k_1}{\rightleftarrows}} n - C_3H_7OH + n - C_3H_7OH^* \tag{25}$$

$$n - C_3H_7OH^* \xrightarrow{k_3} H_2 + C_2H_5CHO \tag{26}$$

$$n - C_3H_7OH^* \xrightarrow{k_4} CH_4 + CH_3CHO \tag{27}$$

$$n - C_3H_7OH^* \xrightarrow{k_5} C_3H_6 + H_2O \tag{29}$$

Where the k_i are the specific reaction velocity constants. Since the concentration of activated n-propanol would be expected to be low, it may be assumed to remain steady and one can then write the rate of concentration change as follows.

$$\frac{d[n - C_3H_7OH^*]}{d(V/F)} = 0 =$$

$$k_1 [n - C_3H_7OH]^2 - k_2 [n - C_3H_7OH][n - C_3H_7OH^*] -$$

$$(k_3 + k_4 + k_5)\ [n - C_3H_7OH^*] \qquad (30)$$

Solution of equation (30) for $[n - C_3H_7OH^*]$ gives

$$[n - C_3H_7OH^*] = \frac{k_1 [n - C_3H_7OH]^2}{k_2 [n - C_3H_7OH] + k_3 + k_4 + k_5} \qquad (31)$$

The rate of decomposition of n-propanol, when measured in a tubular flow reactor, is given by

$$- \frac{d[n - C_3H_7OH]}{d(V/F)} = (k_3 + k_4 + k_5)\ [n - C_3H_7OH^*] \qquad (32)$$

Upon combining equations (31) and (32) to eliminate $[C_3H_7OH^*]$,

$$- \frac{d[n - C_3H_7OH]}{d[V/F]} = \frac{k_1 (k_3 + k_4 + k_5) [n - C_3H_7OH]^2}{k_2 [n - C_3H_7OH] + k_3 + k_4 + k_5} \qquad (33)$$

Due to very low n-propanol conversions, the concentration of n-propanol remains effectively constant and equal to its initial concentration, $[n - C_3H_7OH]_o$ at any space time, (V/F). Therefore, the amount of n-propanol not converted, $[n - C_3H_7OH]_c$, at the space time, $(V/F)_c$, is given as an approximation by equation (37). In the time from 0 to $(V/F)_c$, one can obtain

$$- \frac{d[n - C_3H_7OH]}{d(V/F)} \simeq - \frac{\Delta [n - C_3H_7OH]}{(V/F)} \tag{34}$$

$$= - \frac{[n - C_3H_7OH]_o - [n - C_3H_7OH]_c}{0 - (V/F)_c}$$

$$= \frac{[n - C_3H_7OH \text{ conversion}]}{(V/F)_c} \tag{35}$$

From equations (33), (34) and (35),

$$\frac{\Delta [n - C_3H_7OH]}{(V/F)_c} \simeq \frac{k_1 \ (k_3 + k_4 + k_5) [n - C_3H_7OH]_o}{k_2 [n - C_3H_7OH]_o + k_3 + k_4 + k_5} \tag{36}$$

and

$$\Delta |n - C_3H_7OH| \quad \frac{k_1 (k_3 + k_4 + k_5) [n - C_3H_7OH]_o^2}{k_2 [n - C_3H_7OH]_o + k_3 + k_4 + k_5} (V/F)_c \tag{37}$$

Since k_1, k_2, k_3, k_4, k_5, and $[n - C_3H_7OH]_o$ are each constant, this analysis would require n-propanol conversion to vary linearly with respect to space time according to equation (37). It can be seen in Figure IV-1-B that the conversion curve with respect to space time is not linear at low temperatures. Although the linearity of n-propanol conversion curves in Figures IV-2 to IV-5 improves with increase in temperature. This approach as well as the point of view of chemical sequence mentioned

earlier suggests that the molecular mechanism plays a minor role, if any, in the thermal decomposition of n-propanol. Furthermore, this kinetic treatment when applied to any mechanism starting with equation (25), including free-radical mechanisms, will also show the n-propanol conversion is linear with respect to space time in the region of low conversion. As a result, it is inconclusive to assess the reaction mechanism according to the linearity of the n-propanol conversion curve with respect to space time in the low conversion region.

3. The Free-Radical Mechanism Initiated by Bond Dissociation in n-Propanol

As mentioned in the THEORY AND LITERATURE SURVEY section, the reactions (2) and (3) are considered to be the primary steps. First, let us consider the chemical implications. The reaction (2) could induce the following reaction steps involving radicals:

Chain Initiation

$$n\text{-}C_3H_7OH \longrightarrow CH_3 + CH_2CH_2OH \qquad (2)$$

$$n\text{-}C_3H_7OH + CH_2CH_2OH \longrightarrow C_2H_5OH + CH_3CH_2CHOH \qquad (38)$$

Chain Propagation

$$CH_3CH_2CHOH \longrightarrow CH_3 + CH_3CHO \qquad (39)$$

$$n\text{-}C_3H_7OH + CH_3 \longrightarrow CH_4 + CH_3CH_2CHOH \qquad (40)$$

$$CH_2CH_2OH \longrightarrow H + CH_3CHO \qquad (41)$$

$$n\text{-}C_3H_7OH + H \longrightarrow H_2 + CH_3CH_2CHOH \quad (42)$$

$$CH_3CH_2CHOH \longrightarrow H + C_2H_5CHO \quad (43)$$

Chain Termination

$$2CH_3CH_2CHOH \longrightarrow C_2H_5CHO + n\text{-}C_3H_7OH \quad (44)$$

$$2CH_3 \longrightarrow C_2H_6 \quad (45)$$

The dissociation energies for rupturing bonds in the radicals in reactions such as (41) and (43) are higher than those for the reactions between radicals or between a radical and a molecule, as in reactions (40), (38), (44) and (45). The bond dissociation energy in such radicals is approximately 20 to 40 Kcal (10), while the activation energy of reactions between radicals or between a radical and a molecule is approximately 0 to 15 Kcal (3). Thus it would be anticipated that reaction (38) should be faster than reaction (41). One would expect that if reaction (2) takes place according to this radical mechanism, ethanol should appear in the product. Since ethanol was not detected, the free-radical mechanism induced by the bond dissociation in n-propanol either may be questioned or ethanol is very reactive. Following the latter possibility, one would expect methanol to be formed from the ethanol, analogous to the formation of ethanol from n-propanol, which again was not encountered. Furthermore, if the chain propagation proceeds, a considerable amount of hydrogen should be formed compared

to propionaldehyde. Figure IV-1, IV-2 and IV-3, for instance, do not show this to be the case.

The reaction (3) may induce a second reaction mechanism involving radicals:

Chain Initiation

$$n\text{-}C_3H_7OH \longrightarrow CH_3CH_2 + CH_2OH \qquad (3)$$

$$n\text{-}C_3H_7OH + CH_3CH_2 \longrightarrow CH_3CH_3 + CH_3CH_2CHOH \qquad (46)$$

$$n\text{-}C_3H_7OH + CH_2OH \longrightarrow CH_3OH + CH_3CH_2CHOH \qquad (47)$$

Chain Propagation

$$CH_2OH \longrightarrow H + HCHO \qquad (48)$$

$$CH_3CH_2CHOH \longrightarrow H + C_2H_5CHO \qquad (43)$$

$$CH_3CH_2CHOH \longrightarrow CH_3 + CH_3CHO \qquad (49)$$

$$n\text{-}C_3H_7OH + CH_3 \longrightarrow CH_4 + CH_3CH_2CHOH \qquad (40)$$

$$n\text{-}C_3H_7OH + H \longrightarrow H_2 + CH_3CH_2CHOH \qquad (42)$$

Chain Termination

$$2CH_3CH_2CHOH \longrightarrow C_2H_5CHO + n\text{-}C_3H_7OH \qquad (44)$$

$$2CH_2OH \longrightarrow HCHO + CH_3OH \qquad (50)$$

$$2CH_3CH_2 \longrightarrow C_4H_{10} \qquad (51)$$

In the same way that the previous radical mechanism induced by reaction (2) was discussed, if this mechanism is to be important in the thermal decomposition of n-propanol, methanol should appear in the product. In this investigation methanol was not detected in the products.

Thus, due to the absence of ethanol and methanol from the products and due to the amount of hydrogen encountered compared to the amount of propionaldehyde, it is apparent that a free radical mechanism initiated by direct bond dissociation in n-propanol is not valid.

On the other hand, still considering the radical mechanisms, an examination of the experimental results will be attempted from the point of view of chemical kinetics. Assuming another simple reaction model with steady concentrations of radicals for the thermal decomposition of n-propanol, the following rate equations can be postulated:

$$\text{n-}C_3H_7OH \xrightarrow{k_1} CH_3 + CH_2CH_2OH, \qquad (2)$$

$E_1 = 80$ Kcal

$$\text{n-}C_3H_7OH + CH_2CH_2OH \xrightarrow{k_2} C_2H_5OH + CH_3CH_2CHOH \qquad (38)$$

$$\text{n-}C_3H_7OH + CH_3 \xrightarrow{k_3} CH_4 + CH_3CH_2CHOH \qquad (40)$$

$$CH_3CH_2CHOH \xrightarrow{k_4} CH_3 + CH_3CHO \qquad (49)$$

$E_4 = 15$ to 25 Kcal

[illegible]

[illegible]

[illegible]

[illegible]	[illegible]	[illegible]
[illegible]	[illegible]	[illegible]
[illegible]	[illegible]	[illegible]
[illegible]	[illegible]	[illegible]

$$2CH_3CH_2CHOH \xrightarrow{k_5} C_2H_5CHO + n\text{-}C_3H_7OH \qquad (44)$$

$E_5 = 10$ Kcal

$$\frac{d[CH_3]}{dt} = 0 = k_1[n\text{-}C_3H_7OH] - k_3[n\text{-}C_3H_7OH][CH_3] + k_4[CH_3CH_2CHOH] \qquad (52)$$

$$\frac{d[CH_2CH_2OH]}{dt} = 0 = k_1[n\text{-}C_3H_7OH] - k_2[n\text{-}C_3H_7OH][CH_2CH_2OH] \qquad (53)$$

$$\frac{d[CH_3CH_2CHOH]}{dt} = 0 = k_2[n\text{-}C_3H_7OH][CH_2CH_2OH] + k_3[CH_3][n\text{-}C_3H_7OH] - k_4[CH_3CH_2CHOH] + k_5[CH_3CH_2CHOH]^2 \qquad (54)$$

Solving equations (52), (53) and (54) for these radical species in terms of $[n\text{-}C_3H_7OH]$,

$$[CH_2CH_2OH] = \frac{k_1}{k_2} \qquad (55)$$

$$[CH_3CH_2CHOH] = \left\{\frac{2k_1}{k_5}[n\text{-}C_3H_7OH]\right\}^{\frac{1}{2}} \qquad (56)$$

$$[CH_3] = \frac{k_1}{k_2} + \frac{k_4}{k_3}\left\{\frac{2k_1}{k_5}\,\frac{1}{[n\text{-}C_3H_7OH]}\right\}^{\frac{1}{2}} \qquad (57)$$

The overall n-propanol decomposition rate is now given by,

$$-\frac{d[n\text{-}C_3H_7OH]}{dt} = k_1[n\text{-}C_3H_7OH] + k_2[n\text{-}C_3H_7OH][CH_2CH_2OH] +$$

$$k_3[CH_3][n\text{-}C_3H_7OH] - k_5[CH_3CH_2CHOH]^2 \qquad (58)$$

So that, substituting for $[CH_3]$, $[CH_2CH_2OH]$ and $[CH_3CH_2CHOH]$ into equation (58),

$$-\frac{d[n\text{-}C_3H_7OH]}{dt} = k\,[n\text{-}C_3H_7OH] + k_4\left\{\frac{2k_1}{k_5}[n\text{-}C_3H_7OH]\right\}^{\frac{1}{2}} \qquad (59)$$

In equation (59), that k_1 is much smaller than $k_4\left\{\frac{2k_1}{k_5}\right\}^{\frac{1}{2}}$ can be shown as follows. According to the Arrhenius equation, the ratio of k_1 to $k_4\left\{\frac{2k_1}{k_5}\right\}^{\frac{1}{2}}$ is given as.

$$k_1 : k_4\left\{\frac{2k_1}{k_5}\right\}^{\frac{1}{2}} = 1 : \frac{k_{04}}{k_{01}}\left\{\frac{2k_{01}}{k_{05}}\right\}^{\frac{1}{2}}\exp\left\{\frac{-1}{RT}\{E_4-\tfrac{1}{2}(E_1 + E_5)\}\right\} \qquad (60)$$

Where, k_{0i} is a pre-exponential factor of a reaction rate constant k_i. The pre-exponential factor (35) is of the order of 10^{13} [sec^{-1}] for majority of monomolecular reactions and is of the order of 10^{14}[cu cm/sec·mole] for bimolecular reactions.

Reactions (2) and (49) are monomolecular reactions, so that the quantity of pre-exponential factors k_{01} and k_{04} may be of the order of 10^{13}[sec^{-1}]. Since reaction (44) is a bimolecular reaction, k_{05} may be of the order of 10^{14}[cu cm/sec·mole].

Therefore,

$$\frac{1}{10} < \frac{k_{04}}{k_{01}} < 10 \text{ and} \left(\frac{2}{10^3}\right)^{\frac{1}{2}} < \left(\frac{2k_{01}}{k_{05}}\right)^{\frac{1}{2}} < (2 \times 10)^{\frac{1}{2}}$$

may be possible approximations. Substituting the values of activation energies (E_1 = 80 Kcal, E_4 = 25 Kcal and E_5 = 10 Kcal) and T = 675°K into the exponential term in equation (60),

$$\exp\left(\frac{-1}{RT}\{E_4 - \tfrac{1}{2}(E_1 + E_5)\}\right)$$

$$\simeq \exp\left(\frac{-1}{2 \times 673}\{25 - \tfrac{1}{2}(80 + 10)\} \times 100\right)$$

$$\simeq 2.8 \times 10^6$$

Therefore, one may expect the approximate ratio $k_4\left(\frac{2k_1}{k_5}\right)^{\frac{1}{2}}/k_1$ as,

$$(2.8 \times 10^6)\frac{1}{10}\left(\frac{2}{10^3}\right)^{\frac{1}{2}} < k_4\left(\frac{2k_1}{k_5}\right)^{\frac{1}{2}}/k_1 < (2.8 \times 10^6)(10)(2 \times 10)^{\frac{1}{2}}$$

Therefore,

$$(2.8\sqrt{2}) \times 10^{3.5} < k_4\left(\frac{2k_1}{k_5}\right)^{\frac{1}{2}}/k_1 < (2.8\sqrt{2}) \times 10^{7.5} \qquad (61)$$

Thus, the term $k_1[n\text{-}C_3H_7OH]$ in equation (59) can be neglected. The equation (59), therefore, may be approximated by

$$-\frac{d[n\text{-}C_3H_7OH]}{dt} \simeq k_4\left(\frac{2k_1}{k_5}[n\text{-}C_3H_7OH]\right)^{\frac{1}{2}} \qquad (62)$$

Using the Arrhenius equation again, the overall activation energy is given by

$$E_{overall} = E_4 - \frac{1}{2}(E_1 - E_5),$$

for equation (62).

The activation energy of reaction (2) is around 80 Kcal as mentioned in Appendix VI. The bond dissociation energies in radicals are approximately 20 to 40 Kcal. Bond dissociation energies for some specific reactions are as follows:

Reaction	Bond Dissociation Energy, Kcal	Reference
$CH_3CO \longrightarrow CH_3 + CO$	18	(12)
	15	(10)
$CH_3CH_2CH_2 \longrightarrow CH_3 + CH_2CH_2$	26	(10)
$CH_3CH_2O \longrightarrow CH_3 + CH_2O$	13	(10)

From the values shown above, the activation energy of reaction (49) was estimated to be 15 to 25 Kcal. As mentioned, the activation energy of the reaction between radicals, for example in reaction (44), is low, and may in some cases be less than 10 Kcal. Taking this value and substituting E_1 = 80 Kcal, E_4 = 25 Kcal, and E_5 = 10 Kcal, one can obtain,

$$E_{overall} = 25 + \frac{1}{2}(80 - 10) = 60 \text{ Kcal}$$

or by substituting E_1 = 80 Kcal, E_4 = 15 Kcal and E_5 = 10 Kcal,

$$E_{overall} = 15 + \tfrac{1}{2}(80 - 10) = 50 \text{ Kcal}$$

Thus, the overall activation energy is believed to be higher than 50 to 60 Kcal.

Some overall activation energies and bond dissociation energies for the primary step in the thermal decomposition of organic compounds are shown in Table V-1.

Table V-1

Compounds		Bond Dissociation Energy, Kcal	Overall Activation Energy, Kcal
Acetaldehyde	(12)	76	48
Dimethyl ether	(12)	80	62.5
Acetone	(12)	70	62.5

Comparing the activation energy value calculated for n-propanol decomposition with the trend in values shown in Table V-1, it is reasonable to expect the overall activation energy for n-propanol to be higher than 50 to 60 Kcal. However, the overall activation energy for n-propanol conversion, obtained from the experimental initial rate data mentioned in section IV-B-4, shows a much lower value, 35 Kcal in the higher temperature region and 8 Kcal in the lower temperature region.

Therefore, from a kinetic point of view, it appears that the free-radical mechanisms, initiated by bond dissociation in n-propanol, also do not hold.

4. The Influence of a Foreign Gas

It was noted previously that a foreign gas such as oxygen may influence the rate of thermal decomposition of n-propanol. The foreign gas may either be dissolved in the liquid n-propanol used as the reactant, or it may be a component of air which could have remained in the reactor. In either case, a small amount could have subsequently acted as the initiator. The initiation which could occur from oxygen is discussed in the following section.

The initiation of the thermal decomposition of n-propanol by oxygen may occur (2, 29) according to the reactions (63) and (64),

$$n\text{-}C_3H_7OH + O_2 \longrightarrow CH_3CH_2CHOH + HO_2 \qquad (64)$$

$$n\text{-}C_3H_7OH + HO_2 \longrightarrow CH_3CH_2CHOH + H_2O_2 \qquad (65)$$

Semenov (36) has reported that the reaction of HO_2 with a hydrogen atom proceeds with a subsequent rapid break-up of H_2O_2 into two OH radicals, via

$$H_2O_2 \longrightarrow 2OH \qquad (66)$$

Since OH is so active (37), it may react immediately with n-propanol, as follows,

$$OH + n\text{-}C_3H_7OH \longrightarrow H_2O + CH_3CH_2CHOH \qquad (67)$$

Satterfield and Reid (30) have reported important reactions in the partial oxidation of propane, which are shown as follows.

$$C_3H_7 + O_2 \longrightarrow C_3H_6 + HO_2 \qquad (68)$$

$$HO_2 + C_3H_8 \longrightarrow H_2O_2 + C_3H_7 \qquad (69)$$

$$HO_2 \longrightarrow \text{destruction at the wall} \qquad (70)$$

In the reactions (68), (69) and (70), the behavior of HO_2 with respect to temperature sheds light on the formation of propionaldehyde in the lower temperature region of this investigation. Satterfield and Reid (30) have reported that the ratio of hydrogen peroxide to propylene is independent of residence time at 375°C, but at 475°C the ratio drops rapidly because of the destruction of the perioxide radical at the walls of the reactor. Consequently, it is considered that the maximum amount of HO_2, which induces such consecutive reactions as (65), arises between 375°C and 475°C. This is because the formation rate of HO_2 increases with the increase of temperature and its decomposition rate also increases rapidly with the increase of temperature. If the consecutive reaction of HO_2 proceeds, α-n-propanol radical may be produced in amounts larger than the amount of HO_2 which reacts. The following reactions will show this.

$$n\text{-}C_3H_7OH + HO_2 \longrightarrow CH_3CH_2CHOH + H_2O_2 \qquad (65)$$

$$H_2O_2 \longrightarrow 2OH \qquad (66)$$

$$n\text{-}C_3H_7OH + OH \longrightarrow CH_3CH_2CHOH + H_2O \qquad (71)$$

The α-n-propanol radical is responsible for the formation of

propionaldehyde according to reactions (43) and (44)

$$CH_3CH_2CHOH \longrightarrow H + C_2H_5CHO \tag{43}$$

$$2CH_3CH_2CHOH \longrightarrow C_2H_5CHO + n\text{-}C_3H_7OH \tag{44}$$

Besides the above reactions, α-n-propanol radical may react as follows:

$$CH_3CH_2CHOH \longrightarrow CH_3 + CH_3CHO \tag{49}$$

However, it is unlikely that reactions (43) and (49) will proceed significantly in the lower temperature region, since the bond dissociation energy is higher than the activation energy of such reaction as (44).

It is suggested that the formation of propionaldehyde could arise according to a consecutive reaction of HO_2. If a direct proportionality exists between the amounts of HO_2 and propionaldehyde then, it is expected that a maximum amount of propionaldehyde will occur when the free-radical mechanism is initiated by some substance such as oxygen. The experimental results are consistent with this prediction as shown in Figure IV-8. Furthermore, it may be possible to explain the small amount of hydrogen compared to the amount of propionaldehyde, especially in the lower temperature region, by assuming that propionaldehyde is formed mainly by reaction (44). In the higher temperature region, where HO_2 decomposes rapidly, the chain propagation according to reactions (43) and (49) will become controlling.

[illegible]

[illegible] [illegible]

[illegible] [illegible]

[illegible]

[illegible] [illegible]

[illegible]

[illegible]

[illegible]

The subsequent increase in the amount of propionaldehyde at temperatures higher than 440°C will also be explained by this mechanism (See Figure IV-8).

The following reaction mechanism may then be considered.

Chain Initiation

$$n\text{-}C_3H_7OH + O_2 \longrightarrow CH_3CH_2CHOH + HO_2 \quad (64)$$

$$HO_2 \longrightarrow \text{destruction at the wall} \quad (70)$$

$$n\text{-}C_3H_7OH + HO_2 \longrightarrow CH_3CH_2CHOH + H_2O_2 \quad (65)$$

$$H_2O_2 \longrightarrow 2OH \quad (66)$$

$$n\text{-}C_3H_7OH + OH \longrightarrow CH_3CH_2CHOH + H_2O \quad (71)$$

Chain Propagation

$$CH_3CH_2CHOH \longrightarrow CH_3 + CH_3CHO \quad (49)$$

$$CH_3CH_2CHOH \longrightarrow H + C_2H_5CHO \quad (43)$$

$$n\text{-}C_3H_7OH + CH_3 \longrightarrow CH_4 + CH_3CH_2CHOH \quad (40)$$

$$n\text{-}C_3H_7OH + H \longrightarrow H_2 + CH_3CH_2CHOH \quad (42)$$

Chain Termination

$$CH_3CH_2CHOH + CH_3 \longrightarrow C_2H_6 + CH_3CHO \quad (72)$$

$$CH_3CH_2CHOH + H \longrightarrow CH_3CH{=}CH_2 + H_2O \quad (73)$$

$$2CH_3 \longrightarrow C_2H_6 \qquad (45)$$

$$2CH_3CH_2CHOH \longrightarrow C_2H_5CHO + n\text{-}C_3H_7OH \qquad (44)$$

The products obtained in this investigation are consistent with the above reaction mechanism. Due to the complexity of this mechanism and the low amounts of reaction, it is not possible to calculate the reaction rates quantitatively from the data obtained in this investigation. However, the activation energy for this mechanism can be reasonably expected to be smaller than the values for the molecular mechanism and the free-radical mechanism induced by direct bond dissociation in n-propanol, since the activation energy of the primary step (64) is approximately 40 to 50 Kcal. This can be seen from the data of Semenov (38), while the activation energies of the primary steps in the free-radical mechanism induced by bond dissociation in n-propanol is approximately 80 Kcal.

Semenov (38) has suggested the activation energies shown in Table V-2 in the oxidation of hydrocarbons for such reactions as,

$$RH + O_2 \longrightarrow R + HO_2 \qquad (74)$$

Table V-2

Activation Energies for Reaction,

$$RH + O_2 \longrightarrow R + HO_2$$

Bond	D(R - H), Kcal	Activation Energies for the above Reaction, Kcal
For tertiary C-H bond	89	42
For secondary C-H bond	94	47

[illegible]

[illegible]

[illegible]

[illegible]

[illegible]

[illegible]

[illegible]

[illegible]

[illegible]

[illegible]

Since the overall activation energy will be smaller than that of the primary step, as shown in Table V-1, its magnitude will be consistent with the experimental overall energy of 35 Kcal at higher temperatures (See Figure IV-17). However, there is some uncertainty in the case of the very low activation energy of 8 Kcal encountered in the lower temperature region (See Figure IV-17).

In view of the above considerations, the free-radical mechanism initiated by some substance like foreign gas, such as oxygen, is possibly considered to be consistent with the experimental results with respect to the product compounds encountered, and formation rates of propionaldehyde with respect to temperature, (which is extremely different from the formation rates of others in the temperature region of $380^{o}C$ to $440^{o}C$ as shown in Figure IV-8).

It is believed that some other reaction mechanism, for example catalytic wall effects, occur in the lower temperature region, $380^{o}C$ to $440^{o}C$, resulting in a reduction of the activation energy of the n-propanol conversion step.

It is difficult to anticipate the chemical reactivity of the compounds involved in the possible molecular reaction mechanisms, since the reaction route and its products are unique, or nearly so, in each of the possible cases. For instance, the estimation of an activation energy for this type of reaction will be obtained by an empirical way (7). On the other hand, in the free-radical mechanism, the activation energy for the bond dissociation

reaction step is equal to the bond dissociation energy (7,9) and plays a major role in the chain initiation and in the chain propagation. The contribution of the activation energy in the primary step to the overall activation energy of the chain reaction is the largest as mentioned in the section on THEORY AND LITERATURE SURVEY. Therefore, it may be possible to assess the reactivity of the chemical compound in the free-radical mechanism from point of view of activation energy, if one can obtain the bond dissociation energy of the compound. Much work has been done in studying the bond dissociation energies of organic compounds, as previously described in the literature survey and in Appendix VI. Furthermore, it is learned as a result of these studies that the order of magnitude of the activation energies is the bond dissociation reaction of the molecule, the bond dissociation reaction of the radical, and the reaction between radicals or between a radical and a molecule. Thus, in the free-radical mechanism, it is possible to anticipate the reactivity of a compound and the reaction process as attempted in the preceding discussion.

B. The Effect of Pyrex Glass on the Decomposition of n-Propanol

Figure IV-5 shows that both the amounts of the compounds in the product and the n-propanol conversion decrease slightly with an increase in the amount of Pyrex Glass packed within the glass tubular reactor. Table V-3 shows a comparison of n-propanol conversions obtained with the empty Pyrex Glass reactor (homogeneous

thermal decomposition shown in Figure IV-5), and with additional Pyrex Glass packing within the reactor at the corresponding space times (defined on basis of effective void space of reactor).

Examination of the values, (a) - (b), indicates a difference of such small magnitude that it is doubtful whether one can attach much significance to this quantity. This difference can be attributed to errors such as analysis of products, in plotting and interpolating Figure IV-5, and in calculating the effective space times. Consequently, it was considered that the effect of Pyrex Glass on the thermal decomposition of n-propanol is negligible, i.e. the reaction is essentially a homogeneous one.

C. The Effect of 316 Stainless Steel on the Decomposition of n-Propanol

1. The Change in Product Distribution with Type 316 Stainless Steel Present in the Glass Reactor

Figure IV-16 shows that the amounts of propionaldehyde, hydrogen, propionaldehyde dipropyl acetal, and n-propanol conversion all increase with increase in the contact time. On the other hand, the amounts of acetaldehyde, methane, ethane, and combined propane and propylene decrease. Figure IV-16 also shows no apparent change in the amount of carbon monoxide. The amount of acetaldehyde dipropyl acetal shows a maximum with respect to the contact time. The acetals mentioned above were not encountered in the case of the homogeneous thermal decomposition of n-propanol.

Table V-3

Comparison of n-Propanol Conversion between Decomposition with and without Pyrex Glass Packing

Space Time* [sec]	(a)** Without Pyrex Glass [mole %]	Pyrex Glass Added [gm]	(b) With Pyrex Glass [mole %]	(a) - (b)
7.1	0.4300	15	0.4432	-0.0132
6.8	0.4430	10	0.4488	-0.0055
6.6	0.4500	5	0.4612	-0.0112
6.3	0.4700	0	0.4653	+0.0057

* The space time in the decomposition with Pyrex Glass packing is defined in section IV-C.

** Values are read from Figure IV-5.

2. Catalytic Dehydrogenation by Type 316 Stainless Steel

From the change in chemical product species encountered when stainless steel was placed within the Pyrex Glass reactor, it is apparent that it must be exerting some catalytic influence. From the large amounts of hydrogen and propionaldehyde obtained, the stainless steel may be catalyzing a dehydrogenation reaction. From the homogeneous thermal decomposition of n-propanol which must simultaneously occur, the α-n-propanol radical which appears to be present may also be assumed to have been formed in the gas phase and to have been dehydrogenated. These two dehydrogenations are believed to proceed in the following manner:

$$\text{n-C}_3\text{H}_7\text{OH} \xrightarrow{\text{s.s.}} \text{CH}_3\text{CH}_2\text{CHOH}_{ad} + \text{H}_{ad} \qquad (75)$$

$$2\text{CH}_3\text{CH}_2\text{CHOH}_{ad} \longrightarrow \text{C}_2\text{H}_5\text{CHO}_{ad} + \text{n-C}_3\text{H}_7\text{OH}_{ad} \qquad (76)$$

$$\text{CH}_3\text{CH}_2\text{CHOH} + \text{CH}_3\text{CH}_2\text{CHOH}_{ad} \longrightarrow \text{n-C}_3\text{H}_7\text{OH}_{ad} + \text{C}_2\text{H}_5\text{CHO}_{ad} \qquad (77)$$

$$\text{CH}_3\text{CH}_2\text{CHOH}_{ad} \longrightarrow \text{C}_2\text{H}_5\text{CHO}_{ad} + \text{H}_{ad} \qquad (78)$$

$$\text{H}_{ad} + \text{H}_{ad} \longrightarrow \text{H}_2 \qquad (79)$$

Where the subscript "ad" means that the substance is adsorbed on the surface of stainless steel. If the dehydrogenation proceeds only by the reaction steps, (75), (78) and (79), which are

shown by the overall reaction (80), the amount of hydrogen produced should be the same as the amount of propionaldehyde.

$$n\text{-}C_3H_7OH \xrightarrow{s.s.} C_2H_5CHO + H_2 \qquad (80)$$

It was found that lesser amounts of hydrogen were obtained compared to the amounts of propionaldehyde, as shown in Figure IV-16. This could be explained by including reactions (76) and (77). The concentration of α-n-propanol radical in the gas phase is believed to decrease as the reaction (77) proceeds. Consequently, the formation of acetaldehyde by the reaction (49), which is considered to occur in the gas phase, will decrease. The formation of methane, ethane and combined propane plus propylene should also decrease, since the formation of methyl radical by the reaction (49) decreases.

3. Catalytic Dehydration by Type 316 Stainless Steel

Propionaldehyde dipropyl acetal and acetaldehyde dipropyl acetal are detected in the decomposition of n-propanol with type 316 stainless steel, but not in the homogeneous decomposition of n-propanol. Thus, it is considered that stainless steel has a catalytic dehydration effect as well.

The acetals may be formed as follows:

$$C_2H_5CHO + 2n\text{-}C_3H_7OH \xrightarrow{s.s.} C_2H_5CH(OC_3H_7)_2 + H_2O \qquad (81)$$

$$CH_3CHO + 2n\text{-}C_3H_7OH \xrightarrow{s.s.} CH_3CH(OC_3H_7)_2 + H_2O \qquad (82)$$

Because the stainless steel packing was fabricated from pieces

[illegible]

$$[illegible]$$

[illegible]

[illegible]

[illegible]

$$[illegible]$$

$$[illegible]$$

[illegible]

of 500 mesh screen (specific surface area = 1.3 sq m/gm), the catalytically active sites may not be numerous relative to those on high-surface-area porous catalysts. Since the formation of propionaldehyde by catalytic dehydrogenation increases more rapidly than the formation of acetaldehyde by homogeneous decomposition of n-propanol, one may expect the propionaldehyde to be present in larger amounts and thus to be more subject to condensation with n-propanol than the acetaldehyde.

The ratio of propionaldehyde to that of acetaldehyde will thus increase with contact time. Accordingly in reactions (81) and (82), propionaldehyde dipropyl acetal increases with respect to the contact time but acetaldehyde dipropyl acetal does not increase after a certain contact time as shown in Figure IV-16.

As mentioned earlier, stainless steel contains metal oxides such as Cr_2O_3, and NiO (17). These metal oxides may exhibit catalytic properties for dehydrogenation and dehydration reactions (18). The experimental results, as described above, are consistent with the catalytic activities of these metal oxides.

D. Summary of Proposed Mechanism

1. The Influences of Temperature, Pyrex Glass and Type 316 Stainless Steel Surface

The experimental results were discussed and the influences of temperature, the Pyrex Glass surface and the stainless steel surface

on the decomposition of n-propanol were clarified as shown in Table V-4.

2. Reaction Mechanisms Discussed for Homogeneous Thermal Decomposition of n-Propanol

Three kinds of reaction mechanisms were discussed from points of view of chemical product species in the product, stoichiometry of the product compounds, and reaction kinetics. The mechanisms discussed were the molecular mechanism, the free-radical mechanism induced direct bond dissociation of n-propanol, and the free-radical mechanism initiated by a foreign gas such as oxygen. Table V-5 shows the suitabilities of the mechanisms to the points.

E. <u>Application of These Results to Future Studies</u>

1. The Homogeneous Thermal Decomposition of n-Propanol

Since the n-propanol conversion in the homogeneous thermal decomposition of n-propanol is small (the maximum n-propanol conversion was 0.8651 mole % at the residence time 38.0 sec, and the temperature, 463°C), it is possible to neglect this influence in the study of catalytic reactions of n-propanol when the n-propanol conversion is high, for example, as in the study by Wanke (1) using a silica alumina catalyst treated with NaOH. However, in the investigation at low concentrations, such as the study of initial reaction rates at high space velocities, the influence of the thermal decomposition of n-propanol should be accounted for. Since it is expected as mentioned above that some substance like a foreign gas such as oxygen may initiate the

Table V-4

The Influence of Temperature,

Pyrex Glass and Type 316 Stainless Steel

on n-Propanol Decomposition

Temperature	The radical reactions initiated by a foreign gas such as oxygen occur. The maximum value of n-propanol conversion is 0.8651 mole % at the residence time 38.0 sec, and the temperature 463°C.
Pyrex Glass Surface	No significant influence was found.
Stainless Steel Surface	Catalytic dehydrogenation and dehydration were found.

Table V-5

Suitabilities of the Mechanisms in

Homogeneous Thermal Decomposition of n-Propanol

	Molecular Mechanism	Free-Radical Mechanism Induced by Direct Bond Dissociation in n-Propanol	Free-Radical Mechanism Initiated by a Foreign Gas such as Oxygen
Chemical Product Species	No	No	Yes
Stoichiometry of Product	No	No	Yes
Reaction Kinetics	No	No	Yes At higher temperature ($>440^{\circ}C$) No At lower temperature ($<400^{\circ}C$)

reaction, some treatments of n-propanol which is used as the reactant, such as distillation or treatment with hydroquinone to free it from some substance such as oxygen or peroxide, which may be initiators of radical reactors, should be attempted.

The "map" of n-propanol conversion versus temperature and residence time, shown in Figure IV-14, is helpful to select the reaction conditions at which it is efficient to carry out such an investigation.

2. The Effect of Pyrex Glass on the Decomposition of n-Propanol

It was found in the present investigation that the effect of Pyrex Glass on the decomposition was negligible, so that the reactor fabricated from Pyrex Glass is adequate for future kinetic studies.

3. The Effect of Type 316 Stainless Steel on the Decomposition of n-Propanol

From the results of the present investigation, it is apparent that the stainless steel effects as catalyst on dehydrogenation and dehydration of n-propanol. Therefore, the use of the stainless steel reactor should be avoided.

VI. CONCLUSION

The following conclusions were obtained in the present investigation.

A. The Thermal Decomposition of n-Propanol

1. A maximum conversion of 0.8651 mole % of n-propanol was obtained at the residence time, 38.0 sec, and the temperature of 463°C.

2. The molecular mechanism in the thermal decomposition of n-propanol in the temperature region from 380°C to 463°C is believed to play a minor part, if any.

3. The free-radical mechanism induced by bond dissociation in n-propanol seemingly plays a minor part, if any, in the thermal decomposition of n-propanol.

4. The presence of some foreign substance such as oxygen could account for the thermal decomposition effects. The radical species, α-n-propanol radical is felt to be very significant in this mechanism.

5. A chain reaction seems to proceed to some extent in the decomposition of n-propanol at temperatures above 440°C but not at temperatures below 400°C. The main chain propagation step is thought to be the decomposition of α-n-propanol radical.

B. The Effect of Pyrex Glass on the Decomposition of n-Propanol

The effect of Pyrex Glass on the thermal decomposition is

negligible, if any, at temperatures up to 463°C.

C. <u>The Effect of Type 316 Stainless Steel on the Decomposition of n-Propanol</u>

1. The stainless steel has a catalytic effect on the dehydrogenation of n-propanol and also seems to have an effect on α-n-propanol radical.

2. The stainless steel also has a catalytic dehydration effect resulting in the formation of propionaldehyde dipropyl acetal and acetaldehyde dipropyl acetal.

3. The decomposition of α-n-propanol radical into acetaldehyde and methyl radical may take place in the gas phase.

4. The maximum conversion of n-propanol due to thermal decomposition with the stainless steel present at the temperature of 463°C and a space velocity of 0.0151 [(gm-mole of n-propanol feed)/(hr)(gm-stainless steel)] was 0.7871 mole %.

VII. RECOMMENDATION

1. A reactor made of a stainless steel should be avoided because of its catalytic activity. A reactor made of Pyrex Glass is recommended.

2. Although the magnitude of thermal decomposition of n-propanol in the temperature region of $380^{\circ}C$ to $463^{\circ}C$ is small, it is recommended that precaution is taken to ensure that the n-propanol is free from possible contaminants such as oxygen.

3. The equipment which was constructed and used in the present investigation is excellent for controlling the reaction temperature (the fluctuation was less than $1^{\circ}C$), and for product sampling and handling. It is shown that the equipment may be used in future kinetic investigations of the catalytic dehydrogenation of n-propanol, for example, on an alundum catalyst, providing n-propanol conversions are well above one or two mole %.

4. Using a more precise syringe for the micro-feeder would improve the accuracy of the n-propanol feed rate.

5. The chromatography analytical methods used in the present investigation were sufficient. It is believed that the relative amount of the product components can be detected reliably at lower n-propanol conversions than those obtained in the present investigation.

BIBLIOGRAPHY

1. Wanke, S.E., "Dehydrogenation of n-Propanol on an Alundum Catalyst," M. Sc. Thesis, U. of Alberta, Edmonton, Alberta, April 1966.

2. Semenov, N.N., "Some Problems in Chemical Kinetics and Reactivity," Vol. 1, Vol. 2, Princeton University Press, Princetone, (1958).

3. Steacie, E.W.R., "Atomic and Free-Radical Reaction," Reinhold Publishing Corporation, New York, (1946) 2nd, ed., (1954).

4. Hinshelwood, C.N., "The Kinetics of Chemical Change," The Clarendon Press, Oxford, (1940).

5. Rice, F.O., and Rice, K.K., "The Aliphatic Free-Radicals," Johns Hopkins Press, Baltimore (1935).

6. Kozlov, S.T., Tantsyrev, G.D., and Talroze, V.L., Zavodsk. Lab., 31 (9), 1113-14 (1965).

7. Steacie, E.W.R., Chem. Reviews, 22, 311 (1938).

8. Laidler, K.J., "Chemical Kinetics," McGraw-Hill Book Company, Inc., New York (1950), p. 238.

9. Levenspiel, O., "Chemical Reaction Engineering," John Wiley and Sons, Inc., New York (1962), p. 34.

10. Kerr, J.A., Chem. Rev., 66, 465 (1966).

11. Hinshelwood, C.N., loc. cit., p. 175.

12. Rice, F.O., and Herzfeld, K.F., J. Am. Chem. Soc., 56, 284 (1934).

13. Letort, M., Compt. rend., 197, 1042 (1933).

14. Hinshelwood, C.N., and Askey, P.J., J. Chem. Soc., 812 (1936).

15. Morris, J.C., J. Am. Chem. Soc., 66, 584 (1944).

16. Verhock, F.H., Trans Farady Soc., 31, 1527 (1935).

17. Kubaschewski, O., and Hopkins, B.E., "Oxidation of Metals and Alloys," Butterworths Scientific Publications, London, (1953), p. 76, p. 156.

18. Berkman, S., Morrell, J.C., and Egloff, G., "Catalysis, Inorganic and Organic," Reinhold Publishing Corporation, New York, (1940), p. 735, p. 888.

19. Roberts, J.D., and Caserio, M.C., "Basic Principles of Organic Chemistry," W.A. Benjamin, Inc., (1964), p. 433.

20. Moiseev, I.I., Grigorev, A.A., and Klimenko, M. Ya., U.S.S.R. Patent, 165,436, Oct. 12, (1964).

21. Kondratev, V.N., "Chemical Kinetics of Gas Reaction," Addison-Wesley Publishing Company Inc., London, (1964).

22. Perry, J.H., "Chemical Engineering Handbook," 4th. ed., McGraw-Hill Book Company, New York (1963) p. 3-39.

23. Corning Glass Works Catalogue B-83, "Properties of Selected Commercial Glasses," New York, Corning Glass Works, (1965).

24. Vasudeva, K., "Vapor Phase Reactions of n-Propanol on Solid Catalysts," Ph. D. Thesis, U. of Alberta, Edmonton, Alberta, September 1965.

25. Anderson, N.E., "The Partial Oxidation of n-Butane in a Plug Flow Reactor," Ph. D. Thesis, U. of Alberta, Edmonton, Alberta, January 1966.

26. Sugaku Handbook Hensyn Iinkai, "Sugaku Handbook," Maruzen, Tokyo, (1960) p. 297.

27. Messner, A.E., Rosie, D.M., and Argabright, P.A., Anal. Chem., 31, 230-233 (1959).

28. Gray, P., and Williams, A., Chem. Rev., 59, 239 (1959).

29. Laidler, K.J., loc. cit., p. 258.

30. Satterfield, C.N., and Reid, R.C., J. Chem. & Eng. Data, 6, 302-304 (1961).

31. Steacie, E.W.R., "Atomic and Free-Radical Reaction," Reinhold Publishing Corporation, New York, (1946), p. 81.

32. Laidler, K.J., loc. cit., p. 258.

33. Perry, J.H., loc. cit., p. 23-36.

34. Laidler, K.J., loc. cit., p. 78.

35. Semenov, N.N., loc. cit., Vol. 1, p. 3.

36. Ibid., Vol. 2, p. 204.

37. Ibid., Vol. 1, p. 41.

38. Ibid., Vol. 2, p. 264-265.

39. Nagasako, N., Sato, K., Kiyoura, R.,"Kogyo Kagaku Keisan," Vol. 1, Hirokawa Shoten, Tokyo, (1959), p. 29.

A P P E N D I X   I

CALIBRATION OF MICRO-FEEDER

The micro-feeder was calibrated by feeding n-propanol at a temperature of 80°F. The n-propanol was collected in a 25 ml Erlenmeyer flask after it had passed through the $\frac{1}{16}$ in. stainless steel tubing (P in Figure IV-1). The Erlenmeyer flask was cooled by ice-water in order to prevent the loss of n-propanol by evaporation. The n-propanol was obtained by weighing. Prior to the operation of the micro-feeder, the position of the piston in the syringe was set at a level of 60 cc. The syringe used had a capacity of 100 cc. The calibration of micro-feeder is shown in Table A-I-1.

Table A-I-1

Calibration of Micro-Feeder

Fluid	n-Propanol
Feeder	100 cc glass syringe
Temperature	80°F

Velocity of Piston in Syringe

Run	10 mm/hr	15 mm/hr	20 mm/hr	40 mm/hr
1	6.9370[g]	10.1760[g]	13.7928[g]	27.4700[g]
2	6.7456	10.5066	13.7616	27.5628
3	6.8277	10.1805	13.5522	27.1168
4	7.0970	10.3007	13.5348	27.220
5	6.8024	10.0886	13.6118	
Average	6.8819	10.2505	13.6506	27.3429

[illegible]

[illegible]

[illegible]

[illegible]

[illegible]	[illegible]	[illegible]	[illegible]	[illegible]
[illegible]	[illegible]	[illegible]	[illegible]	[illegible]
[illegible]	[illegible]	[illegible]	[illegible]	[illegible]
[illegible]	[illegible]	[illegible]	[illegible]	[illegible]
[illegible]	[illegible]	[illegible]	[illegible]	[illegible]
[illegible]	[illegible]	[illegible]	[illegible]	[illegible]
[illegible]	[illegible]	[illegible]	[illegible]	[illegible]

The mean of feed rates will be estimated as follows (26). The confidence interval of the mean at confidence coefficient α is given by

$$\overline{X} - t_\alpha \frac{\sigma}{\sqrt{n}} < m < \overline{X} + t_\alpha \frac{\sigma}{\sqrt{n}} \qquad \text{(I-1)}$$

Where, $\overline{X}$ is an arithmatic average of sampling variables X_i

t_α is defined as $\frac{1}{\sqrt{2\pi}} \int_{-t_\alpha}^{t_\alpha} e^{-\frac{1}{2}y^2} dy = \alpha$

n is the number of levels

m is the population mean

σ is the population variance

σ^2 is estimated with the equation, $\frac{1}{n} \sum_{i=1}^{n} (X_i - \overline{X})^2$ (I-2)

Table I-2

Values of σ

Piston Velocity [mm/hr]	10	15	20	40
Variance, σ	0.1242	0.1444	0.1069	0.1804

Table I-2

Values of $t_\alpha\ \sigma/\sqrt{n}$

Piston Velocity [mm/hr]	10	15	20	40
Values of $t_\alpha\ \sigma/\sqrt{n}$	0.3193	0.3713	0.2748	0.5008

t_α at $\alpha = 0.05$ and $n = 5$ is 2.571

t_α at $\alpha = 0.05$ and $n = 4$ is 2.776

[illegible]

$$[illegible]$$

[illegible]

$$[illegible]$$

[illegible]

[illegible]

[illegible]

[illegible]

$$[illegible]$$

Table A-I-3

Means of Feed Rates of n-Propanol

Piston Velocity [mm/hr]	Feed Rates of n-Propanol [g/hr]
10	6.8819 ± 0.3193
15	10.2505 ± 0.3713
20	13.6506 ± 0.2748
40	27.3429 ± 0.5008

The density of n-propanol at 80°F is 0.767 g/cc, so that the feed rates of n-propanol by volume are shown in Table A-I-4. Figure A-I-1 shows the calibration lines of n-propanol feed.

Table A-I-3

Means of Feed Rates of n-Propanol at 80°F

Piston Velocity [mm/hr]	Feed Rates of n-Propanol [cc/hr]
10	5.3 ± 0.24
15	7.9 ± 0.28
20	10.5 ± 0.21
40	21.0 ± 0.39

[illegible]

[illegible]

[illegible]	[illegible]
[illegible]	[illegible]
[illegible]	[illegible]
[illegible]	[illegible]
[illegible]	[illegible]

[illegible]

[illegible]

[illegible]

[illegible]	[illegible]
[illegible]	[illegible]
[illegible]	[illegible]
[illegible]	[illegible]
[illegible]	[illegible]

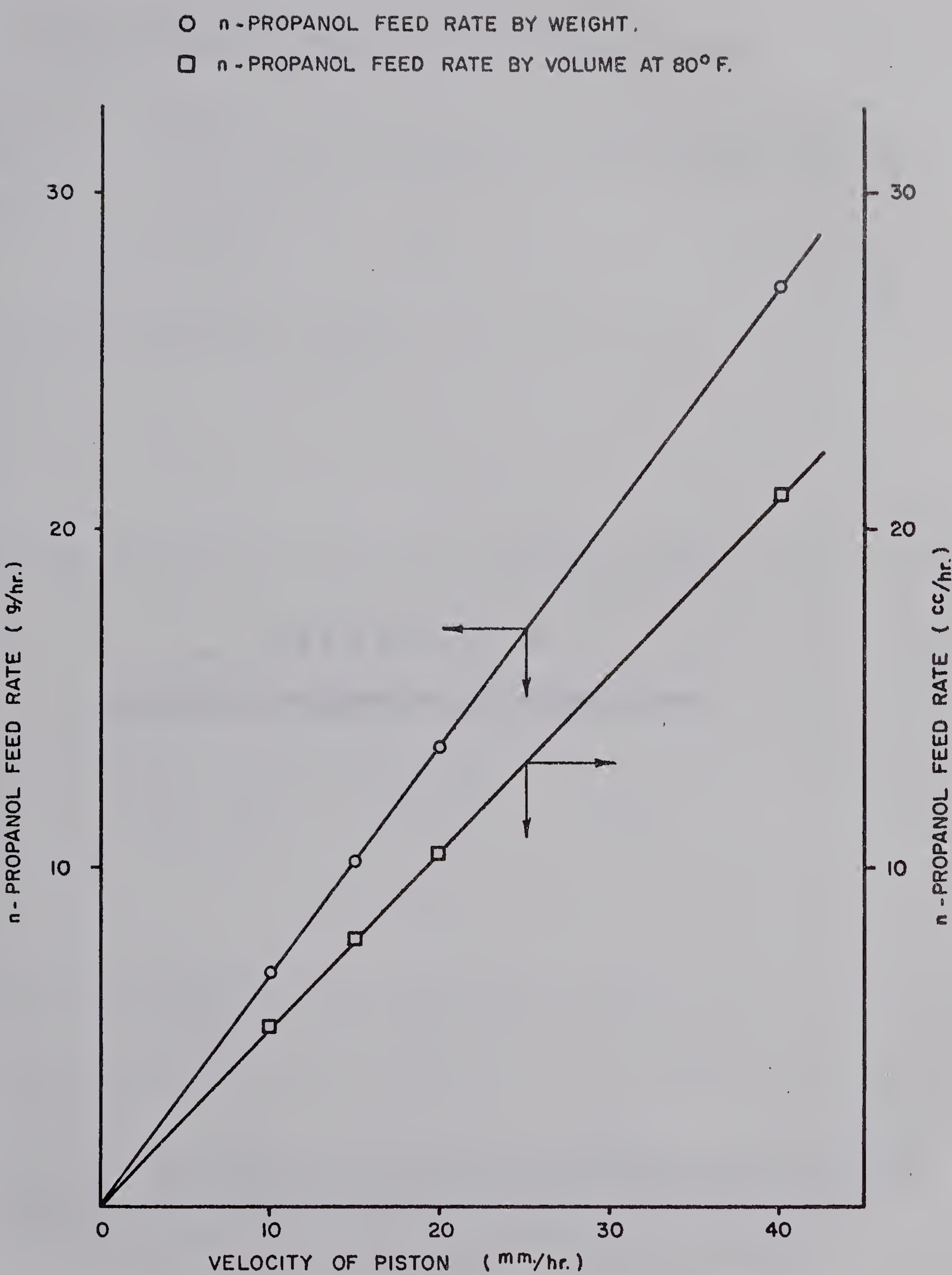

FIGURE A-I-1: CALIBRATION OF MICRO-FEEDER

APPENDIX II

ANALYSIS OF HYDROGEN BY GAS CHROMATOGRAPHY

When helium is used as a carrier gas, the analysis of hydrogen by gas-chromatography is complicated, since not only is the detector sensitivity low, but also the hydrogen peak has a negative polarity at high hydrogen concentrations.

In this investigation however, it was found that the analysis of hydrogen by gas-chromatography, using helium gas as a carrier, was possible in the low concentration regions 0 to 7 mole %. Synthetic mixtures of known amounts of hydrogen with air were analysed to obtain the relationship between mole % and peak area. The gas chromatograph operating variables were the same as described in section III-D-2.

The results are shown in Table A-II-1 and Figure A-II-1.

Table A-II-1

Analysis of Synthetic Known Blends of Hydrogen

True Mole %	Peak Area*	Average
0.670	248	
	237	
	250	245
1.531	473	
	472	
	470	472
2.791	831	
	830	831
7.121	1838	
	1794	
	1834	1822

* Values integrated by a digital integrator (See section III-D).

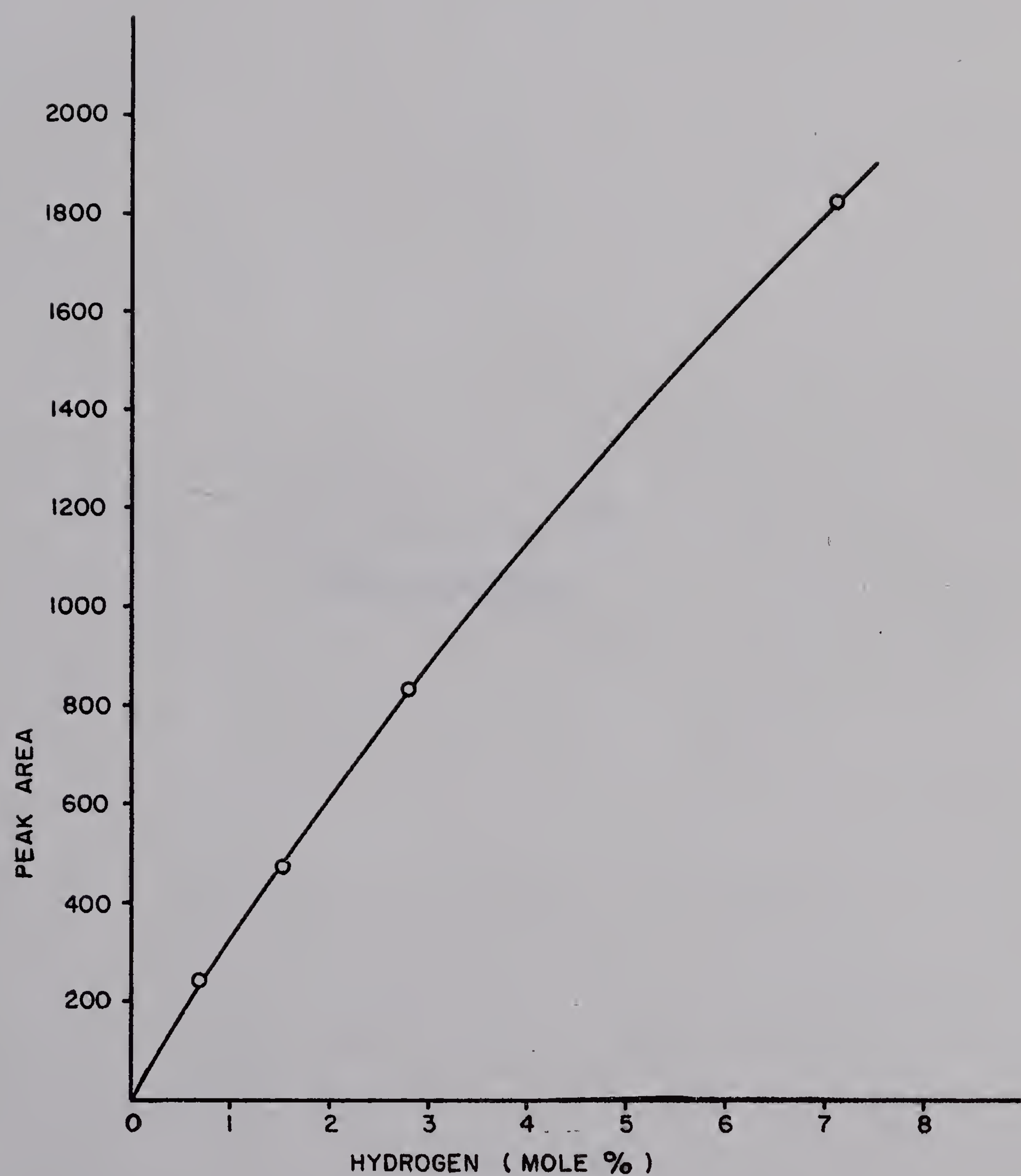

FIGURE A-II-1: CALIBRATION OF HYDROGEN PEAK AREAS

A P P E N D I X III

PRODUCT ANALYSIS

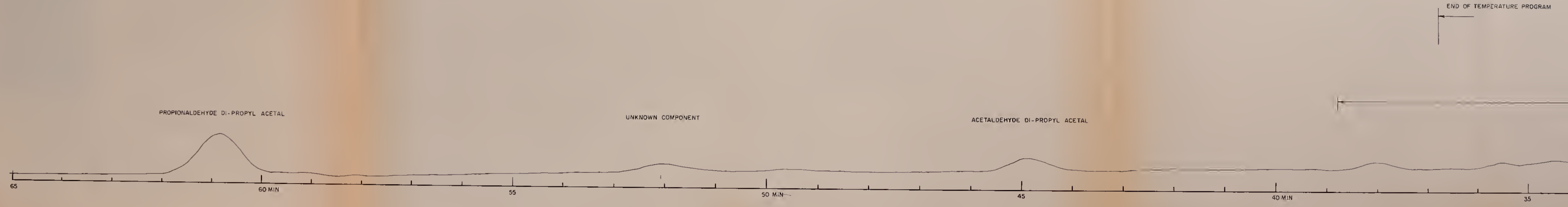
END OF TEMPERATURE PROGRAM
PROPIONALDEHYDE DI-PROPYL ACETAL
UNKNOWN COMPONENT
ACETALDEHYDE DI-PROPYL ACETAL
65
60 MIN
55
50 MIN
45
40 MIN
35

FIGURE A-III-1

LIQUID ANALYSIS USING UCON ON CHROMOSORB W COLUMN

SAMPLE : LIQUID PRODUCT OF RUN 28

COMPONENT	PEAK AREA
ETHANE	3
PROPANE + PROPYLENE	515
ACETALDEHYDE	1646
PROPIONALDEHYDE	8468
n-PROPANOL	2533365
ACETALDEHYDE DI-PROPYL ACETAL	860
PROPIONALDEHYDE DI-PROPYL ACETAL	4300

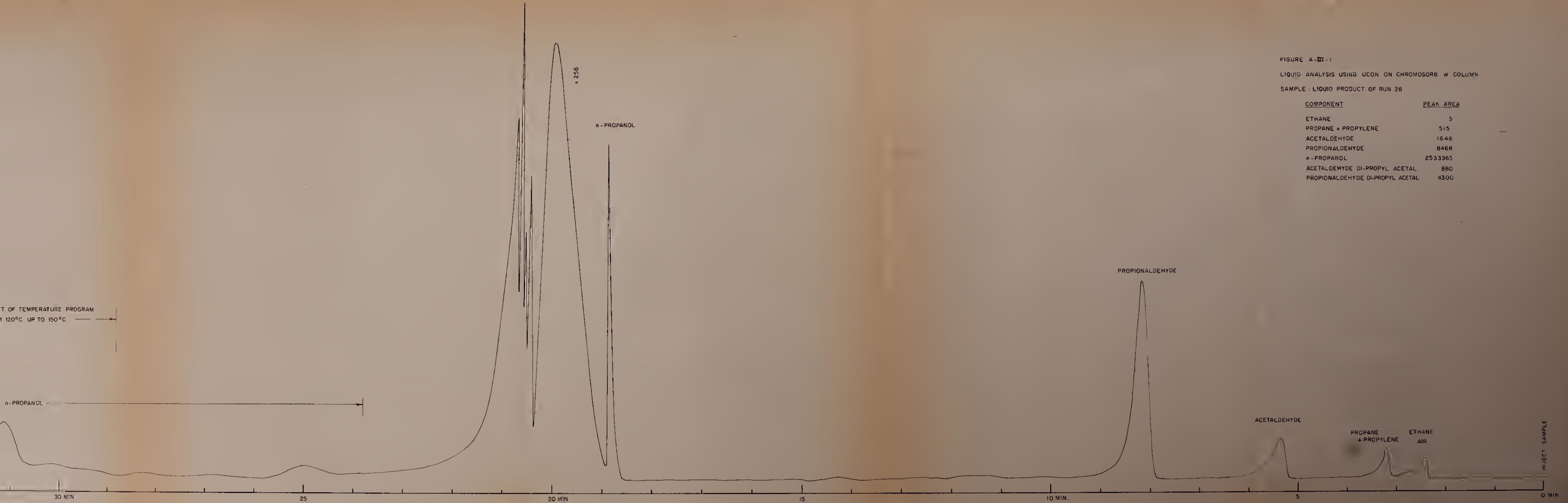

FIGURE A-III-2

GAS ANALYSIS USING UCON ON CHROMOSORB W COLUMN

SAMPLE: GAS PRODUCT OF RUN 28

COMPONENT	PEAK AREA
H_2 + Air + CO + CH_4	(1672, 1368)
ETHANE	1113
PROPANE + PROPYLENE	1105

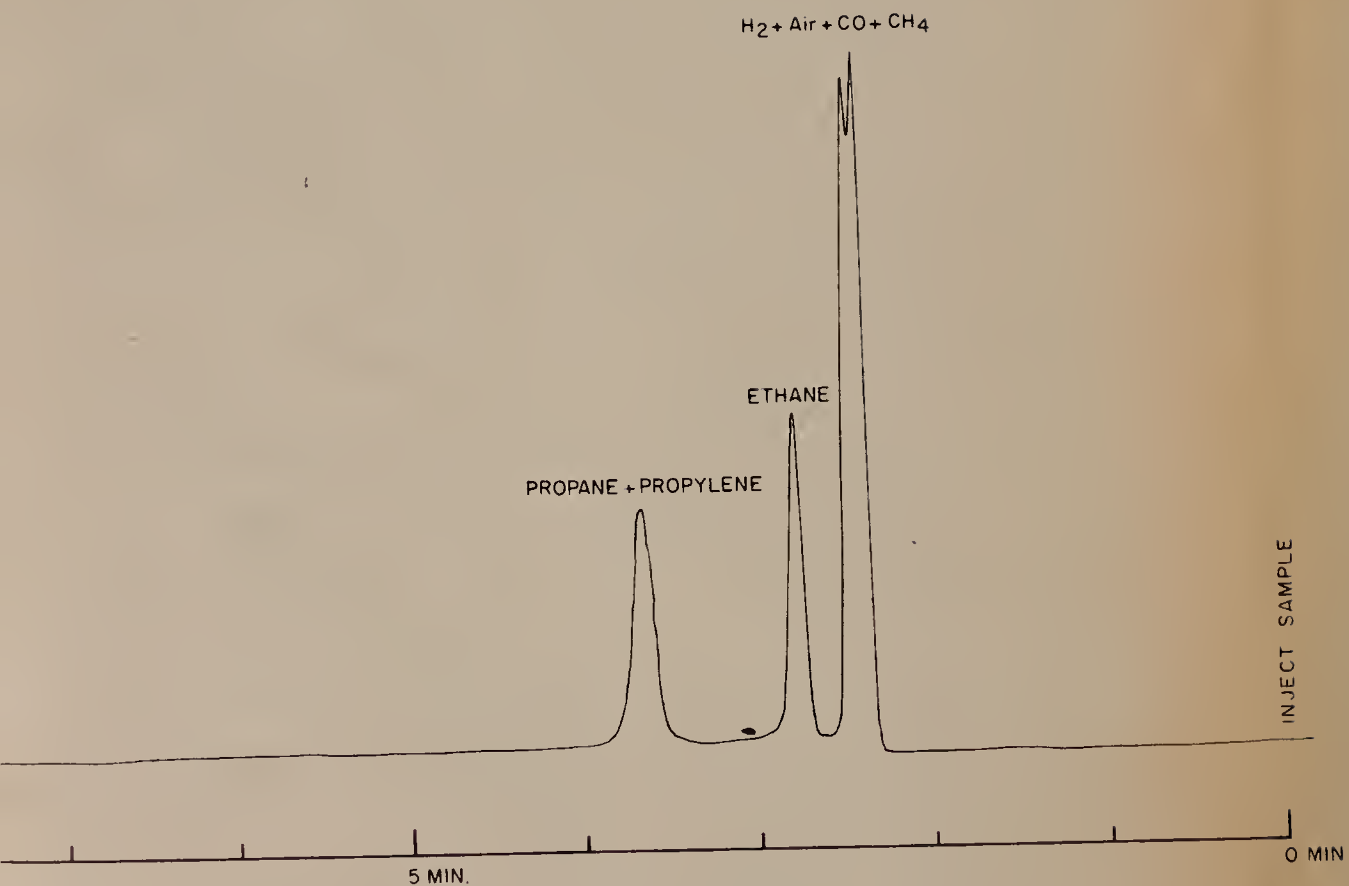

FIGURE A-III-3

GAS ANALYSIS USING ACTIVATED CHARCOAL COLUMN

SAMPLE : GAS PRODUCT OF RUN 28

COMPONENT	PEAK AREA
HYDROGEN	219
OXYGEN	2430
NITROGEN	6767
CARBON MONOXIDE	279
METHANE	1332

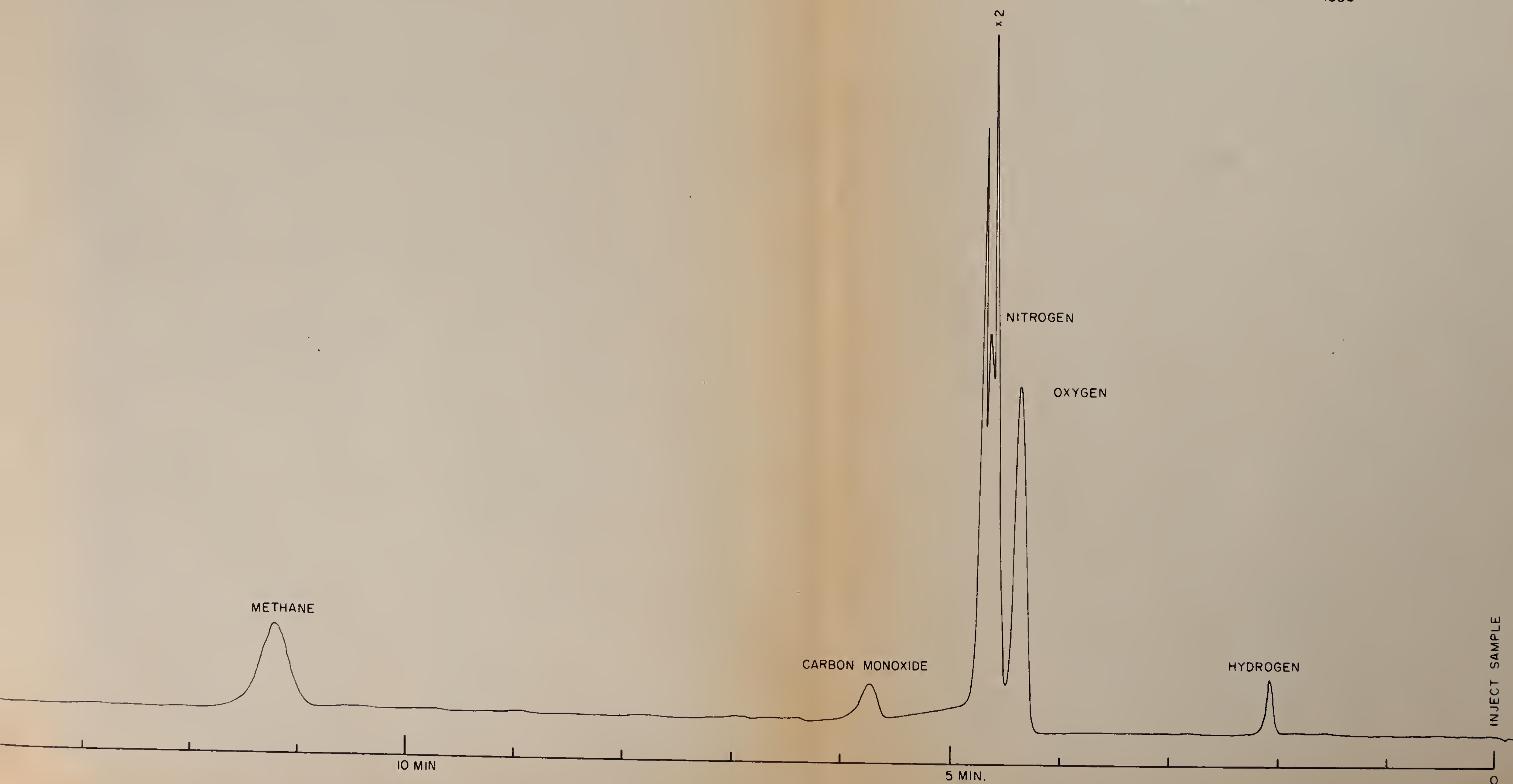

A P P E N D I X IV

RELATIVE THERMAL CONDUCTIVITY

The relative thermal conductivity responses used in the present investigation are shown in Table A-IV-1.

Table A-IV-1

Relative Thermal Conductivity Responses

Component	Thermal Conductivity Responses	Reference
Ethane	0.51	(27)
Propane	0.65	(27)
Propylene	0.63	(27)
Acetaldehyde	0.69	(25)
Propionaldehyde	0.80	(25)
n-Propanol	0.83	(27)
Acetaldehyde di-propyl acetal	1.83*	
Propionaldehyde di-propyl acetal	1.98*	
Diethyl ether	1.10	(27)
Diisopropyl ether	1.30	(27)
Di-n-propyl ether	1.31	(27)
Ethyl-n-butyl ether	1.30	(27)
Di-n-butyl ether	1.60	(27)
Di-n-amyl ether	1.83	(27)

* Estimated from values obtained for ethers.

APPENDIX V

KARL FISCHER TITRATION

An attempt was made to use the Karl Fischer titration for analysis of water in the liquid product. The apparatus consisted of the following components.

a) COLEMAN TITRION Model 32 Automatic Titrator

b) COLEMAN METRION 11 AC pH METER

c) COLEMAN Karl Fischer Adaptor 31-030

d) COLEMAN Glass Electrode 3-410

e) COLEMAN Reference Electrode 3-510

The Karl Fischer reagent used was supplied by Fischer Scientific Company (Catalogue No. So-K-3). The standard water-methanol solution used contained 15.2131[g-water/1000 ml solution]. 15 ml of the standard solution was titrated against the Karl Fischer reagent to obtain the end point of the titration (See Figure A-V-1).

The end point was set at PH 4.61 according to Figure A-V-1 and the standard solution was titrated to obtain the reagent factor [g-water/ml-Karl Fischer reagent]. The results of the titration used to determine the reagent factor are shown in Table A-V-1.

Table A-V-1

Reagent Factor

Run No.	Standard Solution [ml]	K.F.R.* [ml]	Reagent Factor [g-water/ml-K.F.R.*]
1	1.14	0.52	3.33×10^{-2}
2	0.99	0.41	3.67×10^{-2}
3	1.00	0.52	2.93×10^{-2}

* K.F.R. is the Karl Fischer reagent

The size of the titration samples used was approximately 2 ml. The samples were products of Run 19 and 20. Due to the extremely small amount of water in the above samples, the Karl Fischer titration technique was found to be unsatisfactory. A single drop of the Karl Fisher reagent exceeded the end point.

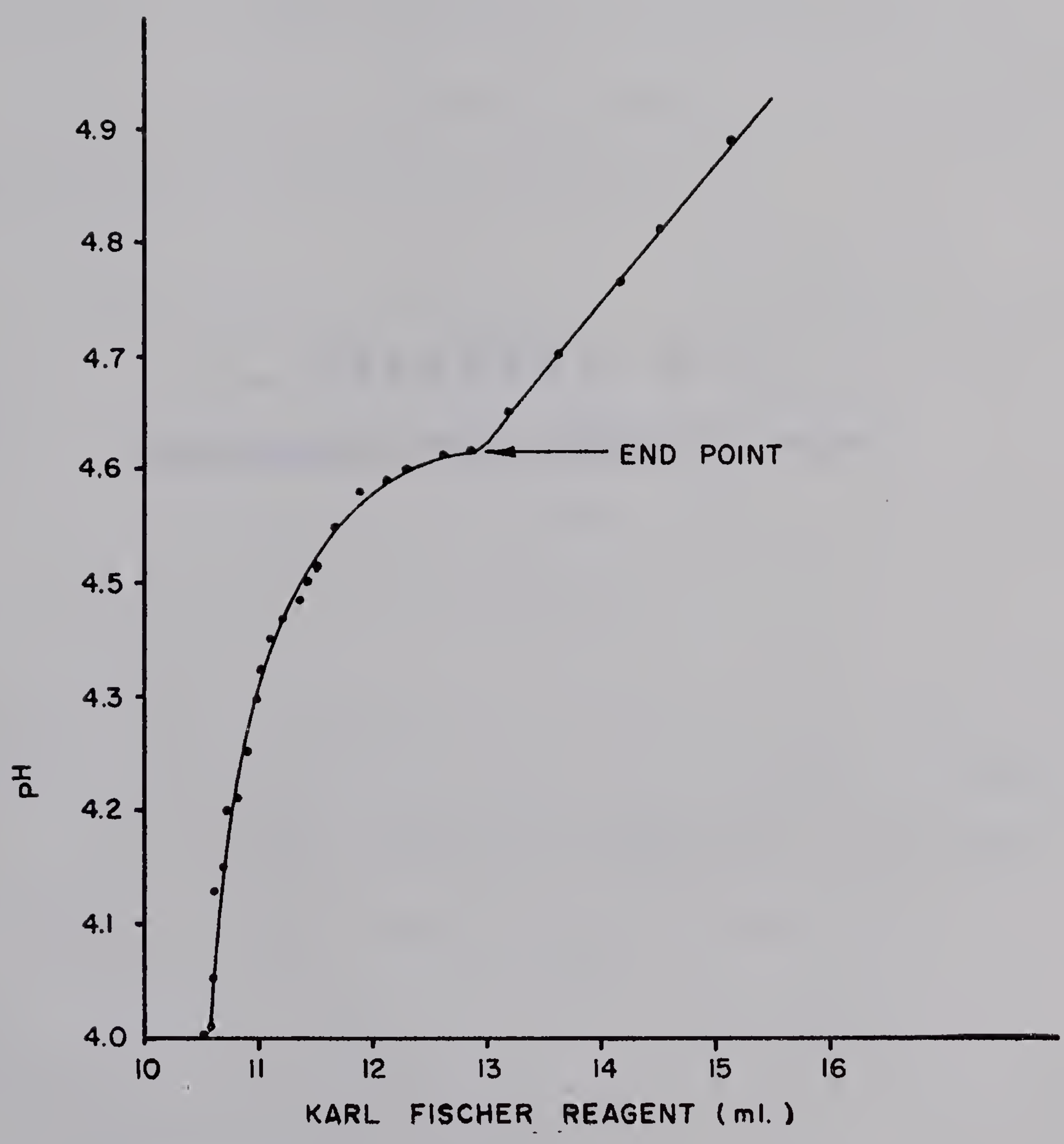

FIGURE A-V-1: TITRATION OF STANDARD SOLUTION

APPENDIX VI

CALCULATION OF BOND DISSOCIATION ENERGY

[illegible]

[illegible]

In the radical decomposition,

$$A\text{–}B \longrightarrow A\cdot + B\cdot \qquad \text{(VI-1)}$$

the dissociation energy D(A–B) is given by

$$D(A\text{–}B) = \Delta H_f^\circ(A\cdot) + \Delta H_f^\circ(B\cdot) - \Delta H_f^\circ(A\text{–}B), \qquad \text{(VI-2)}$$

where, ΔH_f° is the heat of formation at standard state (10).

The following reactions may account for the primary reactions of the thermal decomposition of n-propanol:

$$CH_3CH_2CH_2OH \longrightarrow CH_3 + CH_2CH_2OH \qquad \text{(VI-3)}$$

$$\longrightarrow CH_3CH_2 + CH_2OH \qquad \text{(VI-4)}$$

$$\longrightarrow CH_3CH_2CHOH + H \qquad \text{(VI-5)}$$

$$\longrightarrow CH_3CH_2CH_2 + OH \qquad \text{(VI-6)}$$

$$\longrightarrow CH_3CH_2CH_2O + H \qquad \text{(VI-7)}$$

The dissociation energies of the C–H bonds of the β and γ carbons of n-propanol may be similar to those of the C–H bonds of alkanes.

The dissociation energies, $D(CH_3CH_2CH_2 - OH)$, $D(CH_3 - CH_2CH_2OH)$ and $D(CH_3CH_2 - CH_2OH)$, can be calculated as follows:

a) $D(CH_3CH_2CH_2 - OH)$:

$\Delta H_f^\circ(CH_3CH_2CH_2OH) = -62.2$ Kcal (28)

$\Delta H_f^\circ(CH_3CH_2CH_2) = 21.0$ Kcal (10)

$\Delta H_f^\circ(OH) = 9.3$ Kcal (10)

Therefore, $D(CH_3CH_2CH_2 - OH) = 92.5$ Kcal

b) $D(CH_3 - CH_2CH_2OH)$:

$\Delta H_f^\circ(CH_3CH_2CH_2OH) = -62.2$ Kcal (28)

$\Delta H_f^\circ(CH_3) = 34.0$ Kcal (10)

$\Delta H_f^\circ(C_2H_5O) = -8.5$ Kcal (28)

Hydrogen-atom migration from distant CH_2 group is

$C_2H_5O\cdot \longrightarrow \cdot CH_2CH_2OH = -8.5$ Kcal (28)

Therefore,

$\Delta H_f^\circ(\cdot CH_2CH_2OH) = \Delta H_f^\circ(C_2H_5O) - (-8.5)$

$= -17.0$ Kcal

Therefore,

$D(CH_3 - CH_2CH_2OH) = 79.2$ Kcal

c) $D(CH_3CH_2 - CH_2OH)$:

$\Delta H_f^\circ(CH_3CH_2CH_2OH) = -62.2$ Kcal (28)

$\Delta H_f^\circ(CH_3CH_2^{\cdot}) = 25.7$ Kcal (10)

$\Delta H_f^\circ(CH_3O) = 2$ Kcal (10)

Hydrogen-atom rearrangement of alkoxyl radical is

$CH_3O\cdot \longrightarrow \cdot CH_2OH - 7.5$ Kcal (28)

Therefore,

$\Delta H_f^\circ(\cdot CH_2OH) = -5.5$ Kcal

Therefore,

$D(CH_3CH_2 - CH_2OH) = 82.4$ Kcal

Though it is impossible to calculate the dissociation energy, $D(HOCH(C_2H_5) - H)$, of the reaction VI-5 due to the lack of information about the heat of formation of the radicals, the dissociation energy

is estimated to be approximately 90-92 Kcal from the values shown in Table A-VI-1, (10).

Table A-VI-1

Values of C-H Bond Dissociation Energies of Alcohol (10)

$D(HOCH_2 - H)$	92 Kcal
$D(HOCH(CH_3) - H)$	90 Kcal

The dissociation energies obtained for the reactions IV-3 to VI-7 are shown in Table A-VI-2.

Table A-VI-2

Dissociation Energies of n-Propanol

Values in Kcal/mole

Reaction	Dissociation Energy
VI-3	79.2*
VI-4	82.4*
VI-5	90-92 **
VI-6	92.5*
VI-7	103

* The values calculated by the author

** The value estimated from similar reactions

A P P E N D I X VII

EXPERIMENTAL CONDITIONS

Table A-VII-1

Experimental Conditions

	1	2	3	4	5	6	7	8
Run No.	Feed Rate [mole/hr]	Bath Temp [°C]	Reactor Temp [°C]	Press Dif [mm H_2O]	Atmosphere [mm Hg]	Sampling Period [min]	Liquid Sample [mole]	Gas Sample [mole]
1	0.1143	380	379.0	0	705.0	60	0.1142	0.00002
2	0.1722	380	378.5	0	705.0	40	0.1147	0.00003
3	0.2259	380	378.5	0	705.0	30	0.1129	0.00005
4	0.4621	380	378.0	0	705.0	15	0.1154	0.00007
5	0.1147	400	398.5	0	704.7	60	0.1146	0.00002
6	0.1719	400	398.5	0	704.8	40	0.1145	0.00005
7	0.2333	400	398.5	0	704.8	30	0.1165	0.00006
8	0.4495	400	398.0	0	704.8	15	0.1122	0.00009
9	0.1129	420	419.0	0	704.8	60	0.1128	0.00004
10	0.1693	420	418.5	0	704.8	40	0.1127	0.00008

[illegible]

[illegible]

[illegible]	[illegible]	[illegible]	[illegible]	[illegible]	[illegible]	[illegible]	[illegible]	[illegible]
[illegible]	[illegible]	[illegible]	[illegible]	[illegible]	[illegible]	[illegible]	[illegible]	[illegible]
[illegible]	[illegible]	[illegible]	[illegible]	[illegible]	[illegible]	[illegible]	[illegible]	[illegible]
[illegible]	[illegible]	[illegible]	[illegible]	[illegible]	[illegible]	[illegible]	[illegible]	[illegible]
[illegible]	[illegible]	[illegible]	[illegible]	[illegible]	[illegible]	[illegible]	[illegible]	[illegible]
[illegible]	[illegible]	[illegible]	[illegible]	[illegible]	[illegible]	[illegible]	[illegible]	[illegible]
[illegible]	[illegible]	[illegible]	[illegible]	[illegible]	[illegible]	[illegible]	[illegible]	[illegible]
[illegible]	[illegible]	[illegible]	[illegible]	[illegible]	[illegible]	[illegible]	[illegible]	[illegible]
[illegible]	[illegible]	[illegible]	[illegible]	[illegible]	[illegible]	[illegible]	[illegible]	[illegible]
[illegible]	[illegible]	[illegible]	[illegible]	[illegible]	[illegible]	[illegible]	[illegible]	[illegible]
[illegible]	[illegible]	[illegible]	[illegible]	[illegible]	[illegible]	[illegible]	[illegible]	[illegible]
[illegible]	[illegible]	[illegible]	[illegible]	[illegible]	[illegible]	[illegible]	[illegible]	[illegible]

Table A-VII-2

Experimental Conditions

Run No.	1 Feed Rate [mole/hr]	2 Bath Temp [°C]	3 Reactor Temp [°C]	4 Press Dif [mm H_2O]	5 Atmosphere [mm Hg]	6 Sampling Period [min]	7 Liquid Sample [mole]	8 Gas Sample [mole]
11	0.2262	420	418.5	0	704.8	30	0.1129	0.00011
12	0.4553	420	418.5	0	704.8	15	0.1136	0.00017
13	0.1113	440	438.0	0	704.8	60	0.1112	0.00007
14	0.1717	440	438.0	0	704.8	40	0.1143	0.00014
15	0.2257	440	438.0	0	704.8	30	0.11267	0.00019
16	0.4738	440	438.0	0	704.8	15	0.1181	0.00028
17	0.1134	463	461.5	0	704.8	60	0.1133	0.00013
18	0.1817	463	461.0	0	704.8	40	0.1208	0.00025
19	0.2247	463	461.0	0	704.8	30	0.1120	0.00034
20	0.4553	463	460.5	0	704.8	15	0.1133	0.00050

[illegible]

[illegible]

[illegible]	[illegible]	[illegible]	[illegible]	[illegible]	[illegible]	[illegible]	[illegible]	[illegible]
[illegible]	[illegible]	[illegible]	[illegible]	[illegible]	[illegible]	[illegible]	[illegible]	[illegible]
[illegible]	[illegible]	[illegible]	[illegible]	[illegible]	[illegible]	[illegible]	[illegible]	[illegible]
[illegible]	[illegible]	[illegible]	[illegible]	[illegible]	[illegible]	[illegible]	[illegible]	[illegible]
[illegible]	[illegible]	[illegible]	[illegible]	[illegible]	[illegible]	[illegible]	[illegible]	[illegible]
[illegible]	[illegible]	[illegible]	[illegible]	[illegible]	[illegible]	[illegible]	[illegible]	[illegible]
[illegible]	[illegible]	[illegible]	[illegible]	[illegible]	[illegible]	[illegible]	[illegible]	[illegible]
[illegible]	[illegible]	[illegible]	[illegible]	[illegible]	[illegible]	[illegible]	[illegible]	[illegible]
[illegible]	[illegible]	[illegible]	[illegible]	[illegible]	[illegible]	[illegible]	[illegible]	[illegible]
[illegible]	[illegible]	[illegible]	[illegible]	[illegible]	[illegible]	[illegible]	[illegible]	[illegible]
[illegible]	[illegible]	[illegible]	[illegible]	[illegible]	[illegible]	[illegible]	[illegible]	[illegible]

In Table A-VII-1 and Table A-VII-2,

1. Feed Rate [mole/hr] is n-propanol feed.
2. Bath Temp [°C] is the temperature of a salt bath.
3. Reactor Temp [°C] is the temperature of a reactor bed.
4. Press Dif [mm H_2O] is the pressure difference between the pressure inside the system and the atmosphere.
5. Atmosphere [mm Hg] is the pressure of the atmosphere.
6. Sampling Period [min] is the period during which Sampling was done.
7. Liquid Sample [mole] is the amount of the liquid sample collected.
8. Gas Sample [mole] is the amount of the gas sample collected.

Table A-VII-3

Experimental Conditions

The salt bath temperature is 463°C

Run No.	1 Pyrex Glass Pieces [gm]	2 Feed Rate [mole/hr]	3 Reactor Temp [°C]	4 Press Dif [mm H_2O]	5 Atmosphere [mm Hg]	6 Sampling Period [min]	7 Liquid Sample [mole]	8 Gas Sample [mole]
21	5	0.2250	462.0	0	704.8	30	0.1120	0.00032
22	10	0.2253	462.0	0	704.8	30	0.1125	0.00034
23	15	0.2246	462.0	0	704.8	30	0.1118	0.00031

Table A-VII-4

Experimental Conditions

The salt bath temperature is 463°C

	1	2	3	4	5	6	7	8
Run No.	Stainless Steel [gram]	Feed Rate [mole/hr]	Reactor Temp [°C]	Press Dif [mm H_2O]	Atmosphere [mm Hg]	Sampling Period [min]	Liquid Sample [mole]	Gas Sample [mole]
24	2	0.2270	462.0	0	704.8	30	0.1132	0.00024
25	4	0.2285	462.0	0	700.0	30	0.1140	0.00025
26	6	0.2232	462.0	0	700.9	30	0.1113	0.00025
27	10	0.2257	462.0	0	700.9	30	0.1126	0.00027
28	15	0.2261	462.0	0	702.0	30	0.1128	0.00028

[illegible]

[illegible]

[illegible]

[illegible]	[illegible]	[illegible]	[illegible]	[illegible]	[illegible]	[illegible]	[illegible]	[illegible]
[illegible]	[illegible]	[illegible]	[illegible]	[illegible]	[illegible]	[illegible]	[illegible]	[illegible]
[illegible]	[illegible]	[illegible]	[illegible]	[illegible]	[illegible]	[illegible]	[illegible]	[illegible]
[illegible]	[illegible]	[illegible]	[illegible]	[illegible]	[illegible]	[illegible]	[illegible]	[illegible]
[illegible]	[illegible]	[illegible]	[illegible]	[illegible]	[illegible]	[illegible]	[illegible]	[illegible]
[illegible]	[illegible]	[illegible]	[illegible]	[illegible]	[illegible]	[illegible]	[illegible]	[illegible]
[illegible]	[illegible]	[illegible]	[illegible]	[illegible]	[illegible]	[illegible]	[illegible]	[illegible]

A P P E N D I X VIII

ACCURACY OF DATA

Many factors are considered to produce errors in the experimental data. However, the main factors are believed to be the feed measurement, the product sampling, and the product analyses. Although it is difficult to obtain the overall error in the experimental data from the experimental results in this investigation, the magnitude of the errors of those factors may be useful in appraising the reliability of experimental data.

1. Error in Feed

As mentioned in Appendix I, the error of n-propanol feed by the micro-feed is obtained approximately as

Feed Rate [gm/hr]	Error [%]
6.9 ± 0.32	± 4.6
10.3 ± 0.37	± 3.6
13.7 ± 0.27	± 2.0
27.3 ± 0.50	± 1.8

These values show that the error of the micro-feeder decreases with an increase of feed rate. However, the feed rates employed in this investigation have the magnitude of errors of ±1.8% to ± 4.6%.

2. Error in Sampling

As mentioned in chapter III-A-I, the error of liquid sampling is believed very small. However, the calibration of the wet-test meter used for gas product shown in Table A-VIII-1 indicates.

that the error is approximately ±6% in the region of 0 to 0.01 cu ft. The calibration was performed by feeding air into the wet-test meter from a bottle by replacing it with known amounts of water. In the present investigation, the flow rate of the product gas was very very slow, so that the gas volume was measured statically in this calibration.

3. Error in Chromatography Analysis

A synthetic mixture of known amounts of acetaldehyde with n-propanol was analyzed by Ucon on chromosorb W column. The gas chromatograph operating condition variables were the same as described in section III-D-1.

The results are shown in Table A-VIII-2.

Table A-VIII-2

Analysis of Synthetic Known Blend of Acetaldehyde

True Mole %	Analysis Mole %	Error [%]
9.24	9.30	+0.8
9.24	9.21	-0.3
9.24	9.35	+1.2
9.24	9.20	-0.5

From Table A-VIII-2, the error in gas chromatography analysis may be expected to be approximately ±1.2%.

4. Error in Material Balance

Since the error of n-propanol was large, 1.8 to 4.6%, the

Calibration of Wet-Test Meter

Known Amount of Air [cu ft]	Amount Measured by Wet Test-Meter [cu ft]	Error [%]
0.0132	0.0127	-4.0
0.0131	0.0136	+3.5
0.0135	0.0134	-1.0
0.0055	0.0052	-5.5
0.0051	0.0052	+2.0
0.0056	0.0059	+5.0
0.0021	0.0020	-4.5
0.0019	0.0020	+5.5

amount of the n-propanol feed was defined as follows in this investigation.

Amount of n-propanol feed [gm] =

Amount of liquid product collected [gm] + Amount of gas product collected [gm]

Although the error of the measure of gas product volume is large, ±6%, it is expected that the error does not affect very much since the amount of gas product is very small (The maximum mole ratio of gas product to liquid product is $0.00028/0.2261 \simeq 1.24 \times 10^{-2}$ for Run 28). The material balances obtained in this investigation show very high values as shown in Table IV-1 to IV-4. This may show that the error of liquid sample is very small. However, this does not always indicate the accuracy of analysis or of gas product sampling. Even if there is large error in the analysis of product and/or in the measuring of gas product volume, the material balances do not change much, since the n-propanol conversion is very small.

[illegible]

[illegible]
[illegible]

[illegible]

[illegible]
[illegible]

[illegible]
[illegible]
[illegible]
[illegible]
[illegible]
[illegible]
[illegible]
[illegible]
[illegible]
[illegible]
[illegible]

A P P E N D I X IX

CALCULATION OF DENSITY OF n-PROPANOL

The density of organic compounds (39) are given by

$$\rho = \rho_b (2.0 - T/T_b)^{0.537} \qquad (0.3 < T/T_b < 1.3) \qquad \text{(IX-1)}$$

Where, ρ : density at T°K [gm/cc]

ρ_b : density at T_b°K [gm/cc]

T : temperature [°K]

T_b : boiling temperature [°K]

The density at boiling point, ρ_b, is given by

$$\rho_b = M/V_b \qquad \text{(IX-2)}$$

Where, M : molecular weight

V_b : molecular volume at T_b [cc/mole]

The molecular volume at the boiling point is obtained as the sum of atomic volumes according to a chemical structure for the compound. Atomic volumes for n-propanol are given as follows (39),

Atom	Atomic Volume [gm/atom]
C	14.8
H (for compound)	3.7
O (for alcohols)	12.0

Therefore, the molecular volume of n-propanol, C_3H_8O, at its boiling point is given by

$$V_b = 3 \times 14.8 + 8 \times 3.7 + 12.0$$

$$= 86.0 \quad \text{[cc/mole]}$$

The molecular weight of n-propanol is 60.09, so that substituting into equation IX-2,

$$\rho_b = \frac{60.09}{86.0} = 0.619 \text{ [gm/cc]}$$

The boiling point of n-propanol is 97.8°C, so that the density of n-propanol at 80°F is obtained as follows.

$$T_b = 273 + 97.8 = 370.8 \quad [°K]$$

$$T = 273 + \frac{5}{9}(80 - 32) = 299.7 \quad [°K]$$

Substituting into equation (IX-1),

$$\rho = 0.619\left(2.0 - \frac{299.7}{370.9}\right)^{0.537}$$

$$= 0.619(2.0 - 0.81)^{0.537}$$

$$= 0.767 \quad \text{[gm/cc]}$$